

Charles University
Faculty of Science

Study programme: Molecular and Cellular Biology, Genetics and Virology



Mgr. Maroš Huličiak

Engineering and selection of protein binders recognising medically important cytokines
(Inženýrství a selekce vazebných proteinů rozpoznávajících medicínsky důležité cytokiny)

Doctoral thesis

Supervisor:

prof. Ing. Bohdan Schneider, CSc.

Laboratory of Biomolecular Recognition

Institute of Biotechnology of the Czech Academy of Sciences, v.v.i.

Prague, 2022

Declaration:

I hereby declare that I have completed this PhD thesis independently and thesis is based on my own research. All publications and other used sources have been properly cited. This thesis has not been submitted previously in order to obtain the same or any other academic degree.

In Prague, 25th November, 2022

Mgr. Maroš Huličiak

Acknowledgements

I would like to thank my supervisor prof. Ing. Bohdan Schneider, CSc., DSc. and to my consultant RNDr. Pavel Mikulecký, PhD for their leadership, consultations and scientific advices.

I am also grateful to all my colleagues from the Laboratory of Biomolecular Recognition of Institute of Biotechnology of Academy of Sciences of the Czech Republic for their experimental help and support.

Finally, I want to thank my family for their support and patience during my PhD study.

Abstract

Protein engineering attracts more attention as a powerful tool of biotechnology and medicine. Small, engineered proteins derived from protein molecules of stable fold, the so called scaffolds, are potential replacements of supplements of more widely used antibodies. In this thesis, I introduce utilization of two scaffold molecules designed in our laboratory for development of stable and specific protein binders of high affinity. This thesis discusses the development of binders interacting with medically important human cytokines and their cellular receptors, interleukin-10, interleukin-28 receptor, and interleukin-9 receptor alpha. Recombinant cytokine and receptor proteins were expressed in eukaryotic cells in high yields and quality and served as molecular targets for selections using various display methods of directed evolution. We demonstrated that application of ribosome and yeast display methods or their unconventional combination in a newly developed integrated pipeline leads to successful generation of high affinity and specificity binders based on newly designed protein scaffolds called 57aBi and 57bBi.

Abstract in Czech

Proteinovému inženýrství se dostává čím dál tím více pozornosti jakožto užitečnému nástroji v oblasti biotechnologií a moderní medicíny. Malé, uměle vytvořené molekuly odvozené ze stabilních proteinů, tzv. skafoldů, jsou potenciální náhradou široce používaných protilátek. V této práci představuji využití dvou takovýchto skafoldů navržených v naší laboratoři pro vývoj stabilních vazebných proteinů s vysokou vazebnou afinitou i specifitou. Tato práce pojednává konkrétně o vývoji dvou vazebných molekul interagujících s lékařsky důležitými lidskými cytokiny a jejich buněčnými receptory - jmenovitě s interleukinem-10, receptorem interleukinu-28 a alfa receptorem interleukinu-9. Rekombinantní cytokiny i oba receptory byly ve vysoké kvalitě a s vysokými výtěžky produkovány v eukaryotických buňkách a sloužily jako molekulární cíle pro selekci pomocí displejových metod řízené evoluce. Prokázali jsme, že aplikace ribozomálního a kvasinkového displeje, nebo jejich nekonvenční kombinace vede k úspěšnému generování vysoce afinitních a specifických vazebných molekul založených na nově navržených proteinových skafoldech nazvaných 57aBi a 57bBi.

List of abbreviations

A1M	alpha 1 microglobulin
ABD	Albumin-binding domain
APC	Allophycocyanin
BSA	Bovine serum albumin
cDNA	complementary DNA
DARP	Designed ankyrin repeat protein
DSF	Differential scanning fluorometry
<i>E. coli</i>	<i>Escherichia coli</i>
EDTA	ethylenediaminetetraacetate
ELISA	Enzyme-linked immuno sorbent assay
Env	Envelope
EpCAM	Epithelial cell adhesion molecule
FACS	Fluorescence activated cell sorting
FDA	Food and drug administration
FITC	Fluorescein isothiocyanate
GFP	Green fluorescent protein
GTP	Guanosine triphosphate
HA	hemagglutinin
IFN	Interferon
Ig	Immunoglobulin

IL	interleukin
IL-xR	interleukin receptor
ISGs	IFN-stimulated genes
ISREs	interferon-stimulated response elements
JAK	Janus kinase
MAP	Mitogen-activated protein
MLV	Murine leukaemia virus
mRNA	messenger RNA
MST	Micro scale thermophoresis
NF- κ B	Nuclear factor kappa B
Ni-NTA	Nickel-nitrilotriacetic
Nup	Nuclear pore protein
PCR	Polymerase chain reaction
PDB	Protein Data Bank
PD-L1	Programme-death ligand 1
PI-3	Phosphoinositide-3
PSMA	Prostate specific membrane antigen
PSP94	Prostate secretory protein 94
PVP	Polyvinylpyrrolidone
Ras	Rat sarcoma virus protein
RT-qPCR	Reverse transcription-quantitative PCR

S. cerevisiae

Saccharomyces cerevisiae

SARS-CoV2

Severe acute respiratory syndrome Corona virus 2

SPR

Surface Plasmon resonance

STAT

Signal transducer and activator of transcription

TGF

Tumour growth factor

Th cells

T-helper cells

T_m

Temperature of melting

WT

wild type

γC

gamma chain

Contents

1 Introduction	1
1.1 Interleukins and their receptors	2
1.1.1 IL-10 family cytokines.....	3
1.1.2 common γ chain (γ C) cytokines.....	5
1.2 Protein scaffolds.....	7
1.2.1 Albumin-binding domain.....	9
1.2.2 Adnectin.....	10
1.2.3 Affibodies	10
1.2.4 Affimers	10
1.2.5 Anticalin.....	11
1.2.6 DARPins	12
1.2.7 Knottin	12
1.2.8 Nanobodies	13
1.3 Selection display methods.....	14
1.3.1 Phage display	14
1.3.2 Yeast display.....	17
1.3.3 Bacterial display.....	19
1.3.4 Ribosome display.....	19
1.3.5 mRNA display	22
2 Aims	23
3 Results	24
3.1 Development of 57aBi protein scaffold	25
3.2 Development of bispecific binder signalling via IL-28 receptor.....	28
3.3 Selection of high-specific binders against IL-9 receptor α subunit.....	30
4 Discussion.....	33
4.1 Development of 57aBi protein scaffold	33
4.2 Development of bispecific binder signalling via IL-28 receptor.....	36
4.3 Selection of high-specific binders against IL-9 receptor α subunit.....	39
5 Conclusions	44
6 References	45
7 Supplements	59

1 Introduction

Protein engineering has undergone enormous dynamic development as a modern biotechnological approach over the past twenty years. Small scaffold-derived non-antibody protein binders engineered for high affinity, stability, and specificity to their molecular targets are promising tools as the alternatives to the established, more widely used monoclonal antibodies. In comparison with the latter, the protein scaffolds are smaller in size, do not contain posttranslational modifications, have typically a higher stability, are cheaper to be produced, and do not require lengthy animal immunization.

Combinatorial libraries of the protein scaffolds are selected by so called selection display methods. Evolution of the selection display methods started in the eighties of the 20th century with the development of phage display [1]. Since then, more than ten cell surface-based and cell-free display selection methods were developed and have been used for selection of the protein binders recognizing a wide range of clinically relevant targets.

Proteins of clinical importance also include cytokines and their receptors. Cytokines play a key role in immune system's initial responses to viral or bacterial infections. Also, dysregulation of the cytokines signalling pathways can lead to the development of autoimmune diseases or cancer. Thus, modulation of cytokine pathways using small scaffold-derived proteins can be a promising strategy in therapy or diagnostics of these diseases.

Hereby, I am presenting the results of my work during PhD study published in two impacted scientific journals and one manuscript accepted to be published. The presented research focuses on the strategies for development of small protein binders based on the scaffold concepts developed originally in our laboratory. By using display methods, we have developed binders of human cytokines and their receptors, interleukin-10 (IL-10), interleukin-28 receptor (IL-28R), and interleukin-9 specific receptor subunit alpha (IL-9R α).

1.1 Interleukins and their receptors

Interleukins are secreted signalling molecules belonging to the group of cytokines participating in regulations of immune system. These molecules are produced in various cell types, but leukocytes are their main source. This gave them their name which is composed of two parts: "inter" related to a mean of communication and "leukin" derived from cell population responsible for their major production [2]. The first identified interleukin was Interleukin-2 in 1965, originally named blastogenic factor [3].

Interleukins have varying functions. Some of them can act as pro-inflammatory factors (IL-1, IL-4, IL-6, IL-8, IL-12), others perform the opposite, anti-inflammatory functions (IL-6, IL-10). Thus, the role of interleukins in organism is much greater than was initially thought and their effect depends mainly on the cell population bearing the receptors recognized by the particular interleukin. Interleukins can thus act as growth factors and differentiation inducers [4, 5] but also as pro-apoptotic molecules [6].

Most cytokine receptors are composed of two receptor subunits. The first receptor subunit, its extracellular part, is responsible for interleukin binding with high specificity and affinity. The second subunit then serves as signal transducer with intracellular components of downstream signalling pathways induced by interleukin molecule binding to its receptor. Signalling via interleukin receptors can lead to cell proliferation [7] or apoptosis of the affected cells [8] depending on which signalization cascade is triggered by interleukin. Interleukins can signal via MAP kinase pathway [9], PI-3 kinase pathway [10], NF- κ B pathway [11] and many other pathways but the most typical is JAK-STAT signal pathway [12, 13]. Modulation of the cytokine-induced signalling pathways provides an excellent therapeutic strategy for autoimmune diseases [14, 15] and for inhibition of the progression of various cancer types [16, 17].

There are currently more than 50 cytokines, interleukins, and interferons known to be encoded in the human genome. For greater clarity, cytokines were categorized into subgroups so-called families according to their structure, function, location in genome, receptor usage and biological function [18, 19].

1.1.1 IL-10 family cytokines

The family of the IL-10 related cytokines comprises of nine members, namely IL-10, IL-19, IL-20, IL-22, IL-24, IL-26, and IL-28A, IL-28B, IL-29, the last three are also classified as type III interferons IFN- λ 2, IFN- λ 3, IFN- λ 1. These interleukins are grouped into the IL-10 family based on their shared common receptor usage, downstream signalling, and high similarity in secondary structure. The secondary structure of IL-10 family interleukins is represented by six bundled α -helixes [20]. However, despite the fact the structure of the interleukins in this family is highly conserved, the sequence homology between individual members is very low [21, 22].

Cytokines of the IL-10 family are signalling via heterodimeric receptors. Some of the receptor subunits, IL-10R2, IL-20R1, or IL-20R2, can be shared by the same cytokine [19] (Figure 1). Signalization via receptors leads to activation of the specific kinases JAK1 and Tyk2 that phosphorylate the signal transducer and activator of transcription (STAT) protein molecule. Phosphorylated STAT molecules then form dimers and enter the nucleus, where they act as transcription factors. In IL-10 family signalization, STAT1, STAT2, STAT3 and STAT5 are involved. STAT3 is present in both dimeric states, as homodimer, or heterodimer with STAT1 or STAT5 molecules [23].

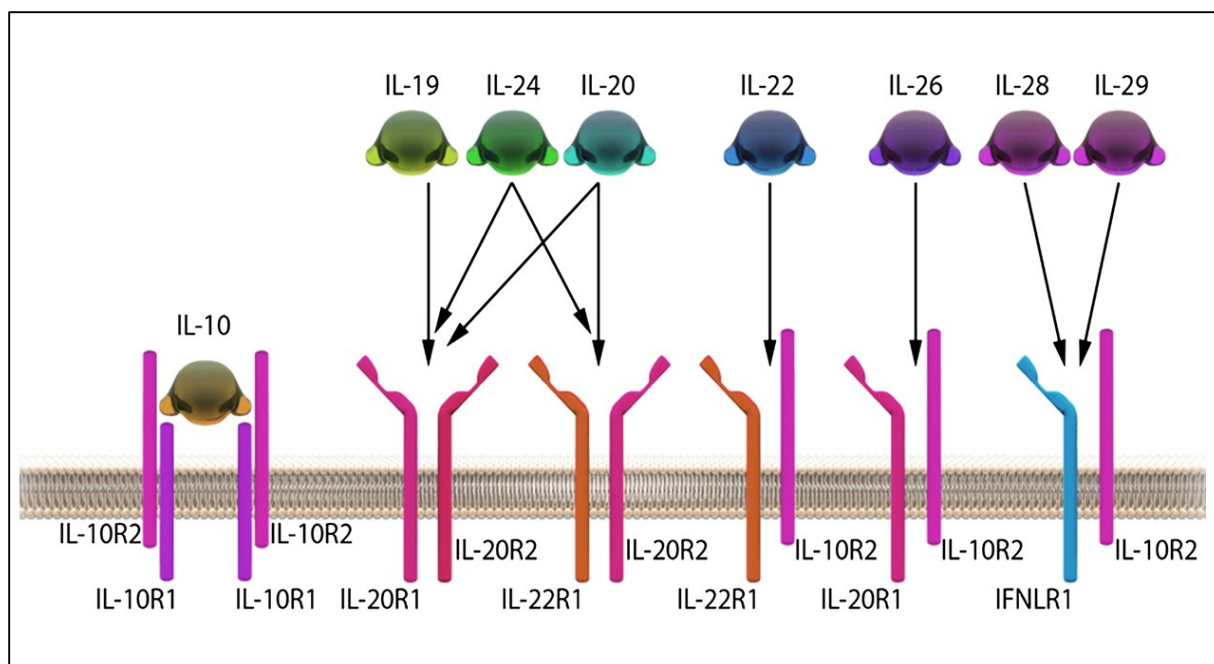


Figure 1. Members of IL-10 family and their cellular heterodimeric receptors. IL-10R2 is shared by IL-10, IL-22, IL-26 and IL-29 cytokine. IL-20R1 is shared by IL-19, IL-24 and IL-26. IL-20R2 is shared by IL-19, IL-20, IL-24. IL-22R1 is common for IL-20, IL-22 and IL-24. Taken from [24].

Interleukin-10 (IL-10) cytokine

IL-10 is an anti-inflammatory cytokine, first described in 1991 as human cytokine inhibitory factor. To be specific, IL-10 is responsible for regulating the expression of pro-inflammatory interleukins, mainly IL-1, IL-6 and IL-8 [25, 26]. IL-10 has significant role in survival of B lymphocytes and their proliferation, typically by inhibition of molecules produced by macrophages and Th1 cells. [27, 28].

The gene of human IL-10 consists of 5 exons and is localized on chromosome 1 [29]. Cytokine is produced by T lymphocytes of Th2 phenotype, regulatory T lymphocytes (T_{reg}), B lymphocytes, monocytes, macrophages, mast cells, NK cells, neutrophils or dendritic cells [30].

In contrast with other IL-10 family members, IL-10 forms homodimer, where each domain consists of 178 amino acids. According to homodimer structure of the IL-10, receptor complex is hetero tetramer consisting of two homodimers: IL-10R1 and IL-10R2 (Figure 1), where IL-10R1 part is responsible for specific binding to IL-10 ligand. Binding of the ligand to the receptor leads to activation of the receptor-associated kinases JAK1 and Tyk2 and phosphorylation and dimerization of STAT3 molecule [31].

Currently, there are many diseases described to be caused by over-expression of IL-10 or its signalling partners. Overproduction of IL-10 cytokine is also associated with autoimmune myocarditis [32],

systemic lupus erythematosus [33], melanoma [34] and other cancer types [35, 36], what makes IL-10 clinically important target.

Interleukin-28 (IL-28) cytokine and its receptor

IL-28 has two isoforms – IL-28A, also called IFN λ 2 and IL-28B (IFN λ 3). Sequence homology of these two isoforms is very high, about 96%. Human IL-28 was discovered in 2002 using genomic screening processes together with IL-29. Amino acid sequence and structure of IL-28 is very similar to IL-29 (IFN λ 1) [37, 38]. Due to this similarity, these interleukins (interferons) are sharing the same receptor, composed of two subunits IFN λ R1 and IL-10R2 (Figure 1).

Genes encoding the human isoforms of IL-28 are located on chromosome 19 on the same arm together with the gene encoding IL-29. Expression of IL-28 is induced as a response to viral infection by T lymphocytes and macrophages [38, 39]. IL-28 has significant role in adaptive immune response and it also increases cytotoxic potential of CD8⁺ T lymphocytes [40].

Signalling via heterodimeric receptor goes along the same principle as in case of IL-10. IL-28 is binding specifically to IFN λ R1. Binding leads to JAK1 and Tyk2 kinases activation followed with downstream STAT phosphorylation, dimerization and nuclear translocation and binding to interferon-stimulated response elements (ISREs) or IFN-stimulated genes (ISGs) [37].

Protective role of IL-28 is well documented and this cytokine is commonly used as supplement to influenza vaccines [40]. Development of the vaccine to HIV is also based on strategy with IL-28B cytokine supplementation [41].

1.1.2 common γ chain (γ C) cytokines

Common γ chain (γ C) cytokines, also referred as IL-2 cytokine family, is represented by IL-2, IL-4, IL-7, IL-9, IL-15 and IL-21. These cytokines signal through heterodimeric or heterotrimeric receptor sharing common γ chain (Figure 2) [42]. First cytokine discovered is member of this family and it was IL-2 in 1965 as growth factor of T lymphocytes. On the top of this, further studies pointed out that IL-2 is crucial for proliferation of the NK cells during immune response [43]. Major signalling pathway of the IL-2 family cytokines is JAK-STAT. Signal transduction is induced via binding of the cytokine to the receptor. The specific receptor subunit then associates with common γ chain. Dissociation constant of binding affinity of the IL-2 to heterodimeric IL-2R β / γ C receptor complex is about 10⁻⁹ M [44]. Receptors subunits of the complex are formed by 3 domains. After activation, short intracellular domain recruit Janus family kinases JAK1 or JAK3. The activation of the JAK kinases results in phosphorylation and subsequent activation of the STAT1, STAT3, STAT5A or STAT5B transcription factors [42].

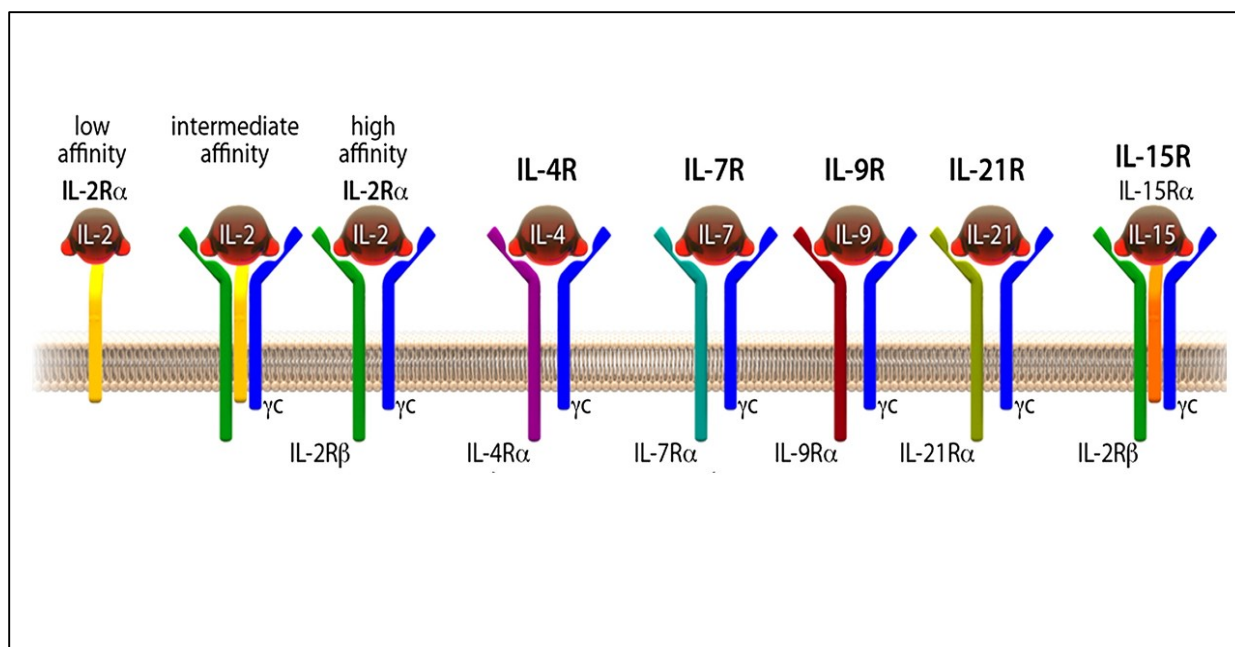


Figure 2. Cytokines of the IL-2 family. Interleukins are sharing common γ chain (γ C) receptor subunit [24].

Cytokines of the IL-2 family belongs to the most studied cytokines due to their application in immunotherapy and tumor inhibition. That was the primary call for development of longer-term circulating and more stable variants derived from IL-2 family cytokines. Using this approach, these engineered cytokines were successfully used in lymphoma treatment as they are associated with reduced toxicity in form of pulmonary edema, one of the most common IL-2 treatment-caused toxicity, where novel designed IL-2-based therapeutic provides improved antitumor response *in vivo* [45, 46].

Interleukin-9 (IL-9) cytokine and its receptor

Identical to IL-2, IL-9 was identified in mice as growth factor of T cells. IL-9 is produced by Th9 helper cells after induction by TGF- β and IL-33 cytokine [42, 47]. Further, the role of IL-9 is to stimulate mast cells and Th17 cells proliferation and prevent them to undergo apoptosis [48].

Molecular weight of IL-9 is 14 kDa. Human IL-9 is a protein formed of 144 amino acids, which can be glycosylated on four different Asparagine sites. The gene of human IL-9 is located on chromosome 5 in association with IL-4, IL-5 and IL-13 genes [49].

IL-9 binds two different receptor subunits, the specific alpha chain, also called IL-9 receptor α (IL-9R α), and the common gamma chain that is conserved and shared with other IL-2 family members. IL-9R α has intracellular, transmembrane and extracellular domain. Whole receptor consists of 522 amino acids [50]. IL-9 receptor is displayed on the T cells and the highest expression was detected on Th2 and Th17 cells [51, 52]. In addition, secreted IL-9 can influence B cells and might lead to an increasing level of IgE molecules. Signalization is initiated by binding of the IL-9 to its heterodimeric receptor and subsequent activation of JAK1 kinase, associated with IL-9R α and JAK3, common γ chain associated kinase, leads to cross-phosphorylation leading to activation of STAT1, STAT3 and STAT5 transcription factors [53]. Despite that IL-9 signals mostly by the JAK/STAT pathway, it can also induce the MAP kinase and NF κ B pathways [54, 55].

An emerging importance of IL-9 was highlighted with increasing number of diseases where it played significant role in pathogenesis or progression. IL-9 overexpression is most often referred to in connection with respiratory diseases, mainly asthma and tuberculosis. Higher levels of secreted IL-9 can also trigger development of coronary diseases, Crohn's disease or Inflammatory bowel disease [56-59]. Modulation of the pathways by blocking IL-9 or its receptor can be one of the promising strategies how to reduce severity of these diseases.

1.2 Protein scaffolds

Novel small non-antibody protein binders derived from protein scaffolds are fast becoming more and more promising tools in field of protein engineering. Their low molecular weight associated with better tissue penetration, absence of posttranslational modification and highly stable fold making them a serious competitor to conventionally used monoclonal antibodies. Proteins derived from scaffolds can be produced in high yields and in soluble form by prokaryotic systems growing in minimal media. Such approach cuts their production costs to minimum, too.

Protein scaffolds are derived from well-known structure, usually small domain of larger protein. Importantly, some of pre-calculated amino acids on the surface can be randomized without disruption of scaffold molecule. Using randomization of amino acids in chosen positions, we can change binding properties of the scaffold and make it to be able to bind different clinically interesting targets [60]. Randomization is set on DNA level during synthesis process where combinatorial libraries of protein scaffolds are generated. There are various strategies in

preparation of combinatorial libraries. The best price-performance ratio has the NNK library synthesis. Compared to fully NNN synthesis approach where all three STOP codons can be introduced into scaffold sequence, NNK offers potential occurrence of only one STOP codon. The most powerful approach is so called TRIM where whole codon triplet for amino acid is added. Using this synthesis strategy, you can avoid presence of all three STOP codons and also codons encoding unwanted amino acid such as cysteine and thus avoiding also formation of disulphide bonds [61].

An approach when amino acid positions on the scaffold chosen for randomization are predetermined by calculations is called directed mutagenesis. Combinatorial libraries can be also created by random mutagenesis tools such as Error-prone PCR. This method is usually selected for secondary mutagenesis for small improvement of binding properties of already existing binders. Error-prone PCR method is based on replication using DNA polymerase with suppressed exonuclease corrective activity. Such polymerase then introduces the mutations into sequence of binder during amplification of combinatorial libraries by PCR. Frequency of occurring mutations can be easily set by number of PCR reaction cycles or by concentration of template DNA [62].

Small protein binders derived from protein scaffolds have already shown their therapeutic potential. There are many scaffold-based proteins in advanced clinical phases of testing. Short overview of the most frequently used protein scaffolds and their structures is displayed in Table 1 and Figure 3. Each scaffold is described in more details in separate chapter with a focus on its clinical application.

Table 1. List of eight most frequently used protein scaffolds, their parental protein and fold type

Scaffold molecule	Parental protein	Fold type
Albumin-binding domain	Streptococcal protein G	α -helical
Adnectin	Fibronectin type III domain	β sandwich
Affibodies	Z domain of protein A	α -helical
Affimers	Phytocystatin	β -sheet, α -helical
Anticalin	Lipocalin	β -barrel, α -helical
DARPin	Ankyrin repeats	α -helical
Knottin	Cellohydrolase	β -sheets
Nanobodies	Camelid antibody	β -sheets

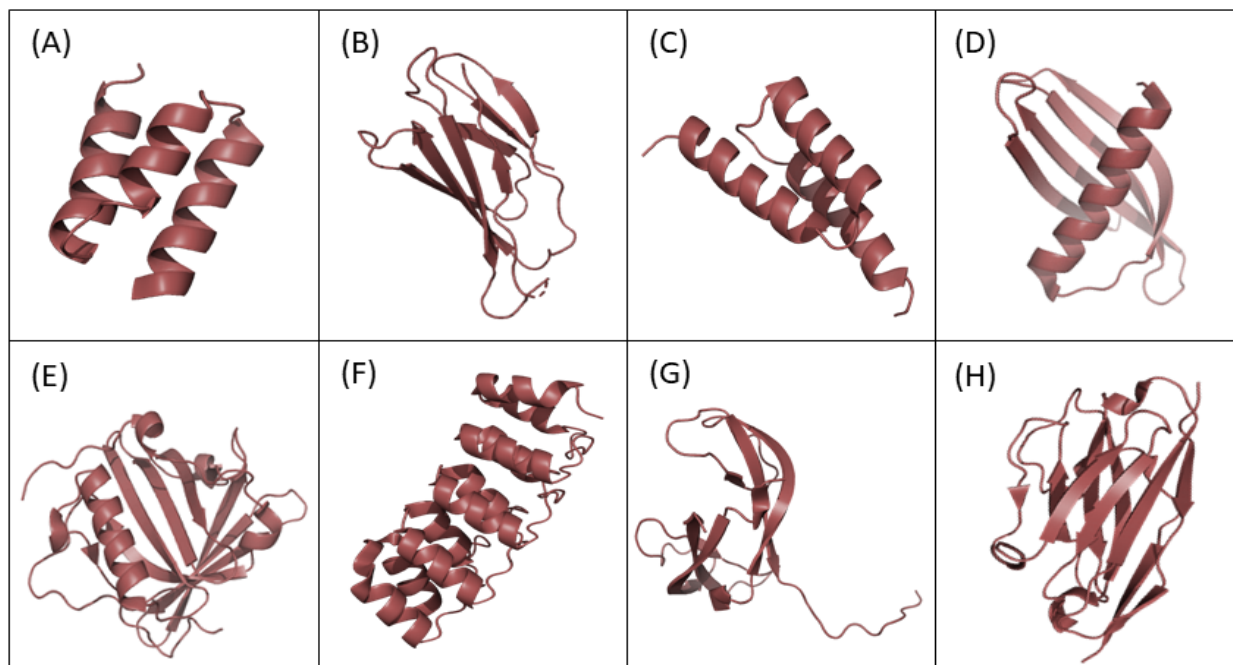


Figure 3. (A) Structure of ABD scaffold design by Ahmad et al. 46 residues long segment of Streptococcal Protein G (PDB ID: 1GJT; residues 20-65) [63]. (B) Structure of Adnectin-1 binding SRC Co-Activator Binding to PXR. Structure taken from complex with human pregnane X receptor ligand domain (PDB ID: 4S0S; residues 7-93) [64]. (C) Structure of Affibody scaffold, 58 residues long segment (PDB ID: 2B87; residues 1-58). Structure solved by [65]. (D) Structure of Affimer type II scaffold - Adhiron, 77 residues long segment (PDB ID: 4N6U; residues 32-108) Structure taken from [66]. (E) Structure of Petrobactin-binding engineered Anticalin, 172 residues long segment (PDB ID: 6GQZ; residues 5-176) Structure taken from [67]. (F) Structure of DARPin molecule, 156 residues long segment (PDB ID: 4J7W; residues 12-167) Source [68]. (G) Structure of CXC-chemokine-binding Knottin scaffold variant, 54 residues long segment (PDB ID: 6I31; residues 12-65) Structure taken from [69]. (H) Structure of BCDO9O-M2 Nanobody variant targeting human ErbB3 receptor, 126 residues long segment (PDB ID: 6F0D; residues 1-126) Structure taken from [70].

1.2.1 Albumin-binding domain (ABD)

ABD scaffold is small three-helical domain from Streptococcal Protein G (Figure 3A). There were more than a hundred ABD variants with altered specificity, increased affinity and stability engineered [71]. Ahmad et al. analysed 46 residue-long segment from the third albumin-binding domain of Streptococcal G protein (PDB ID: 1GJT, residues 20-65) where 15 amino acids residues were chosen for further randomization. Reported thermal stability of circa 70 °C after incorporation of Alanine into chosen randomization positions qualified this domain as promising candidate [63]. Concept was then proven by successful selection of ABD-based protein binders against human prostate secretory protein 94 (PSP94) and Shiga Toxin 1 B subunit [72, 73].

Albumin-binding domain has wide possibilities of use not only as a protein scaffold. Domains are fused with another protein, example g. trichosantin, to help its expression, solubility or stability *in vitro* and *in vivo* [74].

1.2.2 Adnectin

Adnectin protein scaffold is based on the Fibronectin type III domain, naturally occurring in extracellular matrix [75]. The first selection to demonstrate Adnectin for scaffold application was performed in 1998 by phage display aiming at ubiquitin molecule [76]. The methodology for the selection of the binders was extended also to mRNA display and scaffold was commercialized as Trinectin and later as Adnectin. The structure of the scaffold consists of β strands bundled with loops forming β sandwich (Figure 3B). Flexible loops are responsible for binding to the molecular targets and are often chosen for amino acid randomization [77].

Adnectin scaffold-based protein binders were successfully selected to specifically recognise and inhibit Epidermal growth factor receptor and Insulin-like growth factor receptor [78] and also Vascular endothelial growth factor receptor-2, marker of glioblastoma [79].

1.2.3 Affibodies

Scaffold for Affibodies molecules is an engineered IgG-binding domain (called Z domain) of the Staphylococcal protein A. Affibodies have three α -helical fold (Figure 3C), where 13 surface amino acids on helices 1 and 2 were chosen for randomization. Amino acid sequence of helix 3 is constant and responsible for structure stability. Molecular weight of Affibodies is about 6,5 kDa, protein scaffold is composed of 58 amino acids [80, 81].

Affibody scaffold-derived variants have broad range of application. Selected proteins were used for detection of human cancer marker epidermal growth factor receptor 2 in metastasizing cells. Engineered variants were successfully used as colorectal cancer therapeutics and also in commercial ELISA kits as detection components [82-84].

1.2.4 Affimers

Affimer scaffold provides β -sheets and α -helical fold (Figure 3D), where loops connecting these ordered regions are responsible for binding to target molecules after its amino acid randomization. The first type of Affimers is based on human Stefin A protein. The second, more frequently used

type of Affimers, originally called Adhirons, is based on plant Phytocystatin protein engineered for highly soluble and thermostable monomeric form. Molecular weight of Affimers scaffold is 12 kDa [66, 85].

To date, Affimers variants have been selected against a wide range of molecules reaching up to picomolar affinities [86]. Recently, scaffold derived binders K3 and K6 that can recognize specific conformation of the inactive Ras depending on bounded GDP and lock it in its inactive state have been selected. Ras mutation are currently the most often oncogenic drivers of different tumor development. Affimer variants provide a strategy how to maintain Ras GTPase activity at the normal level [87].

1.2.5 Anticalin

Parental proteins of Anticalin scaffold are Lipocalins with molecular weight in range of 16-19 kDa. Tertiary structure of the scaffold is formed by β -barrel with attached α -helix (Figure 3E). Anticalin scaffold was developed and successfully used in many selection processes by research group of prof. Arne Skerra in Munich, Germany. Combinatorial libraries of Anticalin scaffolds are generated by randomization of a set of about 20 amino acids on its surface specifically in loop regions [88, 89].

A huge advantage of this scaffolds is their human origin. Lipocalins are human plasmatic proteins, what minimizes the risk of the immune response and antibody generation after drug administration to patients [90].

Notably, there are several potential drugs candidates based on Anticalin scaffold in preclinical and clinical phases of tests. One of recombinant version of Anticalin-A1M (α_1 -microglobulin) was admitted in 2018 to clinical phase I study by the Swedish Medical Products Agency, while A1M variant is promising drug candidate in treatment of acute kidney injury and preeclampsia [91, 92]. One recombinant Lipocalin-based protein binder is already in the phase III of clinical trials. This engineered Lipocalin variant has origin in blood-sucking tick saliva and is successfully used as inhibitor of human pro-inflammatory C5 protein connected with induction of autoimmune diseases [93].

1.2.6 DARPin

Designed ankyrin repeat proteins (DARPin) are composed of α -helical repeat motifs that are bundled with loops to create a compact stable folded domain (Figure 3F). DARPin usually consist of 4-6 repeats, leading to a right-handed solenoidal structure. One ankyrin repeat used in scaffold is formed of 33 amino acids, in average. [94, 95].

The combinatorial libraries of one ankyrin repeat designed in Plückthun's laboratory contains structurally important fixed positions and six variable non-conserved surface amino acid positions chosen for further randomization, that are engaged in interaction with the target of interest [96].

Whole concept of DARPin is based on immune system of jawless vertebrates. Adaptive immunity of these animals is composed of leucine-rich repeat helical-folded proteins. This system is a homologue to antibody generation in immune response of mammals where sets of antibodies are randomly generated. Similarly, random recombination occurs in these leucine-rich proteins, thanks to which the protein can acquire specificity and affinity to the pathogenic molecule [97].

DARPin-derived protein binders showed their potential as inhibitors of c-Jun N-terminal kinases isoforms 1 and 2 involved in apoptosis and inflammation processes in eukaryotic cells [98]. Another EpCAM-binding DARPin variants are used as diagnostic molecules of this epithelial cell adhesion marker in ovarian cancer, most lethal gynaecological malignancy [99]. Most recently, a set of anti-gephyrin DARPin clones were successfully used in identification of gephyrin clusters in rat neuron culture and mouse brain tissues which were previously overlooked [100].

1.2.7 Knottin

Knottins are versatile class of protein scaffolds known for their robust β -stranded structure (Figure 3G) and small size. Peptides selected from Knottin libraries represent the smallest binders from scaffold molecules listed in Table 1. They have been shown to possess high stability that, together with small size and the ability to penetrate different tissues, makes them a promising diagnostic and therapeutic agents. Of note, they manifest strong resistance to human cell proteases which is supported mainly by presence of so called cysteine knot structure formed by three disulphide bonds improving protein compactness [101].

Getz et al. have identified Knottin scaffold derived from kalata B1 protein, member of cyclotide family. Seven amino acids positions of total 30 amino acid-length protein were chosen for randomization in the sixth loop of protein. Therefore, this loop exhibiting amino acids with highest variability across the cyclotide family was selected for further editing. Combinatorial libraries of scaffold were then selected for binding to α -thrombin using bacterial display selection method assisted with Fluorescence Activated Cell Sorting (FACS). Selected binders provided affinity to α -thrombin in nanomolar range [102].

Using Knottin scaffold molecules, DX-88 Exallantide variant was engineered as a potent Kallikrein inhibitor specifically binding with strong 44 pM affinity. This inhibitor was approved as a drug for the treatment of hereditary angioedema [103]. According to Microscale thermophoresis measurement results, Sankaran et al, developed Knottin-based inhibitors of trypsin with inhibition constants in nanomolar range. These Knottin variants can be so used for immobilization of β -trypsin at the supramolecular surfaces [104].

1.2.8 Nanobodies

Nanobodies are of a similar size as Affimers, their molecular weight is in range of 12-14 kDa. They are derived from variable antigen-binding domain of heavy chains of camelid origin [105]. According to structure of the variable domain of the antibody heavy chain, Nanobodies are composed of anti-parallel β -sheets (Figure 3H). Nanobodies are generated in camelid (camels, lamas, alpacas) or shark by immunization process followed by lymphocyte isolation and their nucleic acid extraction. Specific variable antigen-domain of heavy chains are then amplified by PCR and cloned into bacterial strains for expression. The whole process usually last about four months [106]. Eventhough Nanobodies have antibody origin, their production in prokaryotic system, absence of posttranslational modification such as glycosylation and disulphide bonds formation categorized them to Protein scaffolds class.

Affinities of Nanobodies-based variants are in the picomolar and nanomolar range. The highest affinities using Nanobodies were obtained in selection of binding to the commercial purification ALFA-tag and by detection of Nup proteins in bioimaging [107, 108]. Nanobodies have improved resolution in biological imaging methods. Higher resolution using Nanobodies variants instead of

antibodies is caused by smaller distance between epitope and conjugated fluorophore so the linkage error is reduced (reviewed in [109]).

1.3 Selection display methods

Crucial step after construction of combinatorial libraries of scaffold molecules is their selection against target molecule of interest. Scaffold-derived binders are selected and screened to obtain high affinity, specificity to selected targets or stability improvement by so called display selection methods.

The versatile principle of selection display methods is that there is a linkage between genotype and phenotype during selection process. Nomenclature of these methods is based on that the protein or peptide variants of interest are displayed on cell or virus surface or in cell free systems. Thanks to that, we can conceptually divide selection display methods to surface-based, representing by phage, bacterial or yeast display and cell-free selection display methods including ribosome and mRNA displays [110].

Each of the selection display methods provide some advantages but also has its limitations. In general, cell-free display methods are more suitable for selection of cell-toxic proteins and also for larger combinatorial library selection, because they can cover theoretical complexity up to 10^{14} . On the other hand, cell-based display selection methods guarantee only well-folded and soluble proteins and peptides will be displayed [111, 112].

1.3.1 Phage display

The most often referred and utilized method among combinatorial library selection approaches is phage display. Evolution of phage display started in 1985 by George Smith, who displayed short linear peptide on the surface of bacteriophage envelope. Peptides displayed on viruses were then selected for binding to a predefined antibody [1]. Since that moment phage display has undergone extensive development and moreover laid the foundations for the evolution of new surface-based display methods.

Currently, most frequently used viruses for presenting variants of combinatorial libraries on their envelopes are M13 bacteriophage, Fd filamentary phage and T7 lytic bacteriophage. Peptide libraries are usually displayed in fusions with N-termini of capsid proteins pIII, pVI, pVII or pIX

or their truncated forms. The capsid of M13 bacteriophage allows to present approximately 2700 copies of protein variant on their major coat protein pVII. More copies can be presented using additional minor coat proteins [113, 114].

Initial step of phage display using M13 bacteriophage is its infection of bacterial host (*E. coli*). Subsequently, DNA of phage is injected into the cytoplasm and replicated inside the bacteria. DNA of combinatorial libraries in fusion with p-type envelope protein is transcribed by bacterial system and fused proteins are expressed followed by M13 capsid formation with displayed thousands of copies of protein binder variant. M13 is non-lytic bacteriophage, escaping the host without lysing its membrane which comes with a small limitation, that only small peptides can be presented on their surfaces. In comparison, T7 lytic bacteriophage is able to display protein composed of 1200 amino acids. Amplified and purified viruses are then incubated with immobilized molecular target, followed by series of washing steps while high affinity bounded binders displayed on phage envelope are not washed away. These virus variants are subsequently eluted using acidic or high salt concentrated buffers and amplified in bacterial host cells. Selection process is called Bio panning and usually there are three to five rounds performed. In final round, viral DNA encoding the proteins with best binding properties is isolated and cloned into vector for bacterial expression [114, 115]. The scheme of phage display selection is shown in the Figure 4.

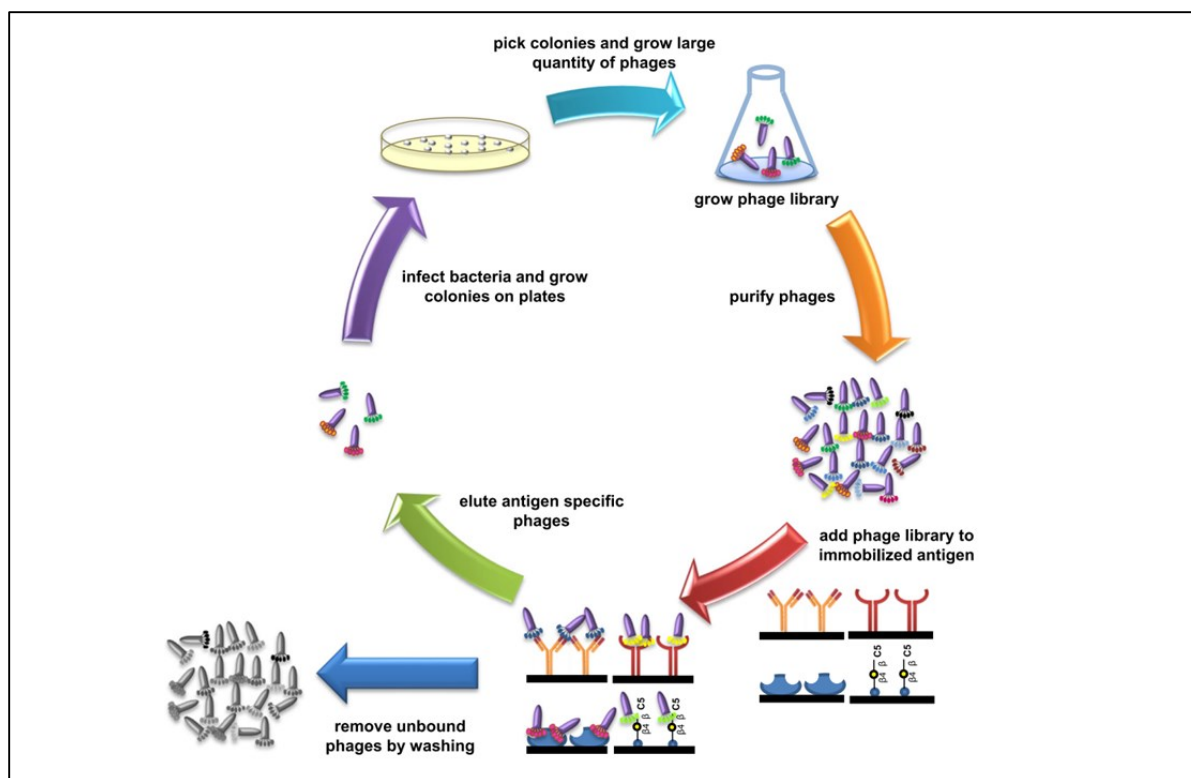


Figure 4. Scheme of Phage display selection. Bacteriophages infect host bacterial cells and are multiplied in them. Phages are then incubated with target molecule. Those variants, which present binders recognizing target with high affinity are used for repeated infection of the host cell [116].

Based on phage display, another viral-envelope derived displays were designed. Retroviral display's usage of eukaryotic mammal host cells is an advantageous option for selection of combinatorial libraries of glycoproteins and proteins requiring posttranslational modifications. Murine leukaemia virus (MLV) envelope spike glycoprotein Env proved to be especially amenable for displaying of foreign peptides or glycoproteins. Limitation of this method is its complexity. Retroviral display is applicable for combinatorial libraries with complexity no more than 10^6 theoretical variants [117, 118]. Equivalent to retroviral display is baculoviral display. Baculoviruses belong to large cDNA viruses group affecting the cells of insect host. According to this, variants selected using baculoviral display method can pose with different posttranslational modification in comparison to modification during retroviral display selection. Baculoviral display is commonly used for development of protein binders which requires posttranslational acylation or phosphorylation [119]. Finally, adenoviruses commonly used as genes delivery systems in a gene therapy showed their ability to display isolated peptides on their envelopes and significantly increased gene transduction, specifically in glioma cell lines [120].

However, phage display is the oldest approach among all display selection methods, it is still successfully utilized in development of therapeutics and diagnostic molecules. Many of those were patented under their trademark and authorized by FDA (Food and drug administration), e.g. Gamifant[®] aiming at IFN γ approved in 2018 or Tremfya[™], inhibitor of IL-23 signalling pathway, helping in Psoriasis treatment [121, 122].

1.3.2 Yeast display

The second most frequently used surface-based selection method is yeast display. This technology is the most powerful affinity screening method because one yeast cells, generally *Saccharomyces cerevisiae*, can display from ten up to hundred thousand copies of protein binder variant on its surface. In comparison with phage display, yeast surface can display even 100x more copies of protein variant than frequently used bacteriophage M13. Displayed protein variant are usually in fusion with cell-wall Agglutinin protein Aga2p, which is bounded to Aga1p protein via two disulphide bonds. Strategy of usage of cell-wall protein Agglutinin as anchor for combinatorial libraries of peptides was developed by Boder and Witrupp in 2000 and to this date, this strategy is the most frequently used in yeast display selection [123, 124]. However, there are different fusion proteins available to exploit in library presentation. As an alternative, proteins can be fused to both C- or N-terminal ends of Cwp2p, Tip1p, Tir1 or Flo1p yeast cell-wall proteins [125].

Plasmid construct for yeast display based on Agglutinin designed by Boder and Witrupp is considered as a golden standard, encoding two epitopes (c-myc and hemagglutinin (HA) tags) for further detection by flow cytometry. These tags can be detected/labelled by fluorescent antibody conjugates as a proof of expression of displayed variants on the yeast surface. These plasmids also contain Galactose or lactose promoter for induction of expression of Agglutinin-displayed binder protein complex. DNA of combinatorial libraries is cloned into this construct, usually by recombination. *S. cerevisiae* yeast cells are then transformed with plasmid construct via electroporation. Yeast cells are cultivated and expression of proteins is induced by activation of one of above-mentioned promoters. Cells presenting library variants on their surface are then incubated with fluorescent antibody conjugate-labelled molecular target. Selection is associated with flow cytometry analysis. Variants with proven expression on yeast surface by fluorophore, attached to target labelled with the second fluorophore are then separately sorted. Selected yeast cells can be used in another selection round or, in case of final round, DNA of selected variants is

isolated, transcribed and translated into protein [123]. Scheme of yeast display selection is shown in Figure 5.

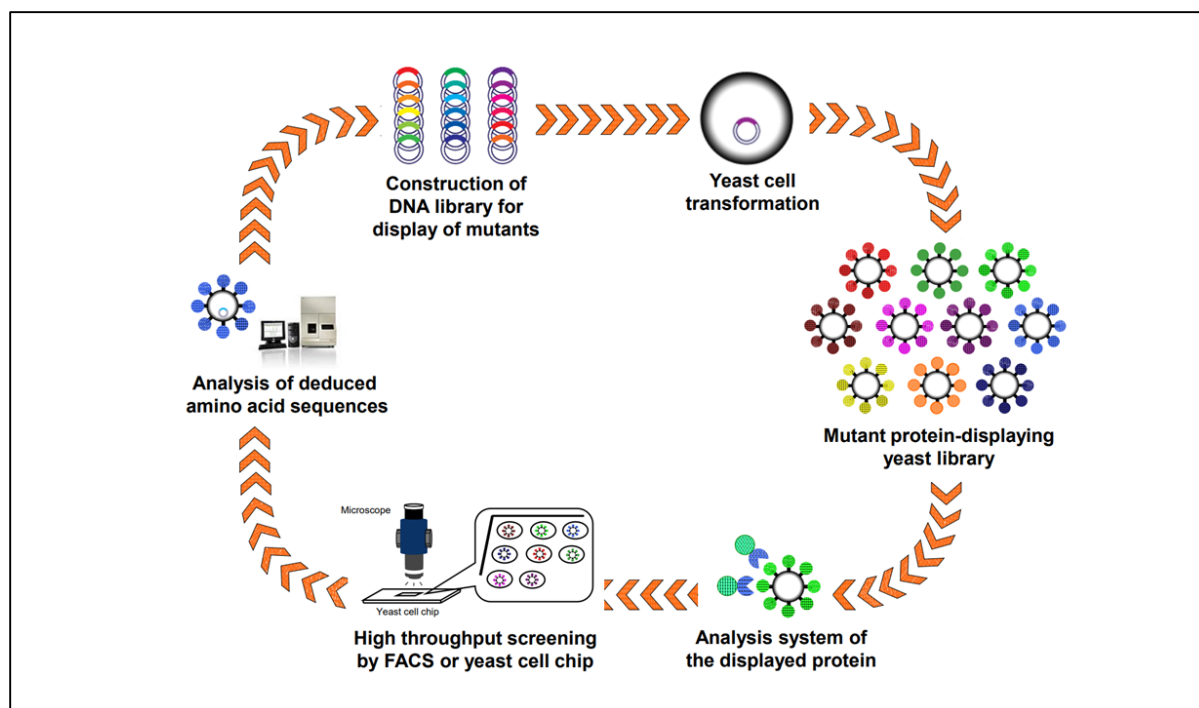


Figure 5. Scheme of yeast display selection. Yeast cells are transformed with plasmid containing DNA combinatorial library in fusion with yeast cell-wall protein. Proteins are displayed on the yeast surface and interact with target molecule. Yeasts with expressed protein and bound target are then sorted by FACS. DNA of this variants is then isolated and analyzed [126].

Methodology of yeast display selection was also a subject for some minor improvements. Of note, Israeli group developed so called Enhanced yeast display platform. Zahradnik et al. introduced surface exposure-tailored reporter eUnaG2, modified GFP encoded in plasmid into Agglutinin protein system. Fluorescent reporter is localized downstream the protein variant sequence which means reporter will be detected only in case of fully-translated and well folded variants after expression. It overcomes requirement to label via antibody which unfortunately might provide some non-specific binding. Thus, system is more stable and importantly, cost of yeast display selection process is significantly reduced [127].

Yeast display was chosen by numerous research groups for development of specific high affinity protein binders and antibodies. Recently, tissue inhibitors of metalloproteases were successfully engineered using this methodical approach [128]. Ban et al. significantly improved the specificity

of 12F6 antibody recognising small hapten molecules by Error-prone mutagenesis approach followed with yeast display selection [129].

1.3.3 Bacterial display

Bacterial prokaryotic cells have very fast generational doubling times and life cycle. According to this, bacterial system is the most frequently used system for expression of recombinant proteins. Nowadays, bacteria are not used only for production of proteins into cytoplasm but also for presenting protein combinatorial libraries on their surface with increasing frequency. To display combinatorial libraries, one can use both, Gram-positive (G+) or Gram-negative (G-) bacteria strains [130]. G+ bacteria, such as *Bacillus subtilis*, display their proteins as fusions with cell wall proteins. In contrast, G- bacteria are presenting recombinant proteins in fusion with outer membrane proteins, lipoproteins or flagellar proteins, well reviewed in [131]. *E. coli* (G- strain) is the most frequently used bacterial strain due to its high transformation efficiency and high expression level. In comparison with G+ bacteria and also yeast display, absence of the cell wall makes isolation of DNA much easier and also much faster.

In 2009, dual biosensor based on bacterial display was developed. Bacterial surface was covered with streptavidin and contains engineered gold-binding peptide which has affinity to SPR (Surface Plasmon resonance) biosensor. *E. coli* can be then immobilized on biosensor surface and provide recognition layer for binding of biotinylated molecules. Such engineered biosensor is promising diagnostic and analytical tool [132]. Another therapeutic application of the binders developed by this selection approach could be found in cancer treatment. For instance, proteins that bind and mediate internalization into breast carcinoma human cells were presented on the surface of non-pathogenic *E. coli* [133].

1.3.4 Ribosome display

Ribosome display is powerful selection method that covers the highest complexity of the combinatorial libraries. The only limitation is the number of ribosomes in cell-free reaction during *in vitro* transcription and translation. As the transcription and translation is performed in bacterial lysate, usually *E. coli* S30 *in vitro* system, transcription and translation is done in one step. Combinatorial libraries to be transcribed and subsequently translated *in vitro* are designed with *in vitro* transcription and translation elements T7 promoter, a stem loop and ribosome binding on its

5' end. On 3' end, there is an absence of the STOP codon what leads to formation of stable complex of mRNA-ribosome and protein where ribosome serves as a linker between genotype and protein phenotype [111]. Whole complex binding to immobilized target on plastic surface or magnetic beads is mediated through the protein molecule. Subsequent selection steps in ribosome display and final mRNA isolation is closely related to the immobilization strategy [134].

According to the protocol developed in 2006 by Plückthun's research team, which is considered as golden standard for ribosome display, target is immobilized on hydrophobic plastic of microtiter plates using coating bicarbonate buffer. Microtiter plate is then blocked by bovine serum albumin (BSA) to cover remaining hydrophobic sites on the plastic. Addition of stable complexes of mRNA-ribosome-protein is followed by binding of complexes via proteins to immobilized target. Unbound or weak-attached complexes are washed away in the series of washing steps. In subsequent rounds of ribosome display, washing conditions are getting stricter. The number of washing steps as well as concentration of used detergent in washing buffer are increasing. The selectivity in the process is safeguarded by decreasing concentration of immobilized target in each round of selection. Only strongly attached complexes bound to target via protein will remain. The mRNA of these complexes is isolated and purified following addition of EDTA containing solution which causes ribosome disruption and mRNA release. Isolated mRNA is then re-transcribed in reverse transcription reaction to cDNA. The result is DNA library with reduced complexity. In the final round of ribosome display selection, DNA library is cloned into a vector suitable for bacterial expression of protein variants, e.g. to analyse binding properties of selected binders [135]. Ribosome display selection process is shown schematically in Figure 6.

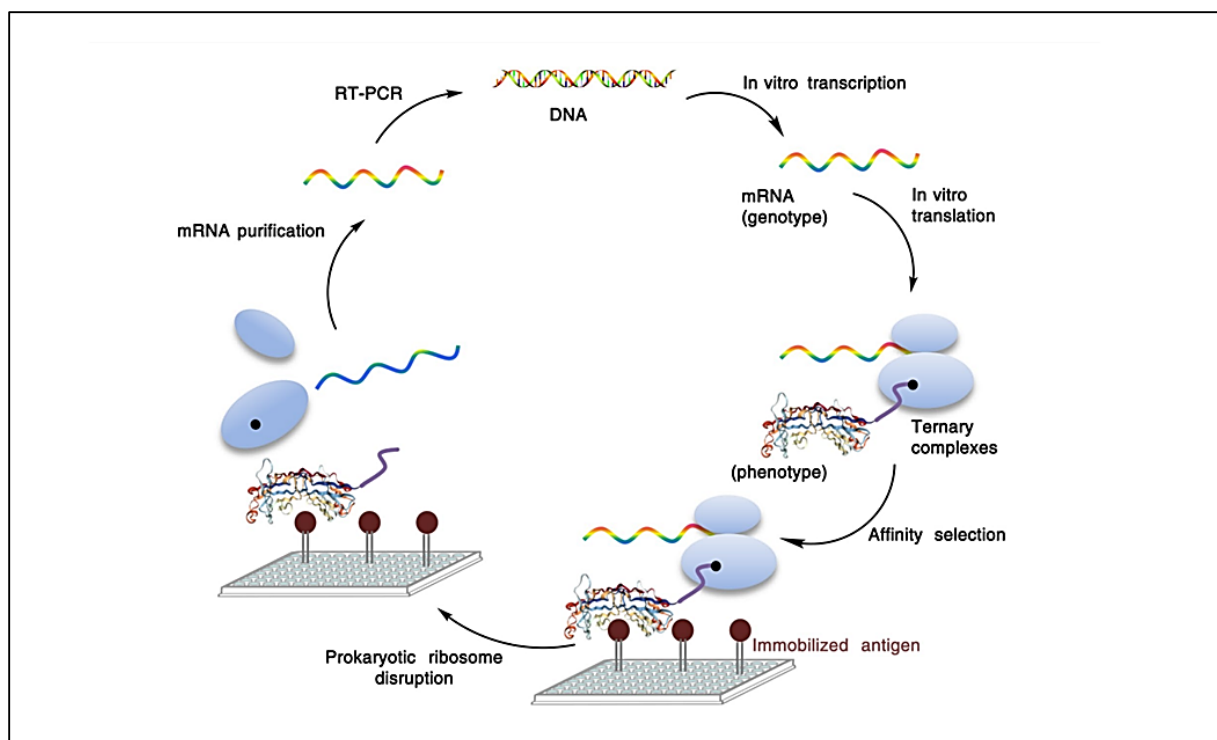


Figure 6. Scheme of ribosome display selection. DNA libraries are transcribed and translated while forming stable mRNA-ribosome-protein complex. Complexes bind immobilized target. Unbound complexes are washed away while bound complexes are a source of isolated mRNA. The resulting DNA, after reverse transcription of eluted mRNA, then enters the next round of selection [136].

Over the past 20 years, ribosome display underwent many improvements and many variations were introduced into this method. Bacterial *in vitro* systems were enriched of GroEL, GroES, DnaJ, DnaK or GrpE chaperones, which help with proper folding of selected proteins to obtain their native conformation [137]. Further, there is a ribosome display based on *in vitro* components purified of bacterial lysates (PURE system) free of nucleases and release factors. This means absence of STOP codon in combinatorial library design is not required [138]. Buchanan et al. improved the stability of their protein binders by unconventional adding of dithiothreitol (DTT) during selection process. This approach of stability optimization is based on altering the redox potential in reaction [139].

There were many successful selections based on prokaryotic *in vitro* ribosome display subsequently using eukaryotic translational systems based on yeast, insect or reticulocyte cell lysates. These systems are suitable for selection of glycosylated binders and proteins with more complexed stabilized quaternary structures, e.g. by cysteine disulphide bonds [140, 141].

Application of ribosome display selection method gave birth to many promising protein binders for medical purposes. For example, diagnostic reagents capable of revealing early symptoms of hepatitis C virus presence [142], synthetic proteins that modulate human Frataxin as prevention of development of Friedreich's Ataxia disease [143] or high-affinity inhibitors of C3-mediated complement occurring in immune disorders affecting mainly kidneys [144].

1.3.5 mRNA display

mRNA display technology was invented in 1997 and together with ribosome display, mRNA display is *in vitro* method which provides many advantages – the biggest complexity coverage, selection of cell-toxic proteins or incorporation of unnatural amino acids into protein binders during selection process. Technique of mRNA display is most often used in selection of short peptides consisting of no more than 100 amino acids [145, 146].

In mRNA display, protein variant of combinatorial library is simply linked to its encoding mRNA. Linkage is accomplished by presence of puromycin antibiotic at 3' end of nucleic acid which mimics 3' end of an attached aminoacylated tRNA. Unlike that, puromycin is not removed but acts like a bridge between protein and mRNA. The big advantage of this method is that after selection against molecular target, mRNA can be directly re-written from bounded mRNA-protein complexes to DNA by reverse transcriptase [145].

Over the last years, mRNA display selection technique has been used to develop specific and high affinity ligands. Proteins composed of synthetic amino acid were successfully selected using this display technique against SARS-CoV2 Spike protein of Corona virus while the affinities of the best binders were in nanomolar range [147]. Recently, there were patented small peptides generated by mRNA display specifically recognizing programme-death ligand PD-L1 [148].

2 Aims

The main aim of my PhD study was to develop small protein binders specifically recognising cytokines or their receptors with an emphasis on innovation of the used methodical approaches.

The main objective can be subdivided into three tasks:

- Engineering of novel scaffold molecules applicable in development of high affinity binders against IL-10 cytokine using ribosome display selection method
- Development of the bivalent binder based on protein scaffold recognising IFN- λ 1 receptors IL-28 receptor 1 (IL-28R1) and IL-10 receptor 2 (IL-10R2) and confirmation that the binder(s) potentiate the IFN- λ 1 signal transduction pathway
- Development of a new methodical platform for selection of high specific scaffold-derived protein binders to IL-9R α subunit

3 Results

The findings presented in this dissertation thesis were published in two articles in peer reviewed journals and one manuscript accepted for publishing. These articles are methodically and topically linked. Each of the articles describes development of a different novel small protein binder derived from scaffold molecules using selection display techniques. The articles and manuscript are attached in the appendix. My contribution to these articles is as listed below:

1. *Protein Binder (ProBi) as a New Class of Structurally Robust Non-Antibody Scaffold for Directed evolution* – molecular biology experiments (cloning of combinatorial libraries of the 57aBi scaffold, ribosome display selection, expression and purification of IL-10 and novel protein binders, ELISA screening method), biophysical experiments (microscale thermophoresis affinity determination, measurements of thermostability of novel protein binders), data analysis, preparation of original draft of the article, graphical content preparation
2. *De novo developed protein binders mimicking Interferon lambda signalling* – molecular biology experiments (cloning of combinatorial libraries of the scaffolds, yeast display selection, expression and purification of novel protein binders), data analysis, preparation of the graphical content
3. *Combined in vitro and cell-based selection display method producing specific binders against IL-9 receptor in high yields* – molecular biology experiments (cloning of combinatorial libraries of scaffolds, ribosome and yeast display selection, expression and purification of IL-9R α novel binders, ELISA specificity tests), biophysical experiments (microscale thermophoresis affinity determination), data analysis, preparation of original draft of the article, graphical content preparation

3.1 Development of 57aBi protein scaffold

Protein Binder (ProBi) as a New Class of Structurally Robust Non-Antibody Scaffold for Directed evolution. *Viruses*. Ngoc P.P., **Huličiak M.**, Biedermannová L., Černý J., Charnavets T., Fuertes G., Herynek Š., Kolářová L., Kolenko P., Pavlíček J., Zahradník J., Mikulecky P., Schneider B. (2021), 13, 190

Because of intellectual property reasons, ProBi scaffolds was in 2022 re-named to 57aBi and this name will be used in all following discussions. Results to be discussed in Discussion section are listed in tables and figures and were taken from [149].

Table 2. The list of potential scaffolds candidates that were selected for detailed analysis.

PDB Code	UniProt	Protein Name	Source Organism	Size (kDa)	Size (aa)	Number of Cysteines
4PSF	Q9NWS0	PIH1D1 N-terminal domain	<i>Homo sapiens</i>	15	138	3
1N3Y	P20702	Alpha-X beta2 integrin I domain	<i>Homo sapiens</i>	22	198	0
4I3B	P0DM59	Fluorescent protein UnaG wild type	<i>Anguilla japonica</i>	15	139	0
2F3L	B1WVN5	Luminal Rfr-domain protein	<i>Cyanotheca</i> sp. 51142	20	184	2
1W2I	P84142	Acylphosphatase	<i>Pyrococcus horikoshii</i>	10	91	0
4NBO	Q9HD15	Steroid receptor RNA activator protein carboxy-terminal domain	<i>Homo sapiens</i>	13	111	2
3APA	O60844	Human pancreatic secretory protein ZG16p	<i>Homo sapiens</i>	16	141	0
4IGI	E9PWQ3	Collagen VI alpha3 N5 domain	<i>Mus musculus</i>	22	203	0
2W4P	P07311	Human common-type acylphosphatase variant, A99G	<i>Homo sapiens</i>	11	99	0
4LKT	Q01469	Human Epidermal Fatty Acid Binding Protein (FABP5)	<i>Homo sapiens</i>	15	138	6
4MJJ	Q14183	C2A domain of DOC2A	<i>Homo sapiens</i>	15	138	5
4JOX	Q939T0	Cry34Ab1 protein	<i>Bacillus thuringiensis</i>	14	123	0

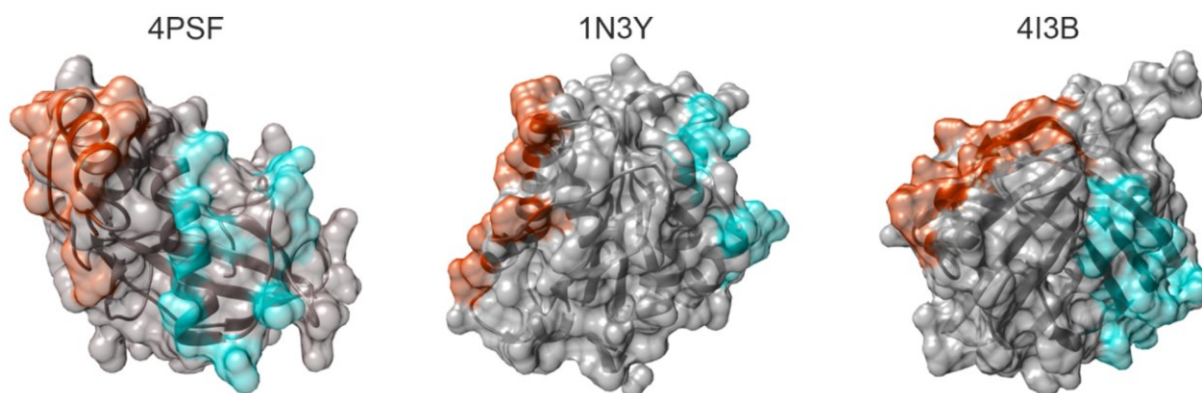


Figure 7. Surface of the 3 most promising scaffold candidates and their Protein data bank (PDB) identification numbers. Regions chosen for mutation are highlighted.

Table 3. Number of mutated residues of the scaffold candidates – WT and their mutants, expression state, level of expressions in soluble form and Melting temperature.

Protein Scaffold Candidate Variant	Number of Mutated Residues	Expression	Solubility	Tm
4PSF-WT	0	Yes	Very good	75 °C
4PSF-allAla-PatchN	10	Yes	Very good	60 °C
4PSF-allAla-PatchC	10	Yes	Very good	67 °C
1N3Y-WT	0	Yes	Very good	57 °C
1N3Y-allAla-PatchN	10	Yes	Good	51 °C
1N3Y-allAla-PatchC	11	Yes	Not soluble	N/A
4I3B-WT	0	Yes	Good	47 °C
4I3B-allAla-PatchN	12	No	No expression	N/A
4I3B-allAla-PatchC	11	Yes	Poor	N/A

Table 4. Amino acid sequences of 57aBi scaffold WT and selected variants against IL-10. Positions of 57 aBi-WT chosen for further mutation are yellow highlighted. Randomized amino acids in selected variants after ribosome display are highlighted in green.

Variant	Position																									
	109	110	111	112	113	114	115	116	117	118	119	120	121	122	123	124	125	126	127	128	129	130	131	132	133	134
WT	R	E	L	V	I	T	I	A	R	E	G	L	E	D	K	Y	N	L	Q	L	N	P	E	W	R	M
A2	R	G	L	V	I	R	I	A	Q	R	G	I	E	F	K	Y	L	L	A	L	N	P	R	W	I	M
A3	R	P	L	V	I	R	I	A	V	G	G	L	E	R	K	Y	G	L	S	L	P	P	L	W	R	M
B4	R	R	L	V	I	R	I	A	R	T	G	L	E	L	K	Y	S	L	N	L	W	P	P	W	S	M
C4	R	V	L	V	I	L	I	A	L	L	G	L	E	V	K	Y	R	L	A	L	Q	P	V	W	Y	M
C11	R	L	L	V	I	L	I	A	I	V	G	L	E	W	K	Y	P	L	P	L	V	P	L	W	E	M
C12	R	G	L	V	I	E	I	A	P	T	G	L	E	W	K	Y	F	L	L	L	E	P	S	W	C	M
E3	R	G	L	V	I	G	I	A	H	R	G	L	E	S	K	Y	Y	L	R	L	G	P	R	W	W	M
F5	R	R	L	V	I	T	I	A	L	R	G	L	E	L	K	Y	P	L	C	L	R	P	A	W	H	M
G3	R	R	L	V	I	A	I	A	P	N	G	L	E	R	K	Y	T	L	H	L	T	P	T	W	S	M
G6	R	G	L	V	I	F	I	A	V	G	G	L	E	S	K	Y	L	L	D	L	E	P	L	W	H	M

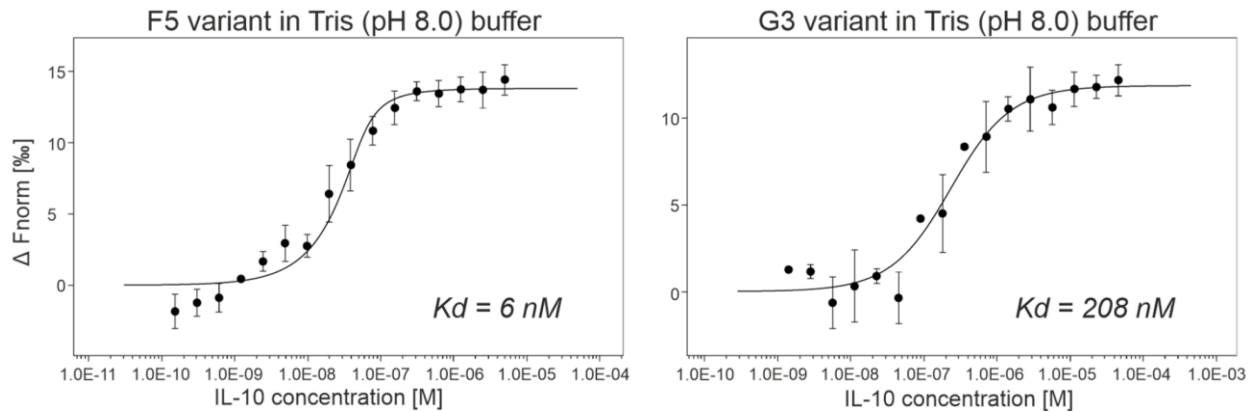


Figure 9. Microscale thermophoresis curves of the two best binders against IL-10 and their determined dissociation constants.

3.2 Development of bispecific binder signalling via IL-28 receptor

De novo developed protein binders mimicking Interferon lambda signaling. FEBS Journal. Kolářová L., Zahradník J., **Huličiak M.**, Mikulecký P., Peleg Y., Shemesh M., Schreiber G., Schneider B.

Results to be discussed in Discussion section are listed in tables and figures and were taken from [150].

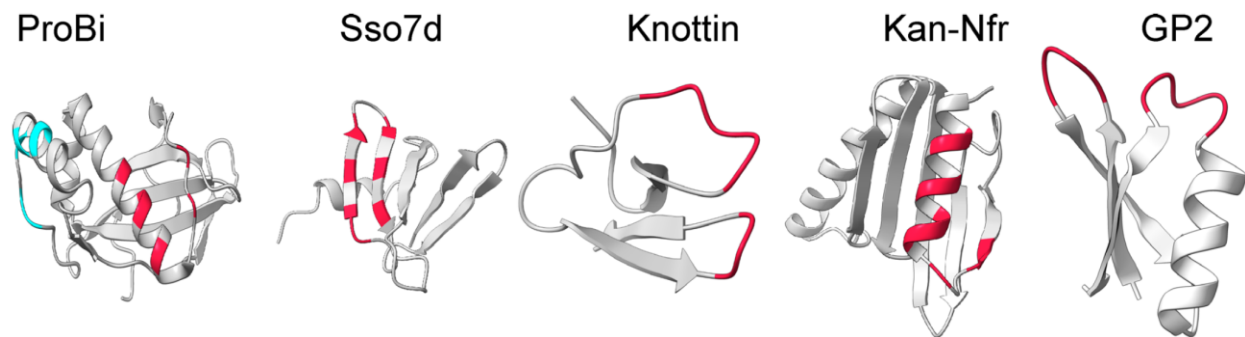


Figure 10. Secondary structures of scaffolds chosen for development of bispecific binders recognising IL-28 receptor. Mutable patches of the scaffolds are highlighted.

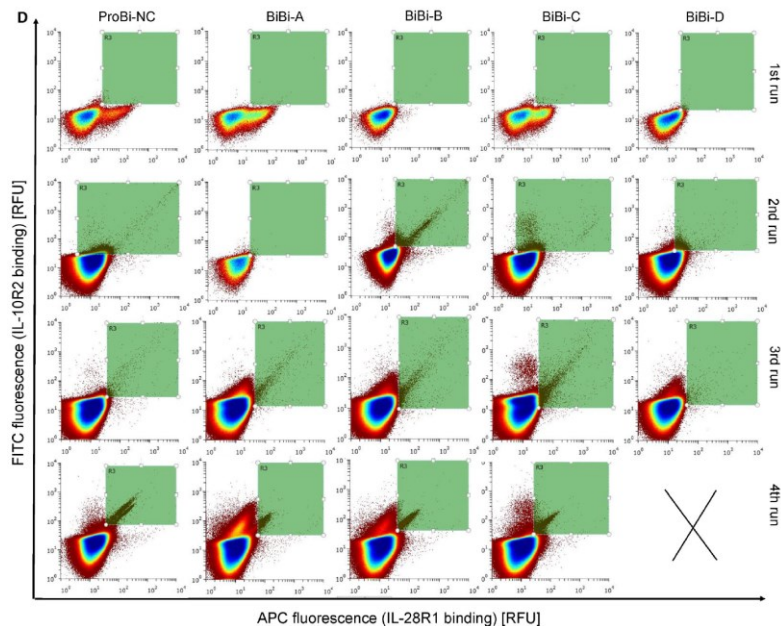


Figure 11. Simultaneous binding of the bivalent binders to IL-28 receptor measured by FACS method. Bivalent proteins recognising both subunit were positive on FITC and APC fluorescence. Green area determined the presence of double binders, which were sorted.

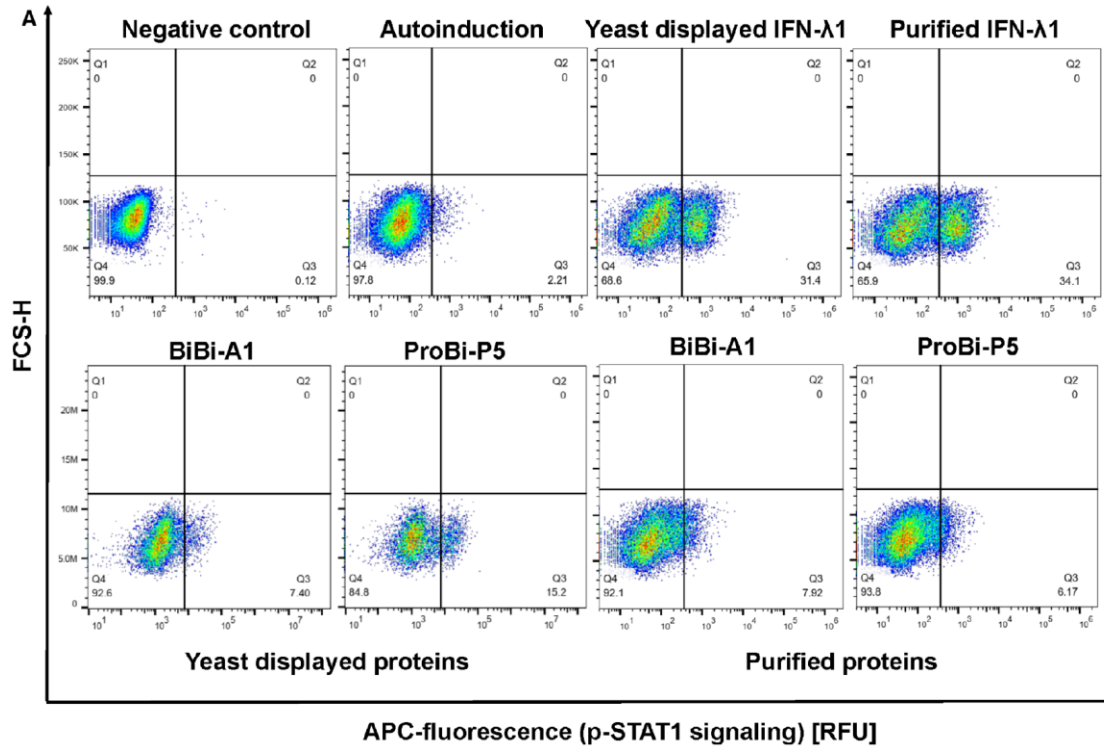


Figure 12. Screening of bispecific binders for their signalling potential via IL-28R measured by flow cytometry. Phosphorylated Tyr701 of STAT 1 molecule was detected after the addition of positive control IFN- λ and bispecific binders. Level of phosphorylated STAT 1 molecule is presented on x-axis as APC fluorescence.

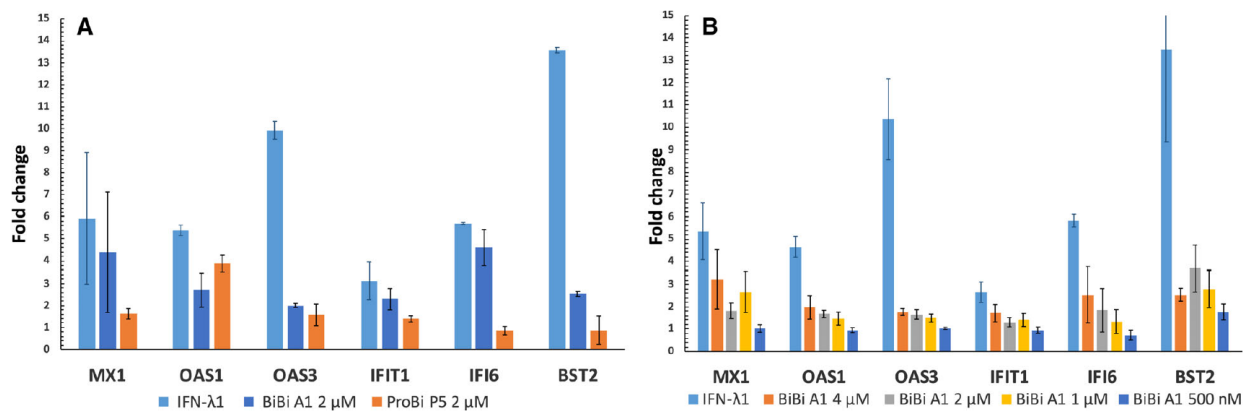


Figure 13. Expression of genes activated by signalling via IL-28 receptor after addition of positive control IFN- λ and bispecific binders in HaCat cells. (A) Gene expression induced by positive control, Bibi A1 and ProBi P5; (B) Gene expression induced by positive control and Bibi A1 at a different concentration.

3.3 Selection of high-specific binders against IL-9 receptor α subunit

Combined in vitro and cell-based selection display method producing specific binders against IL-9 receptor in high yields. FEBS Journal. **Huličiak M.**, Biedermanová L., Berdár D, Herynek Š., Kolářová L., Tomala J., Mikulecký P., Schneider B. (Manuscript to be published).

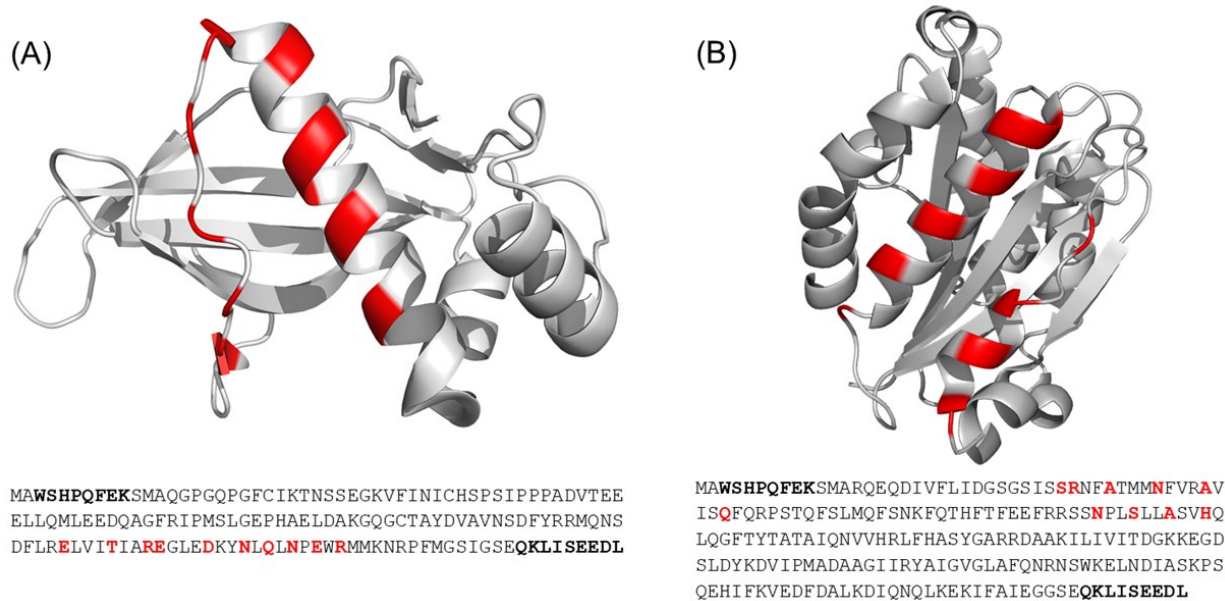


Figure 14. Secondary structures and amino acid sequences of (A) 57aBi scaffold and (B) 57bBi scaffold used in selection process against IL-9R α . Red labelled amino acids were calculated for randomization.

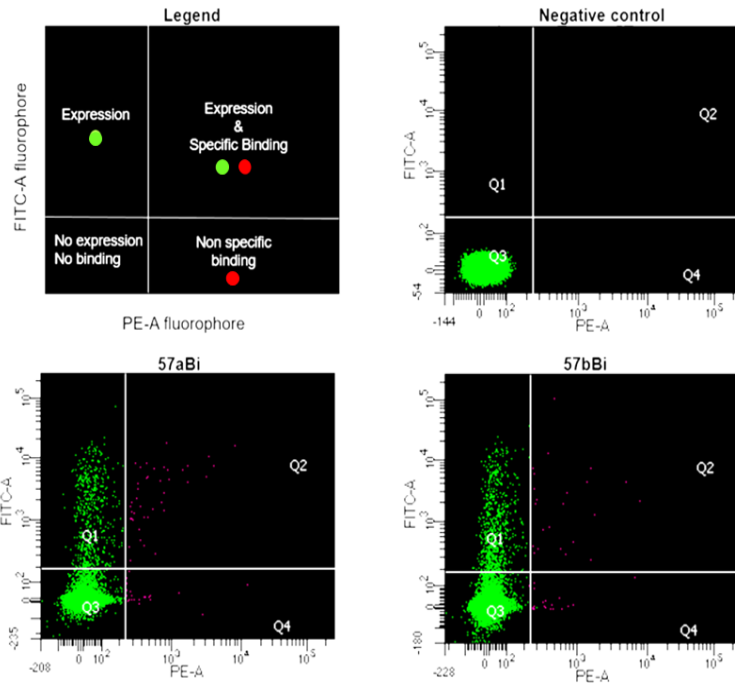
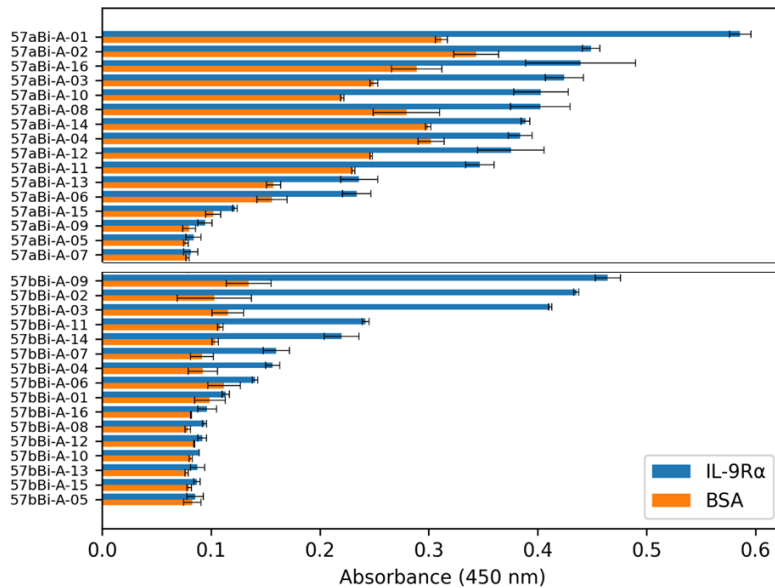


Figure 15. Competitive yeast display selection of the combinatorial libraries of the 57aBi and 57bBi scaffolds by flow cytometry. Expression of protein variant were detected as FITC fluorescence, binding to IL-9R α as PE-A fluorescence. Double fluorescence positives yeast cells from quadrant Q2 were sorted.

(A) ELISA of 57aBi & 57bBi variants after the 5th round of ribosome display



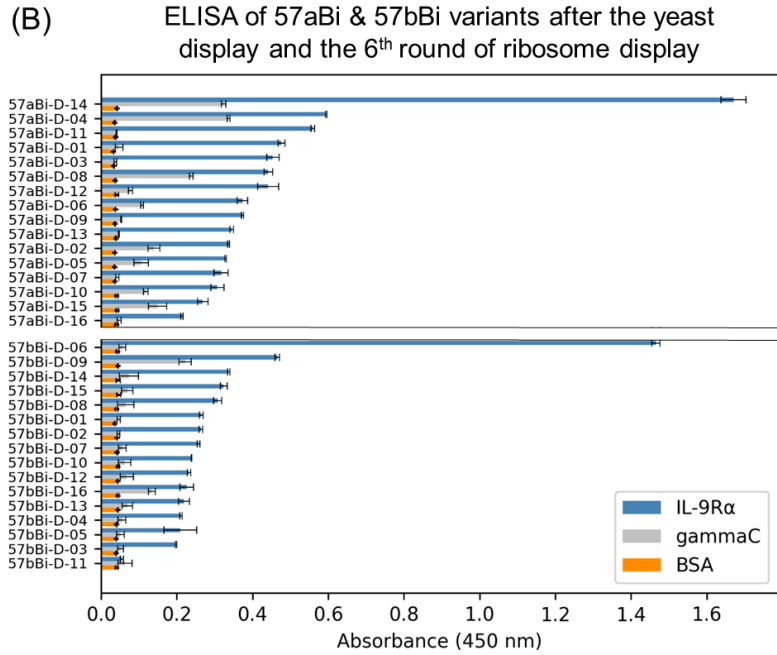


Figure 16. ELISA specificity tests of protein binders selected against IL-9R α by (A) five rounds of ribosome display and by (B) six rounds of ribosome display and one round of yeast display. Binders were testing for binding to (A) IL-9R α and BSA and also to (B) non-specific receptor subunit γ chain.

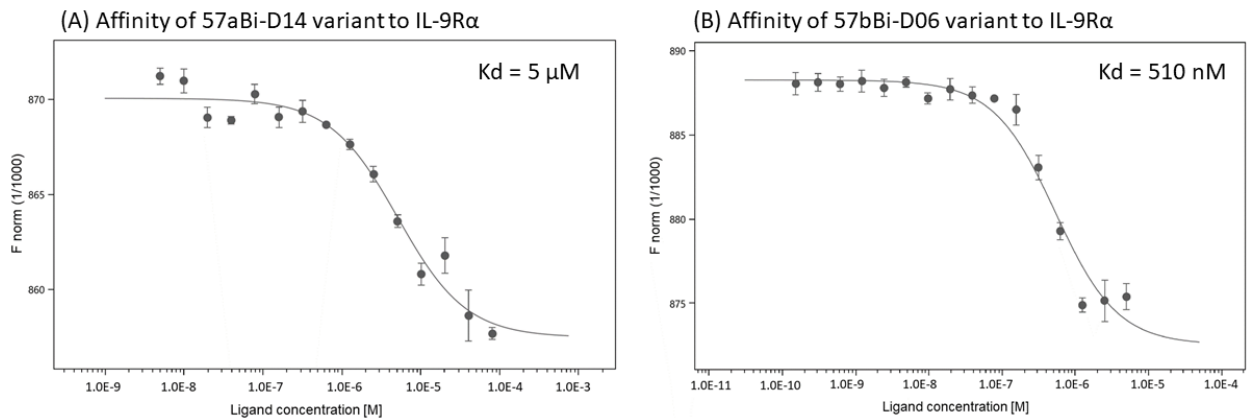


Figure 17. Microscale thermophoresis curves of the best (A) 57aBi and (B) 57bBi scaffold binder to IL-9R α and their determined dissociation constants.

4 Discussion

4.1 Development of 57aBi protein scaffold

Eventhough monoclonal antibodies are considered to be the golden standard for diagnostic and therapeutic purposes with a wide range of applications 21st century witnessed arrival of a new potent rival in the form of non-globulin small protein binders derived from so called protein scaffolds [151]. Small scaffold derived binders are associated with several advantages over antibodies. Because of their smaller size, protein binders are able to better penetrate different tissues. Most frequently used protein scaffolds are Anticalin and DARPin with molecular weight in range of 15-20 kDa, compared to the molecular weight of 150 kDa in case of an prototypic monoclonal antibody [88, 95]. Unlike antibodies the scaffold-based proteins are not posttranslationally modified and can therefore be expressed in bacterial systems. This makes the cost of their production much lower. They also provide an opportunity to avoid the ethical problem with exploitation of animals and their immunization. These are the major calls for novel scaffold molecules development. In our study published by Pham et al [149] in 2021, we described the whole process of development of novel scaffold molecule design which concluded with its successful application for generation of high affinity binders recognising IL-10.

Protein scaffold can be derived from some small independent binding domain of larger well-known protein complex, such as in case of ABD scaffold based on Albumin binding domain of Streptococcal Protein G [63]. We considered this fact during seeking process for potential scaffold candidates. As a part of initial process we searched the Protein Data Bank using following criteria. Firstly, novel protein scaffold should provide well-known structure, solved with high resolution. Secondly, expression of soluble form of the scaffold should be feasible in bacterial strains and thirdly, scaffold candidates should not be toxic or immunogenic. We were also seeking for proteins without cysteine amino acids in the sequence to avoid further problems with scaffold folding in bacterial expression systems. Based on these criteria, we have chosen 12 candidates based mainly on small human and murine protein binding domains. Scaffold candidates are listed in Table 2.

To determine and select the amino acid positions for further randomization we performed *in silico* saturation mutagenesis. Analysis was done by FoldX programme which calculated free energy differences ($\Delta\Delta G$) after substitution of each position of scaffold candidate sequence by all of the

20 standard amino acids. According to calculations we determined amino acids with high level of conservation and structural importance and which surface amino acids can be used for further randomization. Ideally, selected randomized patch should consist of 10 amino acids so that the complexity of the subsequently created combinatorial libraries of the scaffolds could be covered by ribosome display method. Theoretical coverage of complexity by ribosome display is 10^{14} [111]. According to these criteria we continued with five scaffold candidates PIH1D1 N-terminal domain (under PDB ID: 4PSF), Alpha-X beta2 integrin I domain (1N3Y), fluorescent protein UnaG wild type (4I3B), Lumenal Rfr domain protein (2F3L) and *Pyrococcal* Acylophosphatase (1W2I). These five scaffold candidates were expressed in bacterial strains in two versions - with N- and C- terminal His tag for further Ni-NTA affinity chromatography purification. We found that only candidates under PDB ID 4PSF, 1N3Y and 4I3B were expressed in soluble form and were purified with high purity level. We also measured melting temperatures of the candidates to determine their thermostability. In order to verify the correct estimation of calculated mutable positions, we inserted alanine amino acid into positions chosen for randomization in 4PSF, 1N3Y and 4I3B candidates and we repeated the purification and biophysical experiments. Surface patches of mutable residues of these three candidates are displayed in Figure 7.

Table 3 represents the data of expression level of candidates and their mutated variants, their solubility and melting temperatures. 4I3B candidate was excluded from further testing because of its low expression level of the soluble form in *E. coli* BL21 DE3 bacterial strain. 1N3Y candidate can be produced in its soluble form only in N-terminal mutated patch version while it still holds well-folded structure up to a temperature of 51 °C. High, long lasting thermal stability is also a common feature that makes scaffolds more favourable compared to monoclonal antibodies. In 2020, Kalichuk et al. developed small protein binders derived from only 60 amino acids Aho7c scaffold, group of the Affitins molecules, originating from thermophilic archaea *Acidianus hospitalis* that can survive temperatures up to amazing 96 °C and is still functional in pH range 0-12 [152].

The best results of our tested variants were recorded for 4PSF candidate. This molecule can be independently mutated on both N- and C-termini. Both mutated variant has high expression level of their soluble forms and their thermostabilities were over 60 °C. Initial name of scaffold was ProBi, but later, because of intellectual property reasons, it was re-named to 57aBi. C-terminal

mutated patch variant of the 57aBi scaffold was chosen for selection by ribosome display. To demonstrate the 57aBi scaffold potential we decided to select the combinatorial library of the scaffold against Interleukin-10 (IL-10). IL-10 is helical protein of IL-10 family and its overexpression usually leads to development of various types of cancer [34, 35]. IL-10 was isolated from insect cells and purified by affinity chromatography followed with size exclusion chromatography. Proper selection of molecular target in display methods is always a critical step. Selection with inhomogeneous and impure target leads to the generation of binders with low specificity level. We suggest to purify the target at least by two-step purification process. The resulting purified IL-10 met the criteria of a suitable target and was used in ribosome display selection.

Combinatorial library of 57aBi scaffold was synthesized using NNK codon strategy described early in more details (page 8, chapter 1.2 - Protein scaffolds). The constructed library consisted also of N-terminal Strep II tag and C-terminal c-myc tag for its further purification and detection. Combinatorial libraries were then selected by four rounds of ribosome display according to standard ribosome display protocol developed in Plückthun's laboratory [135]. For reduction of non-specificity of the final scaffold-derived binders we introduced some modifications. Instead of classic use of BSA as a blocking agent we altered it in specific rounds of selection by skim milk protein mixture. We also introduced pre-selection process to harness final specificity set up of the binders. Combinatorial libraries were incubated with non-specific targets before specific selection by ribosome display: BSA, skim milk proteins and IL-29 - member of IL-10 family with similar structure fold. Variants recognizing these non-specific targets were excluded before selection process initiation.

Selected variants acquired after ribosome display selection were characterized by ELISA assay to determine the binding level to IL-10 specific target and non-specific binding to BSA, skimmed milk and IL-29. Protein binders and their amino acid sequences with the highest affinity to IL-10 and the lowest affinities to non-specific targets are shown in Table 4. These candidates were selected to undergo final biophysical characterization.

As a final step, we measured the affinity of the candidates by Microscale thermophoresis in different buffers, aggregation level and their melting temperatures. IL-10 was labelled and titrated by 57aBi variants. The results show that two promising binders F5 and G3 variants with highest

affinities in Tris buffer. (50mM Tris, 300mM NaCl) were identified. Dissociation constants of the binders were in nanomolar ratio, which is considered as a very strong binding in nature. According to the results from nanoDSF measurements of the melting temperatures of chosen variants and data from dynamic light scattering, both 57aBi scaffold-derived binders F5 and G3 have high thermal stability (51°C for F5 and 58°C for G3 in Tris buffer) and the level of aggregation was very low.

However, for engineering and development of high-affinity binders against IL-10, candidate under PDB ID 4PSF, currently called 57aBi, was chosen. We also worked with the second scaffold candidate 1N3Y in further selection of binders against IL-9R α . The scaffold was named 57bBi. Both 57aBi and 57bBi scaffolds provide robust structures for development of non-globulin small protein binders. Due to their high thermostabilities and human origin, thus protein variants derived from these scaffolds may be used in future as the drugs for clinical use which will be stable at human body temperature and will not potentiate of immune responses. In comparison, previously mentioned Streptococcal-based ABD scaffold proteins or Affibody-based binding variants with Staphylococcal origin can increase the risk of inflammatory responses after their application into the organism [63, 80].

4.2 Development of bispecific binder signalling via IL-28 receptor

In this study based on Kolarova et al, [150] we aimed to design bivalent binder with specificity to the both IL-28 receptor subunits, IL-28R1 and IL-10R2. Engineered protein binder should mimic biological function of its natural ligand IFN- λ . As signalization triggered by these type of INFs has significant protection role in viral infections [40]. We decided to enhance the signalisation by unnatural bispecific ligand. In case of failure of signalling capabilities of IL-28R natural interferon ligands, our engineered binder can act as backup option how to avoid the dysregulation of the immune system after viral infection and prevent the development of associated diseases. Our hypothesis, i.e. the possibility to use small bispecific scaffold-based binder to trigger the signalization was also supported by similar studies where bispecific antibodies and antibody-drug conjugates were successfully used in cancer therapies. Several drugs and dozens others based on this concept are in various phases of the clinical development or have already been approved by FDA agency. Recently, well reviewed in [153].

Our strategy of the bispecific binder development was divided into two different approaches – to develop two binders independently and then connect them via a flexible protein linker or develop binder based on one scaffold molecule with two mutable patches. For the second purpose was chosen our-designed 57aBi scaffold which can be mutated independently on C- or N- terminus, while these mutations do not lead to disruption of the scaffold structure [149].

In the beginning, we created combinatorial libraries of the five different scaffolds. Used scaffolds and their secondary structures are displayed in Figure 10. 57aBi scaffold (previously called ProBi) was randomized on both termini, so two different combinatorial libraries of this scaffold were created. Libraries were then selected by four rounds of yeast display separately against IL-28R1 and IL-10R2. Recombinant receptors subunits, especially their extracellular domains were produced in *Drosophila* S2 expression system. Both subunits were expressed in soluble form and were purified by two-step process where initial affinity chromatography was followed by size exclusion chromatography. This purification process guaranteed high purity and homogeneity of the extracellular parts of receptor.

After four rounds of the yeast display selection, we obtained the population of the binders recognising receptor subunits only based on 57aBi scaffold (both C- and N- termini randomized variants), Sso7d scaffold and Kan-Nfr scaffold. Sso7d is very small, only 7 kDa ultra-stable scaffold with origin from hyper thermophilic *Sulfolobus solfataricus* [154]. Kan-Nfr is a new 9 kDa protein scaffold developed at the Weizmann Institute of Science in Israel, specifically designed for yeast display selection [127]. Both, Sso7d and Kan-Nfr were kindly provided by our colleagues from Protein-Protein Interaction laboratory of Weizman Institute of Science in Israel. Knotin and GP2 scaffolds, both with randomized positions in loops, were excluded from the next screening for IFN- λ mimicking protein because we did not get satisfactory population of binders after yeast display selection. 57aBi, Kan-Nfr and Sso7d Affitin scaffolds with randomization positions on helices or β – sheets motifs have been shown to have a greater binding preference to IL-28R structure. Strategy to use 5 different scaffolds proved to be very important and beneficial for our intent. Each scaffold provides unique interface for randomization. This also supports our previous work with novel scaffold molecules development and thus expand the platform of successfully used scaffolds such as Anticalin or DARPin.

Binders pre-selected in previous yeast display step were then used for the creation of the five libraries of bivalent binder constructs, that were able to simultaneously bind both subunits of IL-28 receptor. Firstly, the fusions of the best pre-selected binders derived from Sso7d and Kan-Nfr scaffolds were created by their linkage via designed protein linker resulting in creation of four new bivalent binder libraries called Bibi – A, B, C, D. The fifth bivalent binder library called Probi-NC was based on independently mutated patches of 57aBi scaffold, where one patch obtained library with affinity to IL-28R1 and the second to IL-10R2. New constructs of the bivalent binder libraries were tested to bind both receptors subunits at the same time using flow cytometry (Figure 11). 100 000 variants of each library that simultaneously bind both receptor subunits (i.e. variants that were positive for both fluorophore) signals were sorted and screened for their signalling potential via IL-28R.

Final signalization study of the bivalent binders was done by flow cytometer and specific phosphorylation of Tyrosine site 701 of STAT 1 molecule was determined. STAT 1 is normally phosphorylated as a product of Jak kinase activity after binding of the IFN- λ to IL-28 receptor [155]. Assay was performed on human HeLa cells presenting both IL-28 receptor subunits on their surface. To avoid time and material consumption, we decided to first display binders on the surface of the *S. cerevisiae* cells. Those protein variants, which were able to trigger signalization were then purified and tested again to trigger JAK-STAT signalization. Figure 12 shows the comparison between signalization via natural IFN- λ , BiBi-A1 and ProBi-P5 variants displayed on yeast cell or as purified proteins. These variants showed in form of purified protein the highest stability, solubility and low aggregation. Level of signalization via purified proteins is comparable with cell-presented variants. This validates our designed yeast-presenting protein method as powerful well-set screening platform for selection of signalling bivalent binders.

As the final step, we evaluated expression of 10 genes triggered after signalling through IL-28 receptor, specifically MX1, OAS1, OAS3, OASL, IFIT1, IFIT3, IFI6, IFIH1, BST2 and OASL, to be known as over-expressed after IFN- λ signalling [156]. Evaluation was performed by RT-qPCR in HaCaT cells transfected with DNA of both receptor subunits. HaCaT cell system proved to be more suitable for expression of IL-28 receptor than transfected HeLa cells. First, cells were treated with natural ligand IFN- λ 1 as positive control and then with BiBi-A1 and ProBi-P5 purified proteins. To sum up, expression of mentioned genes was induced by both novel bispecific binders,

with BiBi-A1 showing stronger stimulation (Figure 13A). Due to this fact, we repeated the experiment with BiBi-A1 binder only, set in different concentrations. Results from Figure 13B demonstrates that although the signalling followed by activation of gene expression of mentioned genes is initiated after adding BiBi-A1 bivalent binder, expression is at much lower level than after stimulation by natural IFN- λ 1 ligand. To sum up binders' affinities and signalling capacity need to be increased, their production and stability optimized.

Nevertheless, we presented a proof of concept for development of bispecific binders also based on our own-designed scaffold molecule 57aBi and most importantly, powerful platform for their selection. Unfortunately, it is not always certain, that unnatural ligand will modulate the biological activity due to its binding to the molecular target. Another possible optimization in this approach could be small modification of our existing bivalent binders by secondary mutagenesis tools to enhance their signalling potential. For example, Karlsson et al, edited one domain of bivalent protein with an already existing affinity to two viral oncoproteins to develop even more stronger binder to human papillomavirus. Such binder can be used for treatment of chronic infection caused by viruses [157].

4.3 Selection of high-specific binders against IL-9 receptor α subunit

The basic criterion for the evaluation of the quality of antibody or protein binders is their high affinity to their molecular targets. There are protein binders based on scaffolds that have incredibly strong binding affinity to their targets. For example, Lindborg et al, engineered dimeric Affibody molecule that bound to its target staphylococcal protein A with an estimated affinity 16 pM [158]. Another, more recent example is selection of peptide binder with affinity to SARS-CoV-2 Spike receptor binding. Dissociation constant of the binding was 750 pM [159].

Although the high affinity is very important parameter for binding, specificity is often underestimated and even more important. The effect of lower affinity protein binders or antibodies can still be modulated by increasing their concentration. On the other hand, once low specificity is set, binder can interact with any molecule it comes into closer contact and becomes useless. Hereby, in study Huliciak et al, we demonstrate the strategy for development of high specificity protein binders recognising specific subunit of IL-9 receptor.

Indeed, there were attempts for direct blocking of IL-9 by antibodies. In 2013, MEDI-528 monoclonal antibody recognising this interleukin was used in asthma models for inhibition of mucus production during asthma disease in adult patients. The results of this study were not satisfactory. Addition of MEDI-528 antibody has no effect in mucus production and asthma treatment of the patients [160]. We can discuss, that monoclonal antibody probably binds IL-9 in region which is not responsible for receptor binding and do not block interaction between IL-9 and receptor. According to this, we decided to aim directly to the receptor, especially onto its extracellular domain using our protein binders derived from scaffold molecules.

IL-9 belongs to common γ -chain family. That means, that all members of this family are sharing non-specific receptor and have one or two specific receptor subunit [42]. As we wanted to modulate the only IL-9 initiated signalling, we aimed on its specific subunit IL-9R α .

For the purpose of selection of highly specific protein binders we chose two protein scaffolds designed in previous study [149]. 57aBi scaffold, 15 kDa helical domain of chromatin remodelling complex PIH1D1 (PDB ID: 4PSF) and 22 kDa 57bBi integrin domain previously designed under PDB ID: 1N3Y [161, 162]. Secondary structures of scaffolds and their amino acid sequences are displayed in Figure 14. Combinatorial libraries of the scaffolds were synthesized using NNK strategy. Library constructs contained N-terminal Strep II purification tag and C-terminal detection c-myc tag. DNA of these constructs of the scaffolds was then transcribed and translated *in vitro* in lysate of *E. coli* and selected in five rounds of ribosome display against extracellular domain of specific IL-9R α subunit.

Of note, we performed so called subtractive panning before each round of the ribosome display to avoid the presence of the non-specific binders. We have adopted this method from Rothe et al, where the method of subtractive panning was successfully used in selection of human anti-CD28 single chain variable fragments of antibodies [163]. The principle of the method is that you incubate combinatorial libraries of proteins with various non-specific targets before specific selection by ribosome display. In our case, we used bovine serum albumin (BSA) protein. Because we perform ribosome display selections in 96 microplate wells it is enough to simply pipet library into the next well for another negative pre-selection by subtractive panning. This system has great potential for further automation, as well. You can cover 96 wells of microplates with different mixtures of non-specific targets and pre-select your library to high specificity. However, as

mentioned below, we can dramatically improve specificity much easier by implementation of one round of competitive yeast display. Altogether the methodology of subtractive panning should be mainly used for specificity tuning after selection process as negative targets use molecules with similar structures to discriminate the binding of the novel binders to targets with structural similarity.

Another innovation how to increase specificity of our final protein binders is based on utilization of protein-free blocking reagents. In standard ribosome display protocol, hydrophobic surface of the plastic microplate is blocked by protein-based BSA reagent [135]. As an alternative to BSA, proteins of skim milk or fish-gelatine proteins are commonly used [164, 165]. First non-protein blocking reagent was used in 1993 and were based on Polyvinylpyrrolidone (PVP). Currently, there are many commercial protein-free reagents available on the market.

After five rounds of ribosome display, we performed an ELISA specificity screening test. 16 binders derived from the both 57aBi and 57bBi scaffolds were tested for binding to IL-9 specific receptor subunit α and to BSA as negative control. Figure 16A shows binding level and comparison of the binding to IL-9 receptor subunit and to BSA. Protein variants recognise specific subunit of the receptor in the first place, but a residual binding to BSA in some variants is still present. Due to this reason, we decided to continue selections but with a little slightly modified strategy.

Combinatorial libraries after 5th round of ribosome selection were cloned into yeast vector and one round of the competitive yeast display was performed. Yeast cell displaying protein variants on their surface were competing for IL-9R α in a low, only 100 nM concentration. The competitive display was based on the fact that a single yeast cell can display up to hundred thousand copies of the variant on its surface [123]. Only the yeast cells with the best binder expression level which show the highest affinities towards fluorescently-labelled IL-9R α are detected and sorted using flow cytometry assay (Figure 15). Implementation of the yeast display selection method into this methodical platform has another advantage as only properly folded protein variants expressed by yeast system in soluble form can be transported and displayed on the cell wall [123]. By implementing yeast display, we excluded variants which were not fully-translated but passed through previous ribosome display selection rounds.

After yeast display, DNA of selected combinatorial library was isolated and re-cloned again into vector suitable for ribosome display. Additional 6th round of ribosome display was performed, preceded by three rounds of subtractive panning instead of the classical one-step subtractive panning with BSA. From the point of view of binding kinetic, it makes more sense to us to perform 3 fast pre-selection subtractive panning procedures before ribosome display selection.

After the yeast display selection and the sixth round of ribosome display, selected variants were again tested by ELISA specificity test in same conditions as after 5th round of ribosome display. However, in this testing we also coated another negative control, non-specific subunit of IL-9R-common γ chain. Figure 16B shows, that selected binders have significant specificity to IL-9 receptor α subunit while binding to BSA is on the background level. Small group of variants reports the binding to non-specific receptor subunit γ chain, but in comparison with binding to specific receptor subunit is it negligible.

To estimate the affinities of the selected binders, one binder derived from the both scaffolds was chosen for microscale thermophoresis measurement. Figure 17 represents the MST curves of the 57 aBi-D14 and 57bBi –D06, which proved their binding to IL-9R α . We estimated the affinities in micromolar and nanomolar ratio.

However, the biological affinity of the natural IL-9 ligand to IL-9 receptor is much higher, about 100 pM [166], our selected variants can be further matured to obtain higher affinity by secondary mutagenesis tools, for example by Error-prone PCR. One of example, when authors shifted the binding affinity from nanomolar to picomolar range using the Error-prone approach is the development of Anticalin-based protein binder targeting human prostate-specific membrane antigen (PSMA) [167]. We believe that with improved affinities and lasting set specificity level can be our protein binders very promising in their further medical applications.

Finally, here we present our concept of the methodical platform for creation of high specific binders. As initial step is advantageous to use ribosome display selection which is suitable for selection of the combinatorial libraries with the highest theoretical complexity [111]. Critical step was implementation of the yeast display after the 5th round of ribosome display selection. My suggestion for next selection process is that yeast display should be introduced after the 2nd round of ribosome display when is certain the complexity of the library can be covered by yeast display

selection. By implementation of the yeast display in initial rounds of procedure we discriminate the insoluble, bad folded and not fully-translated variants in further selections.

Selected binders produced by these unconventional combination of cell-free and surface-based display methods should serve for next analyses to find out their potential in inhibition of the signalling pathway triggered by IL-9 connected with development of asthma and respiratory diseases. Protein binders might as well serve as detection molecules of overexpressed IL-9 receptors as disease markers. There is well-known methodical approach for generation of fluorescent proteins by using non-canonical amino acids. Non-canonical amino acids provided modified side chains that could be incorporated into protein binders sequence. Fluorescent molecules of various wave lengths could be easily attached to the side chains via so called click chemistry. Elegance of use of non-canonical amino acid is that it can be easily incorporated into protein scaffold sequence during its expression in bacterial expression systems [168].

5 Conclusions

This dissertation thesis describes the development of novel non-antibody small protein binders derived from originally developed scaffold protein molecules targeting medically important cytokines or their receptors.

We successfully introduced two novel scaffold protein molecules called 57aBi and 57bBi. Ten amino acids of each scaffold were chosen for randomization. 57aBi scaffold showed its ability to be mutated on two different surface patches so that it is potentially able to bind two targets. The scaffold concept was proven by selection high affinity protein binders against human interleukin 10 (IL-10) cytokine, where the combinatorial library of the 57aBi scaffold was selected by ribosome display. The potential ability to bind two target molecules by 57aBi was proven by developing bivalent binder mimicking the function of the human IFN- λ 1 cytokine. Scaffold-based binders were trained to interact with both receptor subunits required to trigger the JAK-STAT signalization pathway.

Finally, we extended the available pipelines of the directed evolution by combining cell-free ribosome display and cell-based yeast display. This methodologically unconventional combination of these two selection methods and their thoughtful modifications into one integrated pipeline enabled us to select binders of human IL-9 receptor subunit alpha of sub-micromolar affinity. The combination of both selection methods into one pipeline was motivated by the need to maximize specificity to the target protein. In the project, we succeeded in developing specific IL-9R α binders derived from both 57aBi and 57bBi scaffolds.

6 References

1. Smith, G. P. (1985) Filamentous fusion phage: novel expression vectors that display cloned antigens on the virion surface, *Science*. **228**, 1315-7.
2. Mizel, S. B. & Farrar, J. J. (1979) Revised nomenclature for antigen-nonspecific T-cell proliferation and helper factors, *Cell Immunol.* **48**, 433-6.
3. Kasakura, S. & Lowenstein, L. (1965) A factor stimulating DNA synthesis derived from the medium of leukocyte cultures, *Nature*. **208**, 794-5.
4. Lagoo, A., Tseng, C. K. & Sell, S. (1990) Interleukin 2 produced by activated B lymphocytes acts as an autocrine proliferation-inducing lymphokine, *Cytokine*. **2**, 272-9.
5. Kubin, M., Kamoun, M. & Trinchieri, G. (1994) Interleukin 12 synergizes with B7/CD28 interaction in inducing efficient proliferation and cytokine production of human T cells, *J Exp Med*. **180**, 211-22.
6. Zwicker, S., Hattinger, E., Bureik, D., Batycka-Baran, A., Schmidt, A., Gerber, P. A., Rothenfusser, S., Gilliet, M., Ruzicka, T. & Wolf, R. (2017) Th17 micro-milieu regulates NLRP1-dependent caspase-5 activity in skin autoinflammation, *PLoS One*. **12**, e0175153.
7. Zwingenberger, K., Harms, G., Vergetti de Siqueira, J. G., Correia Dacal, A. R., Jansen-Rossek, R., Bienzle, U. & Feldmeier, H. (1989) T cell phenotype alterations in hepatosplenic schistosomiasis mansoni normalize after chemotherapy, *Immunobiology*. **179**, 342-52.
8. Zychlinsky, A., Fitting, C., Cavaillon, J. M. & Sansonetti, P. J. (1994) Interleukin 1 is released by murine macrophages during apoptosis induced by *Shigella flexneri*, *J Clin Invest*. **94**, 1328-32.
9. Nagata, Y., Moriguchi, T., Nishida, E. & Todokoro, K. (1997) Activation of p38 MAP kinase pathway by erythropoietin and interleukin-3, *Blood*. **90**, 929-34.
10. Wang, L. S., Liu, H. J., Broxmeyer, H. E. & Lu, L. (2000) Interleukin-11 enhancement of VLA-5 mediated adhesion of CD34+ cells from cord blood to fibronectin is associated with the PI-3 kinase pathway, *In Vivo*. **14**, 331-7.
11. Zwicker, S., Martinez, G. L., Bosma, M., Gerling, M., Clark, R., Majster, M., Soderman, J., Almer, S. & Bostrom, E. A. (2015) Interleukin 34: a new modulator of human and experimental inflammatory bowel disease, *Clin Sci (Lond)*. **129**, 281-90.
12. Tanuma, N., Shima, H., Nakamura, K. & Kikuchi, K. (2001) Protein tyrosine phosphatase epsilonC selectively inhibits interleukin-6- and interleukin- 10-induced JAK-STAT signaling, *Blood*. **98**, 3030-4.
13. Zhu, Y., Mao, H., Peng, G., Zeng, Q., Wei, Q., Ruan, J. & Huang, J. (2021) Effect of JAK-STAT pathway in regulation of fatty liver hemorrhagic syndrome in chickens, *Anim Biosci*. **34**, 143-153.

14. Zwerina, K., Koenders, M., Hueber, A., Marijnissen, R. J., Baum, W., Heiland, G. R., Zaiss, M., McLnnes, I., Joosten, L., van den Berg, W., Zwerina, J. & Schett, G. (2012) Anti IL-17A therapy inhibits bone loss in TNF-alpha-mediated murine arthritis by modulation of the T-cell balance, *Eur J Immunol.* **42**, 413-23.
15. Yao, X., Kong, Q., Xie, X., Wang, J., Li, N., Liu, Y., Sun, B., Li, Y., Wang, G., Li, W., Qu, S., Zhao, H., Wang, D., Liu, X., Zhang, Y., Mu, L. & Li, H. (2014) Neutralization of interleukin-9 ameliorates symptoms of experimental autoimmune myasthenia gravis in rats by decreasing effector T cells and altering humoral responses, *Immunology.* **143**, 396-405.
16. Fu, S. & Lin, J. (2018) Blocking Interleukin-6 and Interleukin-8 Signaling Inhibits Cell Viability, Colony-forming Activity, and Cell Migration in Human Triple-negative Breast Cancer and Pancreatic Cancer Cells, *Anticancer Res.* **38**, 6271-6279.
17. Rahal, O. M., Wolfe, A. R., Mandal, P. K., Larson, R., Tin, S., Jimenez, C., Zhang, D., Horton, J., Reuben, J. M., McMurray, J. S. & Woodward, W. A. (2018) Blocking Interleukin (IL)4- and IL13-Mediated Phosphorylation of STAT6 (Tyr641) Decreases M2 Polarization of Macrophages and Protects Against Macrophage-Mediated Radioresistance of Inflammatory Breast Cancer, *Int J Radiat Oncol Biol Phys.* **100**, 1034-1043.
18. Brocker, C., Thompson, D., Matsumoto, A., Nebert, D. W. & Vasiliou, V. (2010) Evolutionary divergence and functions of the human interleukin (IL) gene family, *Hum Genomics.* **5**, 30-55.
19. Renauld, J. C. (2003) Class II cytokine receptors and their ligands: key antiviral and inflammatory modulators, *Nat Rev Immunol.* **3**, 667-76.
20. Walter, M. R. & Nagabhushan, T. L. (1995) Crystal structure of interleukin 10 reveals an interferon gamma-like fold, *Biochemistry.* **34**, 12118-25.
21. Logsdon, N. J., Deshpande, A., Harris, B. D., Rajashankar, K. R. & Walter, M. R. (2012) Structural basis for receptor sharing and activation by interleukin-20 receptor-2 (IL-20R2) binding cytokines, *Proc Natl Acad Sci U S A.* **109**, 12704-9.
22. Zdanov, A. (2004) Structural features of the interleukin-10 family of cytokines, *Curr Pharm Des.* **10**, 3873-84.
23. Ouyang, W., Rutz, S., Crellin, N. K., Valdez, P. A. & Hymowitz, S. G. (2011) Regulation and functions of the IL-10 family of cytokines in inflammation and disease, *Annu Rev Immunol.* **29**, 71-109.
24. Akdis, M., Burgler, S., Cramer, R., Eiwegger, T., Fujita, H., Gomez, E., Klunker, S., Meyer, N., O'Mahony, L., Palomares, O., Rhyner, C., Ouaked, N., Schaffartzik, A., Van De Veen, W., Zeller, S., Zimmermann, M. & Akdis, C. A. (2011) Interleukins, from 1 to 37, and interferon-gamma: receptors, functions, and roles in diseases, *J Allergy Clin Immunol.* **127**, 701-21 e1-70.
25. Fiorentino, D. F., Bond, M. W. & Mosmann, T. R. (1989) Two types of mouse T helper cell. IV. Th2 clones secrete a factor that inhibits cytokine production by Th1 clones, *J Exp Med.* **170**, 2081-95.

26. El Kasmi, K. C., Smith, A. M., Williams, L., Neale, G., Panopoulos, A. D., Watowich, S. S., Hacker, H., Foxwell, B. M. & Murray, P. J. (2007) Cutting edge: A transcriptional repressor and corepressor induced by the STAT3-regulated anti-inflammatory signaling pathway, *J Immunol.* **179**, 7215-9.
27. Zissler, U. M., Jakwerth, C. A., Guerth, F. M., Pechtold, L., Aguilar-Pimentel, J. A., Dietz, K., Suttner, K., Piontek, G., Haller, B., Hajdu, Z., Schiemann, M., Schmidt-Weber, C. B. & Chaker, A. M. (2018) Early IL-10 producing B-cells and coinciding Th/Tr17 shifts during three year grass-pollen AIT, *EBioMedicine.* **36**, 475-488.
28. de Waal Malefyt, R., Haanen, J., Spits, H., Roncarolo, M. G., te Velde, A., Figdor, C., Johnson, K., Kastelein, R., Yssel, H. & de Vries, J. E. (1991) Interleukin 10 (IL-10) and viral IL-10 strongly reduce antigen-specific human T cell proliferation by diminishing the antigen-presenting capacity of monocytes via downregulation of class II major histocompatibility complex expression, *J Exp Med.* **174**, 915-24.
29. Eskdale, J., Kube, D., Tesch, H. & Gallagher, G. (1997) Mapping of the human IL10 gene and further characterization of the 5' flanking sequence, *Immunogenetics.* **46**, 120-8.
30. Saraiva, M. & O'Garra, A. (2010) The regulation of IL-10 production by immune cells, *Nat Rev Immunol.* **10**, 170-81.
31. Pestka, S., Krause, C. D., Sarkar, D., Walter, M. R., Shi, Y. & Fisher, P. B. (2004) Interleukin-10 and related cytokines and receptors, *Annu Rev Immunol.* **22**, 929-79.
32. Zimmermann, O., Homann, J. M., Bangert, A., Muller, A. M., Hristov, G., Goeser, S., Wiehe, J. M., Zittrich, S., Rottbauer, W., Torzewski, J., Pfitzer, G., Katus, H. A. & Kaya, Z. (2012) Successful use of mRNA-nucleofection for overexpression of interleukin-10 in murine monocytes/macrophages for anti-inflammatory therapy in a murine model of autoimmune myocarditis, *J Am Heart Assoc.* **1**, e003293.
33. Peng, H., Wang, W., Zhou, M., Li, R., Pan, H. F. & Ye, D. Q. (2013) Role of interleukin-10 and interleukin-10 receptor in systemic lupus erythematosus, *Clin Rheumatol.* **32**, 1255-66.
34. Kruger-Krasagakes, S., Krasagakis, K., Garbe, C., Schmitt, E., Huls, C., Blankenstein, T. & Diamantstein, T. (1994) Expression of interleukin 10 in human melanoma, *Br J Cancer.* **70**, 1182-5.
35. Lech-Maranda, E., Baseggio, L., Biennu, J., Charlot, C., Berger, F., Rigal, D., Warzocha, K., Coiffier, B. & Salles, G. (2004) Interleukin-10 gene promoter polymorphisms influence the clinical outcome of diffuse large B-cell lymphoma, *Blood.* **103**, 3529-34.
36. Vairaktaris, E., Yapijakis, C., Serefolou, Z., Derka, S., Vassiliou, S., Nkenke, E., Vylliotis, A., Spyridonidou, S., Neukam, F. W., Schlegel, K. A. & Patsouris, E. (2008) The interleukin-10 (-1082A/G) polymorphism is strongly associated with increased risk for oral squamous cell carcinoma, *Anticancer Res.* **28**, 309-14.
37. Sheppard, P., Kindsvogel, W., Xu, W., Henderson, K., Schlutsmeyer, S., Whitmore, T. E., Kuestner, R., Garrigues, U., Birks, C., Roraback, J., Ostrander, C., Dong, D., Shin, J., Presnell, S., Fox, B., Haldeman, B., Cooper, E., Taft, D., Gilbert, T., Grant, F. J., Tackett, M., Krivan, W., McKnight, G.,

- Clegg, C., Foster, D. & Klucher, K. M. (2003) IL-28, IL-29 and their class II cytokine receptor IL-28R, *Nat Immunol.* **4**, 63-8.
38. Kempuraj, D., Donelan, J., Frydas, S., Iezzi, T., Conti, F., Boucher, W., Papadopoulou, N. G., Madhappan, B., Letourneau, L., Cao, J., Sabatino, G., Meneghini, F., Stellin, L., Verna, N., Riccioni, G. & Theoharides, T. C. (2004) Interleukin-28 and 29 (IL-28 and IL-29): new cytokines with anti-viral activities, *Int J Immunopathol Pharmacol.* **17**, 103-6.
39. Zhou, J. H., Wang, Y. N., Chang, Q. Y., Ma, P., Hu, Y. & Cao, X. (2018) Type III Interferons in Viral Infection and Antiviral Immunity, *Cell Physiol Biochem.* **51**, 173-185.
40. Morrow, M. P., Pankhong, P., Laddy, D. J., Schoenly, K. A., Yan, J., Cisper, N. & Weiner, D. B. (2009) Comparative ability of IL-12 and IL-28B to regulate Treg populations and enhance adaptive cellular immunity, *Blood.* **113**, 5868-77.
41. Morrow, M. P., Yan, J., Pankhong, P., Shedlock, D. J., Lewis, M. G., Talbott, K., Toporovski, R., Khan, A. S., Sardesai, N. Y. & Weiner, D. B. (2010) IL-28B/IFN-lambda 3 drives granzyme B loading and significantly increases CTL killing activity in macaques, *Mol Ther.* **18**, 1714-23.
42. Overwijk, W. W. & Schluns, K. S. (2009) Functions of gammaC cytokines in immune homeostasis: current and potential clinical applications, *Clin Immunol.* **132**, 153-65.
43. Malek, T. R. (2008) The biology of interleukin-2, *Annu Rev Immunol.* **26**, 453-79.
44. Mitchell, D. M., Ravkov, E. V. & Williams, M. A. (2010) Distinct roles for IL-2 and IL-15 in the differentiation and survival of CD8⁺ effector and memory T cells, *J Immunol.* **184**, 6719-30.
45. Levin, A. M., Bates, D. L., Ring, A. M., Krieg, C., Lin, J. T., Su, L., Moraga, I., Raeber, M. E., Bowman, G. R., Novick, P., Pande, V. S., Fathman, C. G., Boyman, O. & Garcia, K. C. (2012) Exploiting a natural conformational switch to engineer an interleukin-2 'superkine', *Nature.* **484**, 529-33.
46. Miki, K., Nagaoka, K., Harada, M., Hayashi, T., Jinguji, H., Kato, Y. & Maekawa, R. (2014) Combination therapy with dendritic cell vaccine and IL-2 encapsulating polymeric micelles enhances intra-tumoral accumulation of antigen-specific CTLs, *Int Immunopharmacol.* **23**, 499-504.
47. Beriou, G., Bradshaw, E. M., Lozano, E., Costantino, C. M., Hastings, W. D., Orban, T., Elyaman, W., Khoury, S. J., Kuchroo, V. K., Baecher-Allan, C. & Hafler, D. A. (2010) TGF-beta induces IL-9 production from human Th17 cells, *J Immunol.* **185**, 46-54.
48. Perumal, N. B. & Kaplan, M. H. (2011) Regulating Il9 transcription in T helper cells, *Trends Immunol.* **32**, 146-50.
49. Mock, B. A., Krall, M., Kozak, C. A., Nesbitt, M. N., McBride, O. W., Renauld, J. C. & Van Snick, J. (1990) IL9 maps to mouse chromosome 13 and human chromosome 5, *Immunogenetics.* **31**, 265-70.

50. Renauld, J. C., Druez, C., Kermouni, A., Houssiau, F., Uyttenhove, C., Van Roost, E. & Van Snick, J. (1992) Expression cloning of the murine and human interleukin 9 receptor cDNAs, *Proc Natl Acad Sci U S A.* **89**, 5690-4.
51. Kearley, J., Erjefalt, J. S., Andersson, C., Benjamin, E., Jones, C. P., Robichaud, A., Pegorier, S., Brewah, Y., Burwell, T. J., Bjermer, L., Kiener, P. A., Kolbeck, R., Lloyd, C. M., Coyle, A. J. & Humbles, A. A. (2011) IL-9 governs allergen-induced mast cell numbers in the lung and chronic remodeling of the airways, *Am J Respir Crit Care Med.* **183**, 865-75.
52. Nowak, E. C., Weaver, C. T., Turner, H., Begum-Haque, S., Becher, B., Schreiner, B., Coyle, A. J., Kasper, L. H. & Noelle, R. J. (2009) IL-9 as a mediator of Th17-driven inflammatory disease, *J Exp Med.* **206**, 1653-60.
53. Goswami, R. & Kaplan, M. H. (2011) A brief history of IL-9, *J Immunol.* **186**, 3283-8.
54. Demoulin, J. B., Louahed, J., Dumoutier, L., Stevens, M. & Renauld, J. C. (2003) MAP kinase activation by interleukin-9 in lymphoid and mast cell lines, *Oncogene.* **22**, 1763-70.
55. Richard, M., Louahed, J., Demoulin, J. B. & Renauld, J. C. (1999) Interleukin-9 regulates NF-kappaB activity through BCL3 gene induction, *Blood.* **93**, 4318-27.
56. Wu, B., Huang, C., Kato-Maeda, M., Hopewell, P. C., Daley, C. L., Krensky, A. M. & Clayberger, C. (2008) IL-9 is associated with an impaired Th1 immune response in patients with tuberculosis, *Clin Immunol.* **126**, 202-10.
57. Chen, X., Wang, X., Zhang, Z., Chen, Y. & Wang, C. (2021) Role of IL-9, IL-2RA, and IL-2RB genetic polymorphisms in coronary heart disease, *Herz.* **46**, 558-566.
58. Li, L., Huang, S., Wang, H., Chao, K., Ding, L., Feng, R., Qiu, Y., Feng, T., Zhou, G., Hu, J. F., Chen, M. & Zhang, S. (2018) Cytokine IL9 Triggers the Pathogenesis of Inflammatory Bowel Disease Through the miR21-CLDN8 Pathway, *Inflamm Bowel Dis.* **24**, 2211-2223.
59. Vieyra-Garcia, P. A., Wei, T., Naym, D. G., Fredholm, S., Fink-Puches, R., Cerroni, L., Odum, N., O'Malley, J. T., Gniadecki, R. & Wolf, P. (2016) STAT3/5-Dependent IL9 Overexpression Contributes to Neoplastic Cell Survival in Mycosis Fungoides, *Clin Cancer Res.* **22**, 3328-39.
60. Gebauer, M. & Skerra, A. (2009) Engineered protein scaffolds as next-generation antibody therapeutics, *Curr Opin Chem Biol.* **13**, 245-55.
61. Lebl, M. (1999) Solid-phase synthesis of combinatorial libraries, *Curr Opin Drug Discov Devel.* **2**, 385-95.
62. McCullum, E. O., Williams, B. A., Zhang, J. & Chaput, J. C. (2010) Random mutagenesis by error-prone PCR, *Methods Mol Biol.* **634**, 103-9.

63. Ahmad, J. N., Li, J., Biedermannova, L., Kuchar, M., Sipova, H., Semeradtova, A., Cerny, J., Petrokova, H., Mikulecky, P., Polinek, J., Stanek, O., Vondrasek, J., Homola, J., Maly, J., Osicka, R., Sebo, P. & Maly, P. (2012) Novel high-affinity binders of human interferon gamma derived from albumin-binding domain of protein G, *Proteins*. **80**, 774-89.
64. Khan, J. A., Camac, D. M., Low, S., Tebben, A. J., Wensel, D. L., Wright, M. C., Su, J., Jenny, V., Gupta, R. D., Ruzanov, M., Russo, K. A., Bell, A., An, Y., Bryson, J. W., Gao, M., Gambhire, P., Baldwin, E. T., Gardner, D., Cavallaro, C. L., Duncia, J. V. & Hynes, J., Jr. (2015) Developing Adnectins that target SRC co-activator binding to PXR: a structural approach toward understanding promiscuity of PXR, *J Mol Biol*. **427**, 924-942.
65. Lendel, C., Dogan, J. & Hard, T. (2006) Structural basis for molecular recognition in an affibody:affibody complex, *J Mol Biol*. **359**, 1293-304.
66. Tiede, C., Tang, A. A., Deacon, S. E., Mandal, U., Nettleship, J. E., Owen, R. L., George, S. E., Harrison, D. J., Owens, R. J., Tomlinson, D. C. & McPherson, M. J. (2014) Adhiron: a stable and versatile peptide display scaffold for molecular recognition applications, *Protein Eng Des Sel*. **27**, 145-55.
67. Dauner, M., Eichinger, A., Lucking, G., Scherer, S. & Skerra, A. (2018) Reprogramming Human Siderocalin To Neutralize Petrobactin, the Essential Iron Scavenger of Anthrax Bacillus, *Angew Chem Int Ed Engl*. **57**, 14619-14623.
68. Seeger, M. A., Zbinden, R., Flutsch, A., Gutte, P. G., Engeler, S., Roschitzki-Voser, H. & Grutter, M. G. (2013) Design, construction, and characterization of a second-generation DARPin library with reduced hydrophobicity, *Protein Sci*. **22**, 1239-57.
69. Lee, A. W., Deruaz, M., Lynch, C., Davies, G., Singh, K., Alenazi, Y., Eaton, J. R. O., Kawamura, A., Shaw, J., Proudfoot, A. E. I., Dias, J. M. & Bhattacharya, S. (2019) A knottin scaffold directs the CXC-chemokine-binding specificity of tick evasins, *J Biol Chem*. **294**, 11199-11212.
70. Eliseev, I. E., Yudenko, A. N., Vysochinskaya, V. V., Svirina, A. A., Evstratyeva, A. V., Drozhzhachih, M. S., Krendeleva, E. A., Vladimirova, A. K., Nemankin, T. A., Ekimova, V. M., Ulitin, A. B., Lomovskaya, M. I., Yakovlev, P. A., Bukatin, A. S., Knyazev, N. A., Moiseenko, F. V. & Chakchir, O. B. (2018) Crystal structures of a llama VHH antibody BCD090-M2 targeting human ErbB3 receptor, *PLoS Res*. **7**, 57.
71. Nilvebrant, J. & Hober, S. (2013) The albumin-binding domain as a scaffold for protein engineering, *Comput Struct Biotechnol J*. **6**, e201303009.
72. Zadavec, P., Mareckova, L., Petrokova, H., Hodnik, V., Perisic Nanut, M., Anderluh, G., Strukelj, B., Maly, P. & Berlec, A. (2016) Development of Recombinant *Lactococcus lactis* Displaying Albumin-Binding Domain Variants against Shiga Toxin 1 B Subunit, *PLoS One*. **11**, e0162625.
73. Mareckova, L., Petrokova, H., Osicka, R., Kuchar, M. & Maly, P. (2015) Novel binders derived from an albumin-binding domain scaffold targeting human prostate secretory protein 94 (PSP94), *Protein Cell*. **6**, 774-9.

74. Ren, Z., Zhao, J., Cao, X. & Wang, F. (2022) Tandem fusion of albumin-binding domains promoted soluble expression and stability of recombinant trichosanthin in vitro and in vivo, *Protein Expr Purif.* **200**, 106147.
75. Hohenester, E. & Engel, J. (2002) Domain structure and organisation in extracellular matrix proteins, *Matrix Biol.* **21**, 115-28.
76. Koide, A., Bailey, C. W., Huang, X. & Koide, S. (1998) The fibronectin type III domain as a scaffold for novel binding proteins, *J Mol Biol.* **284**, 1141-51.
77. Lipovsek, D. (2011) Adnectins: engineered target-binding protein therapeutics, *Protein Eng Des Sel.* **24**, 3-9.
78. Emanuel, S. L., Engle, L. J., Chao, G., Zhu, R. R., Cao, C., Lin, Z., Yamniuk, A. P., Hosbach, J., Brown, J., Fitzpatrick, E., Gokemeijer, J., Morin, P., Morse, B. A., Carvajal, I. M., Fabrizio, D., Wright, M. C., Das Gupta, R., Gosselin, M., Cataldo, D., Ryseck, R. P., Doyle, M. L., Wong, T. W., Camphausen, R. T., Cload, S. T., Marsh, H. N., Gottardis, M. M. & Furfine, E. S. (2011) A fibronectin scaffold approach to bispecific inhibitors of epidermal growth factor receptor and insulin-like growth factor-I receptor, *MAbs.* **3**, 38-48.
79. Mamluk, R., Carvajal, I. M., Morse, B. A., Wong, H., Abramowitz, J., Aslanian, S., Lim, A. C., Gokemeijer, J., Storek, M. J., Lee, J., Gosselin, M., Wright, M. C., Camphausen, R. T., Wang, J., Chen, Y., Miller, K., Sanders, K., Short, S., Sperinde, J., Prasad, G., Williams, S., Kerbel, R., Ebos, J., Mutsaers, A., Mendlein, J. D., Harris, A. S. & Furfine, E. S. (2010) Anti-tumor effect of CT-322 as an adnectin inhibitor of vascular endothelial growth factor receptor-2, *MAbs.* **2**, 199-208.
80. Nilsson, B., Moks, T., Jansson, B., Abrahmsen, L., Elmblad, A., Holmgren, E., Henrichson, C., Jones, T. A. & Uhlen, M. (1987) A synthetic IgG-binding domain based on staphylococcal protein A, *Protein Eng.* **1**, 107-13.
81. Lofblom, J., Feldwisch, J., Tolmachev, V., Carlsson, J., Stahl, S. & Frejd, F. Y. (2010) Affibody molecules: engineered proteins for therapeutic, diagnostic and biotechnological applications, *FEBS Lett.* **584**, 2670-80.
82. Malm, M., Bass, T., Gudmundsdotter, L., Lord, M., Frejd, F. Y., Stahl, S. & Lofblom, J. (2014) Engineering of a bispecific affibody molecule towards HER2 and HER3 by addition of an albumin-binding domain allows for affinity purification and in vivo half-life extension, *Biotechnol J.* **9**, 1215-22.
83. Haggblad Sahlberg, S., Spiegelberg, D., Lennartsson, J., Nygren, P., Glimelius, B. & Stenerlow, B. (2012) The effect of a dimeric Affibody molecule (ZEGFR:1907)₂ targeting EGFR in combination with radiation in colon cancer cell lines, *Int J Oncol.* **40**, 176-84.
84. Andersson, M., Ronnmark, J., Arestrom, I., Nygren, P. A. & Ahlborg, N. (2003) Inclusion of a non-immunoglobulin binding protein in two-site ELISA for quantification of human serum proteins without interference by heterophilic serum antibodies, *J Immunol Methods.* **283**, 225-34.

85. Stadler, L. K., Hoffmann, T., Tomlinson, D. C., Song, Q., Lee, T., Busby, M., Nyathi, Y., Gendra, E., Tiede, C., Flanagan, K., Cockell, S. J., Wipat, A., Harwood, C., Wagner, S. D., Knowles, M. A., Davis, J. J., Keegan, N. & Ferrigno, P. K. (2011) Structure-function studies of an engineered scaffold protein derived from Stefin A. II: Development and applications of the SQT variant, *Protein Eng Des Sel.* **24**, 751-63.
86. Al-Enezi, E., Vakurov, A., Eades, A., Ding, M., Jose, G., Saha, S. & Millner, P. (2021) Affimer-Based Europium Chelates Allow Sensitive Optical Biosensing in a Range of Human Disease Biomarkers, *Sensors (Basel).* **21**.
87. Haza, K. Z., Martin, H. L., Rao, A., Turner, A. L., Saunders, S. E., Petersen, B., Tiede, C., Tipping, K., Tang, A. A., Ajayi, M., Taylor, T., Harvey, M., Fishwick, K. M., Adams, T. L., Gaule, T. G., Trinh, C. H., Johnson, M., Breeze, A. L., Edwards, T. A., McPherson, M. J. & Tomlinson, D. C. (2021) RAS-inhibiting biologics identify and probe druggable pockets including an SII-alpha3 allosteric site, *Nat Commun.* **12**, 4045.
88. Flower, D. R., North, A. C. & Sansom, C. E. (2000) The lipocalin protein family: structural and sequence overview, *Biochim Biophys Acta.* **1482**, 9-24.
89. Richter, A., Eggenstein, E. & Skerra, A. (2014) Anticalins: exploiting a non-Ig scaffold with hypervariable loops for the engineering of binding proteins, *FEBS Lett.* **588**, 213-8.
90. Deuschle, F. C., Ilyukhina, E. & Skerra, A. (2021) Anticalin(R) proteins: from bench to bedside, *Expert Opin Biol Ther.* **21**, 509-518.
91. Meining, W. & Skerra, A. (2012) The crystal structure of human alpha(1)-microglobulin reveals a potential haem-binding site, *Biochem J.* **445**, 175-82.
92. Gunnarsson, R., Akerstrom, B., Hansson, S. R. & Gram, M. (2017) Recombinant alpha-1-microglobulin: a potential treatment for preeclampsia, *Drug Discov Today.* **22**, 736-743.
93. Jore, M. M., Johnson, S., Sheppard, D., Barber, N. M., Li, Y. I., Nunn, M. A., Elmlund, H. & Lea, S. M. (2016) Structural basis for therapeutic inhibition of complement C5, *Nat Struct Mol Biol.* **23**, 378-86.
94. Kobe, B. & Kajava, A. V. (2000) When protein folding is simplified to protein coiling: the continuum of solenoid protein structures, *Trends Biochem Sci.* **25**, 509-15.
95. Li, J., Mahajan, A. & Tsai, M. D. (2006) Ankyrin repeat: a unique motif mediating protein-protein interactions, *Biochemistry.* **45**, 15168-78.
96. Steiner, D., Forrer, P. & Pluckthun, A. (2008) Efficient selection of DARPins with sub-nanomolar affinities using SRP phage display, *J Mol Biol.* **382**, 1211-27.
97. Pancer, Z., Amemiya, C. T., Ehrhardt, G. R., Ceitlin, J., Gartland, G. L. & Cooper, M. D. (2004) Somatic diversification of variable lymphocyte receptors in the agnathan sea lamprey, *Nature.* **430**, 174-80.

98. Parizek, P., Kummer, L., Rube, P., Prinz, A., Herberg, F. W. & Pluckthun, A. (2012) Designed ankyrin repeat proteins (DARPin)s as novel isoform-specific intracellular inhibitors of c-Jun N-terminal kinases, *ACS Chem Biol.* **7**, 1356-66.
99. van den Brand, D., van Lith, S. A. M., de Jong, J. M., Gorris, M. A. J., Palacio-Castaneda, V., Couwenbergh, S. T., Goldman, M. R. G., Ebisch, I., Massuger, L. F., Leenders, W. P. J., Brock, R. & Verdurmen, W. P. R. (2020) EpCAM-Binding DARPin)s for Targeted Photodynamic Therapy of Ovarian Cancer, *Cancers (Basel)*. **12**.
100. Campbell, B. F. N., Dittmann, A., Dreier, B., Pluckthun, A. & Tyagarajan, S. K. (2022) A DARPin-based molecular toolset to probe gephyrin and inhibitory synapse biology, *Elife*. **11**.
101. Nygren, P. A. & Skerra, A. (2004) Binding proteins from alternative scaffolds, *J Immunol Methods*. **290**, 3-28.
102. Getz, J. A., Rice, J. J. & Daugherty, P. S. (2011) Protease-resistant peptide ligands from a knottin scaffold library, *ACS Chem Biol.* **6**, 837-44.
103. Lehmann, A. (2008) Ecallantide (DX-88), a plasma kallikrein inhibitor for the treatment of hereditary angioedema and the prevention of blood loss in on-pump cardiothoracic surgery, *Expert Opin Biol Ther.* **8**, 1187-99.
104. Sankaran, S., de Ruiter, M., Cornelissen, J. J. & Jonkheijm, P. (2015) Supramolecular Surface Immobilization of Knottin Derivatives for Dynamic Display of High Affinity Binders, *Bioconjug Chem.* **26**, 1972-80.
105. Pleiner, T., Bates, M., Trakhanov, S., Lee, C. T., Schliep, J. E., Chug, H., Bohning, M., Stark, H., Urlaub, H. & Gorlich, D. (2015) Nanobodies: site-specific labeling for super-resolution imaging, rapid epitope-mapping and native protein complex isolation, *Elife*. **4**, e11349.
106. Liu, W., Song, H., Chen, Q., Yu, J., Xian, M., Nian, R. & Feng, D. (2018) Recent advances in the selection and identification of antigen-specific nanobodies, *Mol Immunol.* **96**, 37-47.
107. Gotzke, H., Kilisch, M., Martinez-Carranza, M., Sograte-Idrissi, S., Rajavel, A., Schlichthaerle, T., Engels, N., Jungmann, R., Stenmark, P., Opazo, F. & Frey, S. (2019) The ALFA-tag is a highly versatile tool for nanobody-based bioscience applications, *Nat Commun.* **10**, 4403.
108. Nordeen, S. A., Andersen, K. R., Knockenhauer, K. E., Ingram, J. R., Ploegh, H. L. & Schwartz, T. U. (2020) A nanobody suite for yeast scaffold nucleoporins provides details of the nuclear pore complex structure, *Nat Commun.* **11**, 6179.
109. Cordell, P., Carrington, G., Curd, A., Parker, F., Tomlinson, D. & Peckham, M. (2022) Affimers and nanobodies as molecular probes and their applications in imaging, *J Cell Sci.* **135**.

110. Georgiou, G., Stathopoulos, C., Daugherty, P. S., Nayak, A. R., Iverson, B. L. & Curtiss, R., 3rd (1997) Display of heterologous proteins on the surface of microorganisms: from the screening of combinatorial libraries to live recombinant vaccines, *Nat Biotechnol.* **15**, 29-34.
111. Pluckthun, A. (2012) Ribosome display: a perspective, *Methods Mol Biol.* **805**, 3-28.
112. Stern, L. A., Lown, P. S. & Hackel, B. J. (2020) Ligand Engineering via Yeast Surface Display and Adherent Cell Panning, *Methods Mol Biol.* **2070**, 303-320.
113. Finlay, W. J., Bloom, L. & Cunningham, O. (2011) Phage display: a powerful technology for the generation of high specificity affinity reagents from alternative immune sources, *Methods Mol Biol.* **681**, 87-101.
114. Piggott, A. M. & Karuso, P. (2016) Identifying the cellular targets of natural products using T7 phage display, *Nat Prod Rep.* **33**, 626-36.
115. Shim, H. (2017) Antibody Phage Display, *Adv Exp Med Biol.* **1053**, 21-34.
116. Wu, C. H., Liu, I. J., Lu, R. M. & Wu, H. C. (2016) Advancement and applications of peptide phage display technology in biomedical science, *J Biomed Sci.* **23**, 8.
117. Karavanas, G., Marin, M., Salmons, B., Gunzburg, W. H. & Piechaczyk, M. (1998) Cell targeting by murine retroviral vectors, *Crit Rev Oncol Hematol.* **28**, 7-30.
118. Urban, J. H. & Merten, C. A. (2011) Retroviral display in gene therapy, protein engineering, and vaccine development, *ACS Chem Biol.* **6**, 61-74.
119. Wang, S. & Balasundaram, G. (2010) Potential cancer gene therapy by baculoviral transduction, *Curr Gene Ther.* **10**, 214-25.
120. Miura, Y., Yoshida, K., Nishimoto, T., Hatanaka, K., Ohnami, S., Asaka, M., Douglas, J. T., Curiel, D. T., Yoshida, T. & Aoki, K. (2007) Direct selection of targeted adenovirus vectors by random peptide display on the fiber knob, *Gene Ther.* **14**, 1448-60.
121. Al-Salama, Z. T. (2019) Emapalumab: First Global Approval, *Drugs.* **79**, 99-103.
122. Markham, A. (2017) Guselkumab: First Global Approval, *Drugs.* **77**, 1487-1492.
123. Boder, E. T. & Wittrup, K. D. (2000) Yeast surface display for directed evolution of protein expression, affinity, and stability, *Methods Enzymol.* **328**, 430-44.
124. Scholler, N. (2018) Selection of Antibody Fragments by Yeast Display, *Methods Mol Biol.* **1827**, 211-233.

125. Kondo, A. & Ueda, M. (2004) Yeast cell-surface display--applications of molecular display, *Appl Microbiol Biotechnol.* **64**, 28-40.
126. Kuroda, K. & Ueda, M. (2013) Arming Technology in Yeast--Novel Strategy for Whole-cell Biocatalyst and Protein Engineering, *Biomolecules.* **3**, 632-50.
127. Zahradnik, J., Dey, D., Marciano, S., Kolarova, L., Charendoff, C. I., Subtil, A. & Schreiber, G. (2021) A Protein-Engineered, Enhanced Yeast Display Platform for Rapid Evolution of Challenging Targets, *ACS Synth Biol.* **10**, 3445-3460.
128. Toumaian, M. R. & Raeeszadeh-Sarmazdeh, M. (2022) Engineering Tissue Inhibitors of Metalloproteinases Using Yeast Surface Display, *Methods Mol Biol.* **2491**, 361-385.
129. Ban, B., Blake, R. C., 2nd & Blake, D. A. (2022) Yeast Surface Display Platform for Rapid Selection of an Antibody Library via Sequential Counter Antigen Flow Cytometry, *Antibodies (Basel).* **11**.
130. Little, M., Fuchs, P., Breitling, F. & Dubel, S. (1993) Bacterial surface presentation of proteins and peptides: an alternative to phage technology?, *Trends Biotechnol.* **11**, 3-5.
131. Lang, H. (2000) Outer membrane proteins as surface display systems, *Int J Med Microbiol.* **290**, 579-85.
132. Park, T. J., Zheng, S., Kang, Y. J. & Lee, S. Y. (2009) Development of a whole-cell biosensor by cell surface display of a gold-binding polypeptide on the gold surface, *FEMS Microbiol Lett.* **293**, 141-7.
133. Dane, K. Y., Suit, L. A. & Daugherty, P. (2007) Selection of peptides internalizing into tumor cells using fluorescent bacterial display libraries, *AIChE Annual Meeting, Conference Proceedings.*
134. Li, H., Liu, L., Ning, B., Sun, Z., Yao, S., Jiang, Y. & Liu, J. (2021) Selection of an artificial paraquat-specific binding protein from a ribosome display library based on a lipocalin scaffold, *Biotechnol Appl Biochem.* **68**, 1372-1385.
135. Zahnd, C., Amstutz, P. & Pluckthun, A. (2007) Ribosome display: selecting and evolving proteins in vitro that specifically bind to a target, *Nat Methods.* **4**, 269-79.
136. Li, R., Kang, G., Hu, M. & Huang, H. (2019) Ribosome Display: A Potent Display Technology used for Selecting and Evolving Specific Binders with Desired Properties, *Mol Biotechnol.* **61**, 60-71.
137. Hoffmann, F. & Rinas, U. (2004) Roles of heat-shock chaperones in the production of recombinant proteins in *Escherichia coli*, *Adv Biochem Eng Biotechnol.* **89**, 143-61.
138. Ueda, T., Kanamori, T. & Ohashi, H. (2010) Ribosome display with the PURE technology, *Methods Mol Biol.* **607**, 219-25.

139. Buchanan, A., Ferraro, F., Rust, S., Sridharan, S., Franks, R., Dean, G., McCourt, M., Jermutus, L. & Minter, R. (2012) Improved drug-like properties of therapeutic proteins by directed evolution, *Protein Eng Des Sel.* **25**, 631-8.
140. Douthwaite, J. A. (2012) Eukaryotic ribosome display selection using rabbit reticulocyte lysate, *Methods Mol Biol.* **805**, 45-57.
141. He, M., Edwards, B. M., Kastelic, D. & Taussig, M. J. (2012) Eukaryotic ribosome display with in situ DNA recovery, *Methods Mol Biol.* **805**, 75-85.
142. Chen, F., Zhao, Y., Liu, M., Li, D., Wu, H., Chen, H., Zhu, Y., Luo, F., Zhong, J., Zhou, Y., Qi, Z. & Zhang, X. L. (2010) Functional selection of hepatitis C virus envelope E2-binding Peptide ligands by using ribosome display, *Antimicrob Agents Chemother.* **54**, 3355-64.
143. Pignataro, M. F., Herrera, M. G., Fernandez, N. B., Aran, M., Gentili, H. G., Battaglini, F. & Santos, J. (2022) Selection of synthetic proteins to modulate the human frataxin function, *Biotechnol Bioeng.*
144. Garlich, J., Cinier, M., Chevrel, A., Perrocheau, A., Eyerman, D. J., Orme, M., Kitten, O. & Scheibler, L. (2022) Discovery of APL-1030, a Novel, High-Affinity Nanofitin Inhibitor of C3-Mediated Complement Activation, *Biomolecules.* **12**.
145. Roberts, R. W. & Szostak, J. W. (1997) RNA-peptide fusions for the in vitro selection of peptides and proteins, *Proc Natl Acad Sci U S A.* **94**, 12297-302.
146. Baggio, R., Burgstaller, P., Hale, S. P., Putney, A. R., Lane, M., Lipovsek, D., Wright, M. C., Roberts, R. W., Liu, R., Szostak, J. W. & Wagner, R. W. (2002) Identification of epitope-like consensus motifs using mRNA display, *J Mol Recognit.* **15**, 126-34.
147. Norman, A., Franck, C., Christie, M., Hawkins, P. M. E., Patel, K., Ashhurst, A. S., Aggarwal, A., Low, J. K. K., Siddiquee, R., Ashley, C. L., Steain, M., Triccas, J. A., Turville, S., Mackay, J. P., Passioura, T. & Payne, R. J. (2021) Discovery of Cyclic Peptide Ligands to the SARS-CoV-2 Spike Protein Using mRNA Display, *ACS Cent Sci.* **7**, 1001-1008.
148. Kamalinia, G., Engel, B. J., Srinivasamani, A., Grindel, B. J., Ong, J. N., Curran, M. A., Takahashi, T. T., Millward, S. W. & Roberts, R. W. (2020) mRNA Display Discovery of a Novel Programmed Death Ligand 1 (PD-L1) Binding Peptide (a Peptide Ligand for PD-L1), *ACS Chem Biol.* **15**, 1630-1641.
149. Pham, P. N., Huliciak, M., Biedermannova, L., Cerny, J., Charnavets, T., Fuertes, G., Herynek, S., Kolarova, L., Kolenko, P., Pavlicek, J., Zahradnik, J., Mikulecky, P. & Schneider, B. (2021) Protein Binder (ProBi) as a New Class of Structurally Robust Non-Antibody Protein Scaffold for Directed Evolution, *Viruses.* **13**.
150. Kolarova, L., Zahradnik, J., Huliciak, M., Mikulecky, P., Peleg, Y., Shemesh, M., Schreiber, G. & Schneider, B. (2022) De novo developed protein binders mimicking Interferon lambda signaling, *FEBS J.* **289**, 2672-2684.

151. Hoogenboom, H. R. (2005) Selecting and screening recombinant antibody libraries, *Nat Biotechnol.* **23**, 1105-16.
152. Kalichuk, V., Kambarev, S., Behar, G., Chalopin, B., Renodon-Corniere, A., Mouratou, B. & Pecorari, F. (2020) Affitins: Ribosome Display for Selection of Aho7c-Based Affinity Proteins, *Methods Mol Biol.* **2070**, 19-41.
153. Shim, H. (2020) Bispecific Antibodies and Antibody-Drug Conjugates for Cancer Therapy: Technological Considerations, *Biomolecules.* **10**.
154. Gocha, T., Rao, B. M. & DasGupta, R. (2017) Identification and characterization of a novel Sso7d scaffold-based binder against Notch1, *Sci Rep.* **7**, 12021.
155. Kotenko, S. V. & Durbin, J. E. (2017) Contribution of type III interferons to antiviral immunity: location, location, location, *J Biol Chem.* **292**, 7295-7303.
156. Diegelmann, J., Beigel, F., Zitzmann, K., Kaul, A., Goke, B., Auernhammer, C. J., Bartenschlager, R., Diepolder, H. M. & Brand, S. (2010) Comparative analysis of the lambda-interferons IL-28A and IL-29 regarding their transcriptome and their antiviral properties against hepatitis C virus, *PLoS One.* **5**, e15200.
157. Karlsson, O. A., Ramirez, J., Oberg, D., Malmqvist, T., Engstrom, A., Friberg, M., Chi, C. N., Widersten, M., Trave, G., Nilsson, M. T. & Jemth, P. (2015) Design of a PDZbody, a bivalent binder of the E6 protein from human papillomavirus, *Sci Rep.* **5**, 9382.
158. Lindborg, M., Dubnovitsky, A., Olesen, K., Bjorkman, T., Abrahmsen, L., Feldwisch, J. & Hard, T. (2013) High-affinity binding to staphylococcal protein A by an engineered dimeric Affibody molecule, *Protein Eng Des Sel.* **26**, 635-44.
159. Yu, L., Wang, R., Wen, T., Liu, L., Wang, T., Liu, S., Xu, H. & Wang, C. (2022) Peptide Binder with High-Affinity for the SARS-CoV-2 Spike Receptor-Binding Domain, *ACS Appl Mater Interfaces.* **14**, 28527-28536.
160. Oh, C. K., Leigh, R., McLaurin, K. K., Kim, K., Hultquist, M. & Molfino, N. A. (2013) A randomized, controlled trial to evaluate the effect of an anti-interleukin-9 monoclonal antibody in adults with uncontrolled asthma, *Respir Res.* **14**, 93.
161. Horejsi, Z., Stach, L., Flower, T. G., Joshi, D., Flynn, H., Skehel, J. M., O'Reilly, N. J., Ogrodowicz, R. W., Smerdon, S. J. & Boulton, S. J. (2014) Phosphorylation-dependent PIH1D1 interactions define substrate specificity of the R2TP cochaperone complex, *Cell Rep.* **7**, 19-26.
162. Vorup-Jensen, T., Ostermeier, C., Shimaoka, M., Hommel, U. & Springer, T. A. (2003) Structure and allosteric regulation of the alpha X beta 2 integrin I domain, *Proc Natl Acad Sci U S A.* **100**, 1873-8.

163. Rothe, A., Nathanielsz, A., Hosse, R. J., Oberhauser, F., Strandmann, E. P., Engert, A., Hudson, P. J. & Power, B. E. (2007) Selection of human anti-CD28 scFvs from a T-NHL related scFv library using ribosome display, *J Biotechnol.* **130**, 448-54.
164. Okda, F., Liu, X., Singrey, A., Clement, T., Nelson, J., Christopher-Hennings, J., Nelson, E. A. & Lawson, S. (2015) Development of an indirect ELISA, blocking ELISA, fluorescent microsphere immunoassay and fluorescent focus neutralization assay for serologic evaluation of exposure to North American strains of Porcine Epidemic Diarrhea Virus, *BMC Vet Res.* **11**, 180.
165. Baldauf, K. J., Salazar-Gonzalez, R. A., Doll, M. A., Pierce, W. M., Jr., States, J. C. & Hein, D. W. (2020) Role of Human N-Acetyltransferase 2 Genetic Polymorphism on Aromatic Amine Carcinogen-Induced DNA Damage and Mutagenicity in a Chinese Hamster Ovary Cell Mutation Assay, *Environ Mol Mutagen.* **61**, 235-245.
166. Uyttenhove, C., Druetz, C., Renauld, J. C., Herin, M., Noel, H. & Van Snick, J. (1991) Autonomous growth and tumorigenicity induced by P40/interleukin 9 cDNA transfection of a mouse P40-dependent T cell line, *J Exp Med.* **173**, 519-22.
167. Barinka, C., Ptacek, J., Richter, A., Novakova, Z., Morath, V. & Skerra, A. (2016) Selection and characterization of Anticalins targeting human prostate-specific membrane antigen (PSMA), *Protein Eng Des Sel.* **29**, 105-15.
168. Amiram, M., Haimovich, A. D., Fan, C., Wang, Y. S., Aerni, H. R., Ntai, I., Moonan, D. W., Ma, N. J., Rovner, A. J., Hong, S. H., Kelleher, N. L., Goodman, A. L., Jewett, M. C., Soll, D., Rinehart, J. & Isaacs, F. J. (2015) Evolution of translation machinery in recoded bacteria enables multi-site incorporation of nonstandard amino acids, *Nat Biotechnol.* **33**, 1272-1279.

7 Supplements

A) Curriculum vitae

B) Publication: Ngoc P.P., Huličiak M., Biedermannová L., Černý J., Charnavets T., Fuertes G., Herynek Š., Kolářová L., Kolenko P., Pavlíček J., Zahradník J., Mikulecky P., Schneider B. (2021) Protein Binder (ProBi) as a New Class of Structurally Robust Non-Antibody Scaffold for Directed evolution. *Viruses.*, 13, 190

C) Publication: Kolarova L., Zahradnik J., Huličiak M., Mikulecky P., Peleg Y., Shemesh M., Schreiber G., Schneider B. (2021) De novo development protein binders mimicking Interferon lambda signaling. *FEBS Journal*

D) Accepted manuscript: Huličiak M., Biedermanová L., Berdár D, Herynek Š., Kolářová L., Tomala J., Mikulecký P., Schneider B. Combined in vitro and cell-based selection display method producing specific binders against IL-9 receptor in high yields. *FEBS Journal*. (Manuscript to be published)

Mgr. Maroš Huličiak – curriculum vitae

Date of birth: 9.2.1994

email: Maros.huliciak@ibt.cas.cz

mobile: +420728057639

Address: Dolná Mariková 737, Slovakia

Jobs:

Doctoral student in Laboratory of Biomolecular recognition (2019 - present), Institute of biotechnology, Biotechnological centre of Czech academy of science and Charles University (BIOCEV) in Vestec

Research assistant in Laboratory of protein engineering (2016 - 2019), Institute of biotechnology, Biotechnological centre of Czech academy of science and Charles University (BIOCEV) in Vestec

Education:

Doctor degree – Molecular and cell biology, genetics and virology (2019-present), Charles University

Master degree – Cell and development biology – Physiology of the cell (2017-2019), Charles University

Bachelor degree – Molecular biology and biochemistry of organism (2013-2017), Charles University

Languages:

Slovak – native speaker

English – B2

German – B1

Achievements:

Scientific competition Genius Olympiad, Oswego – New York (2013), silver medal

Young scientists conference, Olomouc – Czech Republic (2013), the 1st place

Scientific competition INEPO, Istanbul – Turkey (2012), bronze medal

Personal attributes:

Responsibility, Flexibility, Friendliness

Publications:






Pham PN, Huličiak M, Biedermannová L, Černý J, Charnavets T, Fuertes G, Herynek Š, Kolářová L, Kolenko P, Pavlíček J, Zahradník J, Mikulecky P, Schneider B. Protein Binder (ProBi) as a New Class of Structurally Robust Non-Antibody Protein Scaffold for Directed Evolution. *Viruses*. 2021; 13(2):190. <https://doi.org/10.3390/v13020190>

Kolářová, L., Zahradník, J., Huličiak, M., Mikulecký, P., Peleg, Y., Shemesh, M., Schreiber, G. and Schneider, B. (2022), De novo developed protein binders mimicking Interferon lambda signaling. *FEBS J*. <https://doi.org/10.1111/febs.16300>

Huličiak M., Biedermanová L., Berdár D, Herynek Š., Kolářová L., Tomala J., Mikulecký P., Schneider B. Combined in vitro and cell-based selection display method producing specific binders against IL-9 receptor in high yields. *FEBS Journal*. (Manuscript to be published)

Article

Protein Binder (ProBi) as a New Class of Structurally Robust Non-Antibody Protein Scaffold for Directed Evolution

Phuong Ngoc Pham, Maroš Huličiak, Lada Biedermannová, Jiří Černý , Tatsiana Charnavets, Gustavo Fuertes , Štěpán Herynek, Lucie Kolářová, Petr Kolenko , Jiří Pavlíček, Jiří Zahradník, Pavel Mikulecky  and Bohdan Schneider 

Institute of Biotechnology of the Czech Academy of Sciences, BIOCEV, CZ-25250 Vestec, Czech Republic; phuong@ibt.cas.cz (P.N.P.); maros.huliciak@ibt.cas.cz (M.H.); Lada.Biedermannova@ibt.cas.cz (L.B.); jiri.cerny@ibt.cas.cz (J.Č.); tatsiana.charnavets@ibt.cas.cz (T.C.); gustavo.fuertes@ibt.cas.cz (G.F.); Stepan.Herynek@ibt.cas.cz (Š.H.); kolarovalucie007@gmail.com (L.K.); kolenko@ibt.cas.cz (P.K.); jiri.pavlicek@ibt.cas.cz (J.P.); jiri.zahradnik@ibt.cas.cz (J.Z.)

* Correspondence: mikulecky@outlook.com (P.M.); bohdan.schneider@gmail.com (B.S.)

Abstract: Engineered small non-antibody protein scaffolds are a promising alternative to antibodies and are especially attractive for use in protein therapeutics and diagnostics. The advantages include smaller size and a more robust, single-domain structural framework with a defined binding surface amenable to mutation. This calls for a more systematic approach in designing new scaffolds suitable for use in one or more methods of directed evolution. We hereby describe a process based on an analysis of protein structures from the Protein Data Bank and their experimental examination. The candidate protein scaffolds were subjected to a thorough screening including computational evaluation of the mutability, and experimental determination of their expression yield in *E. coli*, solubility, and thermostability. In the next step, we examined several variants of the candidate scaffolds including their wild types and alanine mutants. We proved the applicability of this systematic procedure by selecting a monomeric single-domain human protein with a fold different from previously known scaffolds. The newly developed scaffold, called ProBi (Protein Binder), contains two independently mutable surface patches. We demonstrated its functionality by training it as a binder against human interleukin-10, a medically important cytokine. The procedure yielded scaffold-related variants with nanomolar affinity.

Keywords: directed evolution; protein scaffold; protein engineering; computational saturation; ribosome display; interleukin-10



Citation: Pham, P.N.; Huličiak, M.; Biedermannová, L.; Černý, J.; Charnavets, T.; Fuertes, G.; Herynek, Š.; Kolářová, L.; Kolenko, P.; Pavlíček, J.; et al. Protein Binder (ProBi) as a New Class of Structurally Robust Non-Antibody Protein Scaffold for Directed Evolution. *Viruses* **2021**, *13*, 190. <https://doi.org/10.3390/v13020190>

Academic Editor: Petri Susi
Received: 19 December 2020
Accepted: 23 January 2021
Published: 27 January 2021

Publisher's Note: MDPI stays neutral with regard to jurisdictional claims in published maps and institutional affiliations.



Copyright © 2021 by the authors. Licensee MDPI, Basel, Switzerland. This article is an open access article distributed under the terms and conditions of the Creative Commons Attribution (CC BY) license (<https://creativecommons.org/licenses/by/4.0/>).

1. Introduction

Many biological functions depend on specific protein-protein interactions. Protein engineering offers the possibility to tune these interactions by developing de novo binding partners [1–3] or by mutating the interaction partners using computational design [4,5]. A powerful tool of protein engineering is to generate protein binders by the in vitro directed selection techniques [6–8] or to use evolution-based approaches to increase the stability of recombinant proteins [9–11].

A prototype of a binding protein is an antibody, a highly selective and adaptive molecule capable of binding to a huge spectrum of partners. The antibody-based binders have been indispensable not only in research experiments but also in clinical trials and tens of them are biologicals approved by Federal Drug Administration. However, several suboptimal properties of these molecules such as their large size (~150 kDa), cross-reactivity, and necessity of animal immunization during the preparation, motivated the development of binders with alternative structures [12,13]. These novel artificial high-affinity binders are called “small non-antibody protein scaffolds” [14–16]. The advantage of scaffolds over antibodies is their typically higher stability and lower cost of production. The most widely

used scaffolds are designed Ankyrin repeats (dARPins), lipocalin domain (anticalins), and Ig-binding domain of Staphylococcal Protein A (affibodies) [17–19]. Some of the small protein scaffolds were already proven to be useful in a wide range of applications, from academic research to clinical imaging, diagnostics, or therapeutics [20–23], and others are even in clinical trials [24,25]. In our previous work, we used the albumin-binding domain (ABD) of Streptococcal Protein G as a scaffold protein. We engineered its binding against human IFN γ [26] and interleukin-23 receptor [27] using computational design and ribosome display.

The exploration of non-antibody protein scaffolds is still a young field compared to the research of antibodies and the full potential of scaffolds has not yet been uncovered. Therefore, we are convinced that there is ample space to expand the current portfolio of protein scaffolds so that they can complement antibodies and interact with new target molecules. Therefore, a systematic method to streamline the development of new scaffolds with desired properties would be beneficial but relatively few attempts can be found in the literature [18,28,29]. In general, a good small protein scaffold should display a high stability, together with flexibility of binding. The desired properties thus include tolerance to mutations during diversification, thermostability, *in vivo* integrity, and non-immunogenicity. Moreover, the variants of the protein scaffold must be efficiently evolvable to achieve high affinity and specificity towards target proteins. Therefore, the properties of the potential small protein scaffold must be thoroughly evaluated.

In this work, we present a systematic stepwise procedure for the selection of new and structurally robust protein scaffolds. The procedure starts with a wide search of suitable structures in the Protein Data Bank (PDB) [30], followed by a series of computational and experimental screens to select the most robust candidates as novel, small protein scaffolds. We demonstrate the applicability of our method by selecting a protein scaffold called ProBi (Protein Binder) that fulfills all the criteria of stability and mutability, and comprises not one, but two independently mutable surface patches.

We tested the applicability of the ProBi scaffold by generating its variants with high affinity to a target protein using *in vitro* directed evolution techniques. As the target, we selected a medically important protein, interleukin-10 (IL-10), a member of the cytokine superfamily. IL-10 is an immune repressor [31], with numerous investigations suggesting its major impact in inflammatory, malignant, and autoimmune diseases. IL-10 overexpression was found in certain tumors and is considered to promote tumor development [32]. Also, some viral homologs can bind to the IL-10 receptor 1 [33] and mimic the immunosuppressive effects of IL-10. Thus, proteins binding IL-10 and interfering with its signaling have a great potential for diagnostic and therapeutic purposes.

To generate ProBi-based binders to IL-10, we created a DNA library by randomization of 10 amino acids on one of the ProBi surface patches and used the ribosome display technique to screen for ProBi variants with the highest affinity. We successfully generated binders of the newly developed ProBi protein scaffold with affinities of ~10 and ~200 nM against IL-10.

2. Materials and Methods

2.1. Selection of Suitable Protein Structures from the Protein Data Bank

The Protein Data Bank (PDB) [30] was searched for potential protein scaffolds using the following criteria: (1) small size (molecular weight in range of 10–25 kDa); (2) monomeric protein with a reasonably high-resolution X-ray structure (<3.0 Å); and (3) produced in Expression Organism of *E. coli* for ease of expression. Proteins matching these initial search criteria were then manually curated to meet additional rules: structure (protein fold class) (1) should differ from the previously published protein scaffolds; (2) should differ from the other selected structures in the set; (3) should contain a low number of cysteine residues and disulfide bonds, (4) should not be toxic or immunogenic, (5) should not contain any ligand or cofactor, and (6) should be soluble and easy to purify (according to the source literature).

2.2. In Silico Identification of Mutable Surface Patches on Protein Scaffolds Candidates

(a) Multiple sequence alignment. For each of the scaffold candidate proteins, a similarity search was performed for the related amino acid sequences from different species using the UniProt BLAST service (www.uniprot.org/blast) with default parameters (Target database = UniProtKB, E-Threshold = 10, Matrix = blosum62, Filtering = None, Gapped = yes, Hits = 250). The identical sequences were subsequently removed using a script and the remaining ones were aligned using Clustal W [34] in the UGENE program [35]. The conservation of each sequence position was calculated.

(b) In silico saturation mutagenesis. The mutability of the surface amino acid residues was evaluated by in silico mutation scanning using the FoldX program [36] by applying the “positionscan” FoldX Keywords: In all proteins, each position was substituted by all of the 20 standard amino acid residues, and the corresponding free energy differences ($\Delta\Delta G$) between the mutant and the wild-type (WT) structure were calculated; the calculations included self-mutations leading to $\Delta\Delta G = 0$. Positions in which most of the mutations were stabilizing ($\Delta\Delta G < 0$), or only slightly destabilizing ($\Delta\Delta G < 0.5$ kcal/mol), were identified and the mutability score for each position was calculated as a percentage of mutations fulfilling these criteria.

(c) Sequence and structural evaluation. The mutable residues, identified by multiple sequence alignment and in silico saturation mutagenesis, were located on the 3D structure of each protein scaffold candidate. We then visually searched for continuous surface regions consisting of mutable residues. The regions where the mutable residues were close together in both sequential and structural space we termed the mutable surface patch. Ideally, the patch should contain 10–12 residues to fulfill the theoretical complexity suitable for ribosome display. If the identified patch contained less than 10–12 residues with the highest mutability score, we completed the patch by a small number of neighboring surface residues with slightly lower mutability scores.

2.3. Production of Proteins

(a) Cloning of recombinant proteins. The genes coding the selected five protein scaffold candidates—4PSF, 1N3Y, 4I3B, 1W2I, and 2F3L, were ordered in the form of DNA strings (ThermoFisher Scientific, Waltham, MA, USA) with codons optimized for expression in *Escherichia coli* but without a stop codon. The DNA strings were cloned into the pET-26b(+) vector using NdeI and XhoI restriction enzymes in frame with C-terminal His-tag. Also, the DNA strings were used as templates for polymerase chain reaction (PCR) to add the N-terminal His-tag and stop codon. These N-terminally tagged proteins were cloned into the pET-26b(+) vector using NdeI and XhoI restriction enzymes. Final constructs were labeled as pET26b-4PSF-WT, etc.

The genes coding the variants of three protein scaffold candidates—4PSF, 1N3Y, and 4I3B, with all mutable residues changed to alanine amino acid, referred to as allAla mutants, were ordered in the form of DNA strings with N-terminal His-tag and C-terminal stop codon. The DNA strings were digested by NdeI and XhoI restriction enzymes and cloned into the pET-26b(+) vector. Final constructs were labeled as pET26b-4PSF-allAla, etc.

The ProBi-WT protein and its variants were amplified by the PCR method using the ProBi-cloning-for and ProBi-cloning-rev primers (Table S1). The created fragments were cleaved by NcoI and BamHI restriction enzymes and cloned into the pRDVsm or pETsm vectors (Figure S1).

The genes encoding the interleukin-10 (residues 19–179 of UniProt entry P22301) and interleukin-29 (residues 20–200 of UniProt entry Q8IU54) were ordered in the form of a DNA string with codons optimized for expression in *Drosophila melanogaster*. The DNA was cleaved by BglII and XhoI restriction enzymes and cloned into a pMTH vector (a modified version of pMT-BiP-V5-His_A vector where recognition site for the AgeI restriction enzyme is exchanged for XhoI enzyme). The final construct contained IL-10 or IL-29 protein with N-terminal BiP signal peptide and C-terminal His-tag. Final constructs were labeled as pMTH-IL10cd and pMTH-IL29cd.

(b) Expression and purification of recombinant proteins. The recombinant protein scaffold candidates were produced in *E. coli* BL21(DE3) strain. In addition, the expression of 1W3I scaffold was tested in *E. coli* C41(DE3) and C43(DE3) strains. The bacteria were cultivated in LB medium (Sigma-Aldrich, St. Louis, MO, USA) at 37 °C until OD₆₀₀ = 0.6, followed by the addition of 1 mM isopropyl-beta-D-thiogalactopyranoside (IPTG) for induction of expression. Then the cultivation continued for 4 h at 37 and 30 °C or overnight at 25 and 16 °C. The cells were harvested by centrifugation (5000× *g*, 15 min, 4 °C) and stored at −20 °C. The cells were resuspended in LH buffer (20 mM Na-Phosphate buffer, pH 7.3, 100 mM NaCl), and disrupted by ultrasound. The soluble fraction was separated by centrifugation (40,000× *g*, 20 min, 4 °C) and passed over the Ni-NTA agarose beads equilibrated in LH buffer. The beads were washed by LH buffer supplemented by 10 mM imidazole and proteins were eluted by LH buffer containing 200 mM imidazole.

The recombinant ProBi variants were produced in *E. coli* BL21-Gold(DE3) in LB medium (Sigma-Aldrich) at 37 °C until OD₆₀₀ = 0.6, followed by the addition of 1 mM IPTG for induction of expression. Then cultivation continued overnight at 18 °C. The cells were harvested by centrifugation (5000× *g*, 15 min, 4 °C) and stored at −20 °C. The cells were resuspended in LS buffer (50 mM Tris, pH 8.0, 150 mM NaCl, 1 mM EDTA), and disrupted by ultrasound. The soluble fraction was separated by centrifugation (40,000× *g*, 20 min, 4 °C) and passed over the StrepTactin XT resin equilibrated in LS buffer. The resin was washed by LS buffer and proteins were eluted by BXT buffer (100 mM Tris, pH 8.0, 150 mM NaCl, 1 mM EDTA, 50 mM biotin).

The constructs pMTH-IL10cd and pMTH-IL29cd for expression of recombinant IL-10 and IL-29, respectively, in insect S2 cells were produced and purified similarly as IFN γ R2 in the previous report [37]. Briefly, S2 cells were cultivated in Insect-XPRESSTM Protein-free Insect Cell Medium (Lonza) and protein expression was induced by the addition of CuSO₄. IL-10 and IL-29 proteins were secreted into the medium and stored at −80 °C.

All proteins were further purified to homogeneity by size exclusion chromatography at 16 °C using Superdex 75 10/300 Increase, Superdex 200 10/300 Increase, or Superdex 75 16/600 column (GE Healthcare, Chicago, IL, USA). The column was equilibrated in phosphate-buffered saline (PBS) pH 7.4 (for protein scaffold proteins and all Ala mutants), 20 mM Tris, pH 7.5, 100 mM NaCl (for preliminary crystallization trials), or in 50 mM Tris, pH 8.0, 300 mM NaCl (for ProBi variants and IL-10 protein). Samples were analyzed by 15% sodium dodecyl sulphate–polyacrylamide gel electrophoresis (SDS-PAGE).

2.4. Biophysical Characterization of Recombinant Proteins

(a) Oligomerization and melting temperature of protein scaffold candidates and allAla mutants. The oligomeric state of proteins and their monodispersity was measured by dynamic light scattering (DLS) using a ZetaSizer Nano ZS90 (Malvern Panalytical, Malvern, UK) instrument and quartz cuvette ZEN2112. The secondary structure and folding of proteins were analyzed by circular dichroism (CD) spectra using a Chirascan Plus spectrometer (Applied Photophysics, Surrey, UK) in steps of 1 nm over the wavelength range 200–260 nm. Samples were diluted with PBS buffer, pH 7.4, to a concentration of 0.2 mg/mL. The individual spectra were measured in a 0.01 cm path-length quartz cell at a temperature of 25 °C. The CD signal was recorded as the ellipticity, and the resulting spectra were buffer-subtracted. The melting temperatures of proteins were evaluated using either the CD spectrometer or nanoDSF technology. The CD melting measurements were performed by using the 0.1 cm path-length quartz cell. The samples were heated from 20 to 85 °C, and the sample absorption was recorded at 280 nm in 1 °C increments at a rate of 0.5 °C/min. The nanoDSF technology was implemented in the Prometheus NT.48 instrument (NanoTemper, München, Germany). The samples were loaded into standard capillaries and heated from 20 to 95 °C at a rate of 1 °C/min. The melting temperatures (T_m) were estimated from the first derivative of the melting curves.

(b) Testing protein suitability for affinity measurements. The applicability of protein scaffold candidates and allAla mutants for affinity measurements using the microscale

thermophoresis (MST) and surface plasmon resonance (SPR) was tested. For MST, proteins were labeled using the Monolith Protein Labeling Kit RED-NHS (Amine Reactive) according to the manufacturer's protocol. The samples were loaded into three types of capillary (standard, hydrophilic, and hydrophobic) and inserted into the Monolith NT.115 instrument (NanoTemper). The capillary scan was performed immediately, and then samples were incubated in the instrument for 1 h and re-measured. An alternative approach was implemented for SPR. The GLC sensor chip was inserted into the ProteOn XPR36 instrument, washed but not activated. The samples in different channels were passed over the un-activated chip to estimate the non-specific binding of proteins to the surface of the chip itself. The running buffer (PBS, pH 7.4, 0.005% Tween-20) was used in the control channel.

2.5. Crystallization and Structure Determination

The crystallization solution included J61 at a concentration of 10 mg/mL in a buffer containing 100 mM NaCl, 20 mM Tris, pH 8.0. Crystals were prepared using the hanging-drop vapor-diffusion method with the reservoir solution containing 5% (*v/v*) glycerol and 4 M sodium formate. Crystals required cryo-protection with 20% glycerol before flash freezing in liquid nitrogen and the diffraction experiment.

The final diffraction data were collected at the Helmholtz-Zentrum Berlin (Bessy II) on a beamline 14.1 at 100 K. The diffraction images were processed using the XDS program [38] and scaled using the AIMLESS program [39] from the CCP4 program package [40]. The phase problem was solved by molecular replacement using PHASER [41] using monomeric 4PSF structure [42] as a search model. The structure was refined using the REFMAC5 program [43] using 95% of reflections as a working set and 5% or reflections as a test set. Manual corrections to the model were done using the graphic COOT program [44]. The last run of several cycles of refinement was performed using all reflections and anisotropic ADPs. The structure quality was checked using the validation tools implemented in CCP4, MOLPROBITY [45], and the PDB. Final data processing statistics and structure refinement statistics are shown in Table S2.

2.6. Construction of DNA Library of ProBi Scaffold (PatchC)

The earlier design of the DNA library [46] was adopted with small changes regarding restriction enzyme recognition sites and N- and C-terminal tags. Our ribosome display DNA construct contained a T7 promoter, 5' stem-loop, ribosome binding site, N-terminal Strep-tag, open reading frame encoding the ProBi scaffold library, and C-terminal c-Myc-tag fused to TolA-spacer without stop codon. The library of ProBi scaffold (PatchC) was prepared by the GENEWIZ company using NNK codons technology. We selected ten residues to be randomized. The initial synthetic DNA library was amplified by PCR and then used in the first selection round of ribosome display.

2.7. Selection of Novel Binders by In Vitro Ribosome Display

The previous protocols from Pluckthun's laboratory regarding the in vitro selection by ribosome display [46,47] were adopted and adjusted. All the following steps were first performed with the ProBi-WT scaffold to establish and verify the protocol.

(a) Preparation of the mRNA-ribosome-protein (MRP) complex. The DNA library was amplified by PCR (supplemented by 6% DMSO) with primers T7b and TolAk (Table S1) using Q5 polymerase (New England Biolabs, Ipswich, MA, USA) with an annealing temperature of 66 °C. As a template, either the starting DNA library in the first selection round was used or the sorted DNA library cloned into the pRDVsm vector in the next rounds. The resulted amplicon contained a T7 promoter, 5' stem-loop, ribosome binding site (RBS), start codon, N-terminal Strep-tag II, scaffold library, C-terminal c-Myc-tag, tolA spacer, and 3' stem-loop without stop codon. The amplicon was purified from 1% agarose gel and used in the following cell-free protein synthesis step. We utilized RTS 100 *E. coli*

HY Kit (Biotecrabbt) according to manufacturer recommendations to create the MRP complex composed of mRNA, ribosome, and protein scaffold variants.

(b) Ribosome display selection rounds. The Nunc PolySorp plate (Invitrogen, Carlsbad, CA, USA) was coated with anti-His antibody (His-tag Monoclonal Antibody (HIS.H8) by Invitrogen) diluted to a final concentration of 25 µg/mL in bicarbonate coating buffer (pH 9.6). All following steps were undertaken in the TBS buffer, pH 7.4. Blocking of plate and incubation of scaffold variants with proteins were undertaken either by an initial preselection process or an optimized preselection process described below.

(c) Initial preselection process. The plate was blocked by 3% bovine serum albumin (BSA) during all rounds. The MRP complex supplemented by 0.5% BSA and heparin (200 mg/mL) was added to the Preselection well that was coated with a mixture of 3% BSA, interferon-gamma (IFN γ , 25 µg/mL), and the 4PSF wild type protein (4PSF-WT, 25 µg/mL). The reaction was incubated for 1 h at 4 °C.

(d) Optimized preselection process. The plate was blocked by either 3% BSA (used in the first and third round) or by 3% dry skimmed cow milk (used in the second and fourth round). The MRP complex supplemented by 0.5% BSA and heparin (200 mg/mL) was added to the Preselection well that was coated with a mixture of 3% BSA, IFN γ (25 µg/mL), IL-29 (25 µg/mL), and 4PSF-WT (25 µg/mL). The reaction was incubated for 1 h at 4 °C.

(e) Selection process. The preselected MRP complex was transferred into the Selection well that contained IL-10 (25 µg/mL) as a target molecule and incubated again for 1 h at 4 °C. In each round, the well was washed by different cycles of washes and increasing concentration of Pluronic F-127 in TBS buffer. The conditions were as follows: First round–5 wash cycles with 0.10%, second round–10 wash cycles with 0.15%, third and fourth-round–10 wash cycles with 0.20%. The library complex was incubated with an EB buffer (50 mM Tris-Acetate, 150 mM NaCl, 50 mM EDTA, pH adjusted to 7.5) containing *S. cerevisiae* RNA (1 mg/mL) and heparin (200 mg/mL) to release the mRNA. The mRNA was purified by the High Pure RNA Isolation Kit (Roche, Basel, Switzerland) according to the manufacturer's instructions and used in the GoScript Reverse Transcription System (Promega, Dane County, WI, USA) with ProBi-cloning-rev primer according to the manufacturer's instruction. The created cDNA was amplified by PCR (supplemented by 6% DMSO) with primers ProBi-cloning-for and ProBi-cloning-rev using Q5 polymerase (New England Biolabs). The resulted amplicon was cloned into the pRDVsm vector using NcoI and BamHI restriction enzymes and T4 ligase (New England Biolabs). The pRDVsm-ProBi was used in the following preselection and selection process. After the fourth round, the amplicon was cloned into the pETsm vector and transformed into BL21(DE3)-Gold (Agilent, Santa Clara, CA, USA) for affinity estimation by enzyme-linked immunosorbent assay (ELISA) and characterization.

2.8. Characterization of Novel Binders

(a) ELISA assay. The Nunc PolySorp plate (Invitrogen) was coated with anti-His antibody (His-tag Monoclonal Antibody (HIS.H8) by Invitrogen) diluted to a final concentration of 5 µg/mL in bicarbonate coating buffer (pH 9.6). All following steps were done in the PBS-P buffer (PBS buffer, pH 7.4, 0.1% Pluronic F-127). For the first evaluation of the binding of 190 variants, the wells were blocked by 1% BSA, then IL-10 (10 µg/mL) was attached as a target molecule, and samples were applied in the form of cell lysates. For initial specificity mapping of 47 variants, the wells were blocked by 3% dry skim milk, 3% BSA, or 1% BSA. The wells with 1% BSA were further incubated with either IL-10 or IL-29 (10 µg/mL), and samples were applied in the form of cell lysates. For affinity estimation of 10 selected variants, the wells were blocked by 1% BSA and then incubated with IL-10 (10 µg/mL) as a target molecule. Then the samples in the form of proteins purified on StrepTactinXT were applied. Finally, the binders were detected by horseradish peroxidase (HRP)-conjugated antibody against the C-terminal c-Myc-tag and TMB-2 as substrate.

(b) Inhibitory assay. Murine RAW264.7 cells were cultured in DMEM medium supplemented with 10% FBS. The mixture containing IL-10 (final concentration of 10 ng/mL)

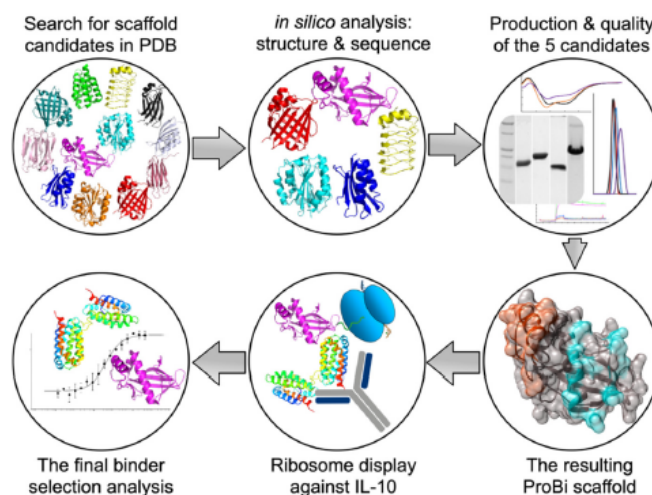
and ProBi variants (concentrations ranging from 160 ng to 100 µg/mL) was added to the cells and incubated for 30 min. The plates with cells were placed on ice, medium discarded, and washed with a cold PBS buffer. The cells were disrupted by a cold RIPA buffer supplemented by protease and phosphatase inhibitors. An amount of 20 µg of total protein was resolved using 10% Tris-Glycine SDS-PAGE gel and transferred to nitrocellulose membrane using Trans-Blot Turbo Transfer System according to the manufacturer's instructions. Membranes were blocked by 5% BSA in TBST buffer and incubated with antibodies against Y705-STAT3 (dilution 1/700) and alpha-tubulin (dilution 1/5000) diluted in 5% BSA in TBST buffer. Blots were washed in TBST buffer and incubated with appropriate HRP-conjugated secondary antibodies diluted in 1% BSA in TBST buffer. Membranes were treated with ECL solution (Merck Millipore, Burlington, MA, USA) and visualized on the Azure c600 instrument.

(c) Affinity measurements. The binding affinity in a solution was measured using the Monolith NT.115 instrument to monitor microscale thermophoresis (MST). The composition of the Assay buffer was 50 mM Tris, pH 8.0, 300 mM NaCl, and 0.1% Pluronic F-127. The IL-10 with C-terminal His-tag was labeled in assay buffer using the Monolith His-tag Labeling Kit RED-tris-NTA kit according to the manufacturer's instructions. The labeled IL-10 was titrated by ProBi variants diluted in an assay buffer and incubated for 10 min at room temperature. The reaction mix was loaded into standard capillaries and MST was monitored using Medium MST power and 60% of LED power. The analysis of interaction was done in MO.Affinity Analysis v2.3 software.

(d) Circular dichroism. The folding of new ProBi variants was measured by Circular dichroism spectra the same way as done with allAla mutants of protein scaffold candidates but with a final concentration of 0.1 mg/mL.

3. Results and Discussion

This work aimed to formulate and test a general procedure for selecting “small engineered non-antibody protein scaffolds” [15,16] suitable for generating artificial recombinant high-affinity binders by methods of targeted *in vitro* evolution. The systematic procedure for the development and testing of a new stable small protein scaffold presented in this work consists of two main parts comprising the steps graphically represented in Scheme 1 and summarized below:



Scheme 1. The procedure for the development of a new stable small protein scaffold.

(I) Development of a novel scaffold:

- (i) Selection of suitable protein candidates from the Protein Data Bank.
- (ii) In silico identification of mutable patches on the surfaces of the scaffold candidates.
- (iii) Characterization of soluble wild-type variants of the scaffold candidates.
- (iv) Testing the stability of the potential scaffolds.
- (v) Testing the suitability of the scaffold candidate(s) for in vitro evolution.
- (vi) Construction of the final ProBi scaffold.
- (II) Application of the ProBi scaffold on the IL-10 target as a model system:
 - (i) Selection of novel ProBi-based binders by ribosome display.
 - (ii) Characterization of the novel ProBi-based binders.
 - (iii) Further development of scaffold selection and improvement of ProBi-based binders.

3.1. Development of a Novel Scaffold

3.1.1. Selection of Suitable Protein Structures from the Protein Data Bank

The first step of the procedure was to search for appropriate structures within the Protein Data Bank (PDB) database [30] performed by the members of the laboratory. The initial search was based on visual inspection of several hundred structures of small (less than 25 kDa) monomeric proteins solved by X-ray crystallography. The search results were limited to proteins known to be expressed in *Escherichia coli*. We finally selected about 100 structures that were further evaluated based on the literature data. Our selected candidates should (i) be new protein scaffolds, (ii) be based on different folds, (iii) preferably contain no or low number of cysteines, (iv) not to be toxic, (v) not to need any cofactor to maintain the structure, and (vi) be easy to purify.

We chose 12 proteins (Table 1) for closer structural examination and a more in-depth literature review. During this step, we excluded 2W4P [48] and 4LKT [49] because of structural similarities with other selected non-human candidates, 1W2I [50] and 4I3B [51], respectively. Furthermore, we eliminated 4MJJ and 4JOX because the manuscripts were not published at that time and we could not check their expression and purification protocols. To the best of our knowledge, none of the eight finally selected proteins had previously been used as a scaffold for directed evolution.

3.1.2. In Silico Identification of Mutable Surface Patches on the Protein Scaffold Candidates

On the surface of the eight candidate scaffolds, we looked for continuous patches consisting of residues that may be mutated without destabilizing the overall structure. To identify such mutable residues, we combined the analysis of protein sequence conservation with in silico saturation mutagenesis. We did not limit our search only for loop segments [28] because protein scaffolds could be mutated also at flat surfaces or combinations of loops and helices [18].

(a) Multiple sequence alignment. Sequences of protein homologs from different organisms for the eight protein scaffold candidates were aligned and the conservation of each amino acid position was calculated.

(b) In silico saturation mutagenesis. To evaluate the mutability of the residues, we performed in silico mutation scanning using the FoldX program [36]. Every amino acid position in each of the eight candidates was substituted by all of the 20 standard amino acid residues, and the corresponding free energy differences ($\Delta\Delta G$) between the mutant and the wild-type structure were calculated. Thus, each position in the protein sequence was characterized by 20 $\Delta\Delta G$ values. We identified spots in which most of the mutations were stabilizing ($\Delta\Delta G < 0$), or only slightly destabilizing ($0 < \Delta\Delta G < 0.5$ kcal/mol). We calculated the mutability score for each position as a percentage of mutations fulfilling these criteria.

(c) Sequence and structural evaluation. For the selection of mutable residues, we combined the evolutionary conservation and mutability scores. Positions with identity conservation $< 90\%$ and FoldX mutability score $> 50\%$ were considered mutable. Next, we mapped the mutable residues onto the protein 3D structures. We visually identified mutable positions and selected those constituting compact patches on the protein surface.

We preferred those patches consisting of residues that were not only structurally, but also sequentially close together, for ease of the subsequent library construction. To achieve a high variability of the designed DNA library, we selected 10–12 mutable residues, the numbers typically used in ribosome display experiments [57,58]. In cases where the patches contained less than 8–10 predicted mutable residues, we chose additional neighboring solvent-accessible residues to bring the total number of residues to 10.

Table 1. List of protein scaffold candidates that were selected for closer in silico structural analysis and literature review. The first five candidates were chosen for further experimental characterization.

PDB Code	UniProt	Protein Name	Source Organism	Size (kDa)	Size (aa)	Number of Cysteines	Reference
4PSF	Q9NWS0	PIH1D1 N-terminal domain	<i>Homo sapiens</i>	15	138	3	[42]
1N3Y	P20702	Alpha-X beta2 integrin I domain	<i>Homo sapiens</i>	22	198	0	[52]
4I3B	P0DM59	Fluorescent protein UnaG wild type	<i>Anguilla japonica</i>	15	139	0	[51]
2F3L	B1WVN5	Lumenal Rfr-domain protein	<i>Cyanothece</i> sp. 51142	20	184	2	[53]
1W2I	P84142	Acylphosphatase	<i>Pyrococcus horikoshii</i>	10	91	0	[50]
4NBO	Q9HD15	Steroid receptor RNA activator protein carboxy-terminal domain	<i>Homo sapiens</i>	13	111	2	[54]
3APA	O60844	Human pancreatic secretory protein ZG16p	<i>Homo sapiens</i>	16	141	0	[55]
4IGI	E9PWQ3	Collagen VI alpha3 N5 domain Human	<i>Mus musculus</i>	22	203	0	[56]
2W4P	P07311	common-type acylphosphatase variant, A99G	<i>Homo sapiens</i>	11	99	0	[48]
4LKT	Q01469	Human Epidermal Fatty Acid Binding Protein (FABP5)	<i>Homo sapiens</i>	15	138	6	[49]
4MJJ	Q14183	C2A domain of DOC2A	<i>Homo sapiens</i>	15	138	5	To be published
4JOX	Q939T0	Cry34Ab1 protein	<i>Bacillus thuringiensis</i>	14	123	0	To be published

In five candidate proteins, we found at least one mutable surface patch, in three of them even two independent patches (Figure 1). We excluded three proteins—4NBO [54], 3APA [55], and 4IGI [56], since they did not contain any suitable surface patch.

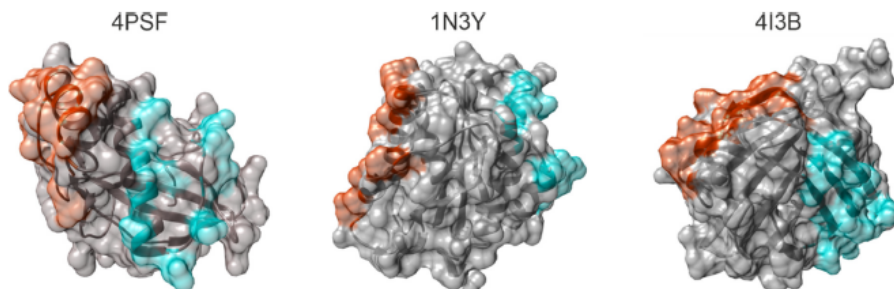


Figure 1. Surface patches of mutable residues identified in the structures of Protein Data Bank (PDB) IDs 4PSF [42], 1N3Y [52], and 4I3B [51]. The proteins are shown as ribbons in semitransparent surface representation. Residues constituting PatchN and PatchC in each protein are colored red and cyan, respectively.

3.1.3. Characterization of Soluble Wild-Type Variants of the Potential Scaffolds

We continued with five small protein scaffold candidates—4PSF [42], 1N3Y [52], 4I3B [51], 1W2I [50], and 2F3L [53]. We analyzed the expression level, solubility, purification simplicity, oligomerization state, secondary structure, and thermal stability of their wild-type (WT) variants.

(a) Protein expression and solubility. We prepared two versions of each scaffold candidate, first with N-terminal His-tag and second with C-terminal His-tag. We tested the expression and solubility of these five proteins in *E. coli* BL21(DE3) at four different temperatures, 37, 30, 25, and 16 °C. We detected high expression levels and excellent solubility of 4PSF, 1N3Y, 4I3B, and 2F3L with the N-terminal His-tag at 16 °C. The solubility varied with temperature. We were not able to express 4PSF, 1N3Y, and 4I3B proteins with the C-terminal His-tag. In the case of 1W2I, the proteins were not expressed in *E. coli* BL21(DE3) strain, only in *E. coli* C41(DE3) and C43(DE3) cells which are usually used for the expression of toxic proteins. Therefore, we decided to exclude the 1W2I protein.

(b) Protein purification. We continued with the purification of the remaining four proteins—4PSF, 1N3Y, 4I3B, and 2F3L, all of them as variants with the N-terminal His-tag. We performed a two-step purification procedure, first on Ni-NTA agarose beads and second by size exclusion chromatography. We isolated the 4PSF, 1N3Y, and 4I3B proteins at very high purity, but the 2F3L showed a minor band of either a homodimer or a non-relevant protein contaminant on SDS-PAGE (Figure 2A). The purified proteins retained solubility without aggregation and degradation at 4 °C in 20 mM sodium phosphate buffer at pH 7.5 and 100 mM NaCl in the range of days and weeks.

(c) Oligomerization. We used dynamic light scattering (DLS) to measure the oligomerization of purified proteins. The 4PSF, 1N3Y, and 4I3B proteins were monodisperse and monomeric based on the intensity-based particle size distribution with Z-averages of 4.6, 5.4, and 4.4 nm in diameter, respectively (Figure 2B). Although the 2F3L protein was monodisperse, the Z-average of 7.8 nm in diameter was higher than expected. It correlates with the impurities appearing on SDS-PAGE (Figure 2A). Since other than monomeric states of a protein would complicate biophysical measurements and binding assays, we decided to exclude 2F3L.

(d) Secondary structure. We checked the folding of the remaining three protein scaffold candidates, 4PSF, 1N3Y, and 4I3B, by circular dichroism (CD) measurements in the ultraviolet (UV) range (Figure 3). Based on the standard analysis of CD spectra using the CDNN software [59], the spectra of all three proteins showed features of regular secondary structures. In case of 4PSF and 1N3Y the combination of alpha-helices and beta-sheets, in case of 4I3B mainly of beta-sheets, agreeing qualitatively with the features of the respective crystal structures.

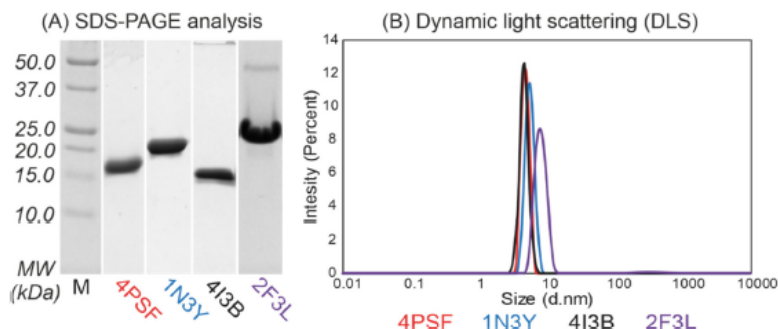


Figure 2. (A) Sodium dodecyl sulphate–polyacrylamide gel electrophoresis (SDS-PAGE, 15%) analysis and (B) dynamic light scattering (DLS) measurement of the purified protein scaffold candidates with N-terminal His-tags after size exclusion chromatography. The 4PSF, 1N3Y, and 4I3B proteins were isolated to high-purity as monomeric proteins. On the contrary, 2F3L showed minor contaminations around 45 kDa on SDS-PAGE gel and DLS measurement confirmed the presence of bigger particles.

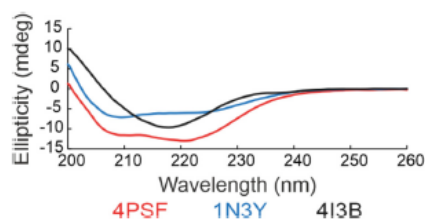


Figure 3. Far-ultraviolet (UV) circular dichroism (CD) spectra of three scaffold candidates. The results indicate that all three proteins acquire the expected secondary structure features. The 4PSF (red) and 1N3Y (blue) showed a combination of alpha-helices and beta-sheets, whereas the 4I3B (black) formed mainly beta-sheets.

(e) **Thermal stability.** We determined the thermal stability of proteins by measuring their melting temperature (T_m) using a circular dichroism technique. The melting temperatures of the WT variants of 4PSF, 1N3Y, and 4I3B were 75 °C, 57 °C, and 47 °C, respectively.

3.1.4. Testing the Stability of the Potential Scaffolds

Before starting a directed molecular evolution campaign, we experimentally verified the mutability of the predicted surface patches, for which we mutated all selected residues in each surface patch to alanines. The alanine-scanning mutagenesis is a method used to identify the structural role of protein residues [60–62]. The idea was that the protein scaffold candidate should sustain the expression, solubility, and folding upon forming a large relatively hydrophobic surface patch of alanines.

Each of three small protein scaffold candidates, 4PSF, 1N3Y, and 4I3B, has two mutable surface patches, either closer to N-terminus (PatchN) or C-terminus (PatchC) (Figure 1). Therefore, we constructed six allAla mutants. We performed the same characterization of the allAla mutants as for the WT proteins. The number of mutated residues, protein expression, solubility, and melting temperatures are summarized in Table 2. Based on these results, we decided not to continue with the 4I3B candidate because its allAla mutants did not express well or were only poorly soluble. The 1N3Y-allAla mutants were both expressed, but only the PatchN was soluble. The best results were achieved for 4PSF because both its allAla-PatchN and allAla-PatchC variants were expressed and soluble.

Table 2. Properties of three most promising wild-type (WT) protein scaffold candidates and their allAla variants. The melting temperatures (T_m) were measured by circular dichroism.

Protein Scaffold Candidate Variant	Number of Mutated Residues	Expression	Solubility	T_m
4PSF-WT	0	Yes	Very good	75 °C
4PSF-allAla-PatchN	10	Yes	Very good	60 °C
4PSF-allAla-PatchC	10	Yes	Very good	67 °C
1N3Y-WT	0	Yes	Very good	57 °C
1N3Y-allAla-PatchN	10	Yes	Good	51 °C
1N3Y-allAla-PatchC	11	Yes	Not soluble	N/A
4I3B-WT	0	Yes	Good	47 °C
4I3B-allAla-PatchN	12	No	No expression	N/A
4I3B-allAla-PatchC	11	Yes	Poor	N/A

Next, we performed control measurements to check for non-specific binding of the 1N3Y and 4PSF scaffold candidates and their allAla mutants. We measured their binding to the capillaries used for microscale thermophoresis (MST) and to sensor chips for surface plasmon resonance (SPR) (Figure S2). We determined that the 1N3Y-WT and 1N3Y-allAla-PatchN were applicable for MST but not for SPR because they non-specifically bind to a clean surface of the SPR sensor chip. We observed no such effects with any of the 4PSF variants.

Considering all the findings, we chose the 4PSF protein as the best scaffold candidate. The WT protein as well as the allAla mutants were expressed at high yield, soluble and easy to purify, were monodispersed and folded, and possessed appropriate characteristics for MST and SPR affinity measurements. We selected the 4PSF C-terminal surface patch (PatchC) for further work because the 4PSF-PatchC-allAla mutant had the highest melting temperature among the allAla mutants.

3.1.5. Testing the Suitability of the Scaffold Candidates for In Vitro Evolution

First, we constructed a degenerate DNA library for ribosome display. The selected PatchC of the 4PSF scaffold candidate had 10 calculated mutable residues (Figure 4). The random mutagenesis of these 10 positions gave rise to the maximal diversity of more than 1012 variants, which agreed with the potential diversity suitable for ribosome display [57,58]. The DNA library was synthesized by GENEWIZ company by the degenerate NNK codons technology. The same company estimated library correctness as being 78%, which was sufficient for further work.

Next, we performed pilot ribosome display selection and crystallization of variants. We took advantage of directed evolution to train the 4PSF scaffold candidate to bind the IL-10 protein as the target molecule. Pilot experiments were undertaken to establish the ribosome display protocol for the initial preselection process (see section Section 3.2.2 below). After the fourth selection round of ribosome display, we selected eight random colonies for two-step purification and crystallization trials. We used commercial screens for preliminary crystallization trials and then manually optimized the conditions to get better diffracting crystals. We started the crystallization with seven variants (G14, G21, H25, H33, J61, J70, and J93). We observed a crystallization process of six variants, and only the G21 did not result in any crystal form in our tested screens. Four variants created crystals with low diffraction quality (ranging 6 to 8 Å). Crystallization of the J61 variant resulted in crystals diffracting up to a high resolution (1.2 Å). We have solved the structure with the molecular replacement method using the original 4PSF structure [42]. The structure, deposited under the PDB entry ID 7AVC, was similar to the original 4PSF structure with root mean square deviation of 0.93 Å calculated on 129 C α atoms (Figure S3). The fold remains stable even after nine mutations at the selected positions. Thus, we established the suitability of the 4PSF scaffold candidate for in vitro evolution by ribosome display. Because the affinity

of the J61 variant to IL-10 was only in the micromolar range we continued in the effort to develop higher affinity binders.

Variant	Position																									
	109	110	111	112	113	114	115	116	117	118	119	120	121	122	123	124	125	126	127	128	129	130	131	132	133	134
WT	R	E	L	V	I	T	I	A	R	E	G	L	E	D	K	Y	N	L	Q	L	N	P	E	W	R	M
A2	R	G	L	V	I	R	I	A	Q	R	G	I	E	F	K	Y	L	L	A	L	N	P	R	W	I	M
A3	R	P	L	V	I	R	I	A	V	G	G	L	E	R	K	Y	G	L	S	L	P	P	L	W	R	M
B4	R	R	L	V	I	R	I	A	R	T	G	L	E	L	K	Y	S	L	N	L	W	P	P	W	S	M
C4	R	V	L	V	I	L	I	A	L	L	G	L	E	V	K	Y	R	L	A	L	Q	P	V	W	Y	M
C11	R	L	L	V	I	L	I	A	I	V	G	L	E	W	K	Y	P	L	P	L	V	P	L	W	E	M
C12	R	G	L	V	I	E	I	A	P	T	G	L	E	W	K	Y	F	L	L	L	E	P	S	W	C	M
E3	R	G	L	V	I	G	I	A	H	R	G	L	E	S	K	Y	Y	L	R	L	G	P	R	W	W	M
F5	R	R	L	V	I	T	I	A	L	R	G	L	E	L	K	Y	P	L	C	L	R	P	A	W	H	M
G3	R	R	L	V	I	A	I	A	P	N	G	L	E	R	K	Y	T	L	H	L	T	P	T	W	S	M
G6	R	G	L	V	I	F	I	A	V	G	G	L	E	S	K	Y	L	L	D	L	E	P	L	W	H	M

Figure 4. The amino acid sequences of the wild-type (WT) 4PSF protein scaffold and its selected variants with the highest affinity to interleukin-10 and the lowest affinity to interleukin-29, bovine serum albumin (BSA), and skimmed milk. The yellow color represents amino acids of 4PSF-WT protein that were mutated (in green) in scaffold variants. The residue numbering corresponds to the PDB entry 4PSF.

3.1.6. Construction of the Final ProBi Scaffold

The final 4PSF scaffold construct used for directed evolution experiments, termed ProBi-WT hereafter, consists of three sequence segments (Figure 5): (i) the N-terminal Strep-tag to simplify purification; (ii) the 4PSF scaffold segment; (iii) the C-terminal c-Myc-tag. It was added to detect variants expressed properly to the c-Myc tag and exclude fragments emerging because of premature stop codons or frameshifts in the randomized DNA library. The expression level, solubility, and biophysical features of this new ProBi scaffold construct were similar to the original scaffold candidate.

MAW*SHPQFEK SMAQGPGQPG FCIKTNSSSEG KVF***INICHSP SIPP***PADVTE EELLQMLEED*
AGFRIPMSL *GEPHAELDAK GQGCTAYDVA VNSDFYRRMQ NSDFLRELVI* **TIAREGLEDK**
YNLQLNPEWR *MKNRPFMGS IGSEQKLISE EDL*

Figure 5. The amino acid sequence of the wild type ProBi-WT protein scaffold. The N-terminal Strep-tag and C-terminal c-Myc-tag are in bold, the 4PSF scaffold segment is in italic. The ten mutable amino acid residues forming the PatchC are highlighted in red.

3.2. Application of the ProBi Scaffold on the Interleukin-10 (IL-10) Target as a Model System

3.2.1. Selection of the Target Protein

Cytokines from the family of interleukin-10 are medically important signaling proteins of native immunity [31–33]. Immunosuppressive effects of the prototypical member of the family, IL-10, which may hinder immunotherapeutic strategies of cancer therapy [32], are not completely understood. In addition, monodispersity, CD spectra, and signaling on the RAW264.7 murine cell line of recombinant IL-10 produced in the laboratory encouraged use of this cytokine as the biologically relevant and molecularly well-defined target for our study.

3.2.2. Selection of Novel ProBi-Based Binders by Ribosome Display

(a) Initial preselection process. We performed four selection rounds of ribosome display, with the following preselection conditions: incubation for an hour with a mixture of BSA, IFN γ , and ProBi-WT scaffold; blocking solution 3% BSA for all rounds. After the fourth round, we selected 190 random colonies (together with ProBi-WT) for a small-scale expression in deep-96-well plates and for detection of binding to IL-10 using the ELISA assay. We took advantage of the C-terminal c-Myc-tag to reveal those clones that have the correct open reading frame and bind the IL-10. From these, we selected 47 clones with the highest signal for larger-scale expression in deep-24-well plates. These 47 clones were tested for binding to IL-29, which shares the IL-10R2 receptor with IL-10 [63]. We discovered that most of the clones showed binding to IL-29 as well as to IL-10. Most variants also displayed non-specific binding to BSA and skimmed milk.

(b) Optimized preselection process. To decrease the non-specific binding of ProBi variants to BSA and milk proteins, we optimized the preselection conditions. The initial preselection conditions were extended in three ways. We (1) included IL-29 to the preselection mix; (2) varied the blocking solution between BSA (used in the first and third round) and skimmed milk (used in the second and fourth round); and (3) performed the preselection reaction in three consecutive wells. Otherwise, we completed the ribosome display the same way as in the point a) above. The optimization of the preselection monitored on 190 variants led to a decrease of non-specific binding to the BSA and milk to 50% and 60%, respectively, of the binding to IL-10. For further characterization, we selected 10 variants (Figure 4) with high affinities to IL-10 and low affinities to IL-29, BSA, and milk. We created the phylogenetic tree that is described in Supporting Information (Figure S4).

3.2.3. Characterization of Novel ProBi-Based Binders

(a) Affinity estimation by ELISA assay. We expressed and purified ten selected variants by one step purification on affinity StrepTactinXT resin and performed ELISA measurements to estimate their affinities to IL-10 and BSA (data not shown). We discarded six variants with the highest binding background to BSA and continued with four variants for more detailed characterization.

(b) Affinity measurements by MST. We expressed and purified ProBi-WT and its four variants labeled F5, G3, A2, and G6 by two-step purification on affinity StrepTactinXT resin and size exclusion chromatography. We successfully measured the IL-10 binding affinities of two variants, G3 and F5 (Figure 6). Their dissociation constants (K_d) are shown in Table 3. The F5 variant had the highest affinities, 6 nM in Tris (pH 8.0) buffer, and 15 nM in Hepes (pH 7.5) buffer, respectively. We detected binding of the A2 variant to IL-10 but we were not able to reach the bound (saturation) state of the binding curve. Therefore, we only estimated the affinities to be higher than 1 μ M. The G3 variant assembled into a dimer, and the A2 and F5 variants behaved the same way as the ProBi-WT protein. The G6 variant showed the highest tendency to form oligomers (data not shown) and, therefore, it was discarded.

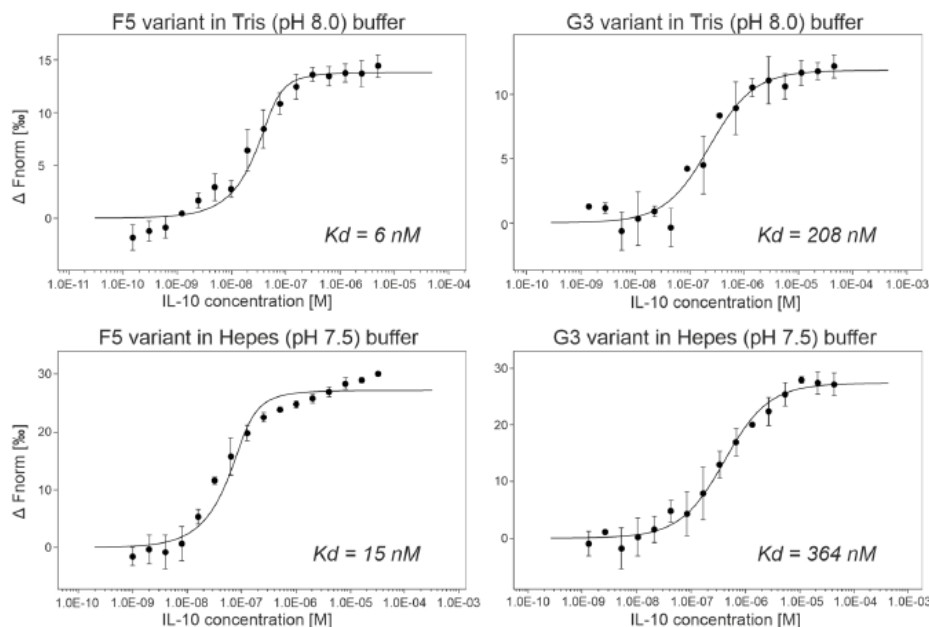


Figure 6. The microscale thermophoresis (MST) curves of two best ProBi IL-10 binders, F5 and G3. The results showed that the change of buffer from Tris to Hepes and pH from 8.0 to 7.5 did not affect the affinities.

Table 3. Variants of the ProBi scaffold sorted by their affinities to IL-10. The table shows affinities, response amplitude during microscale thermophoresis (MST) measurements, number of replicates of the MST measurements, and melting temperatures (T_m) measured by the nanoDSF method. Not measurable indicates that the affinity is so low that it falls beyond the dynamic range of the MST technique.

ProBi Variant (Buffer)	Affinity	Response Amplitude	Replicates	T_m
WT (Tris)	Not measurable	Not measurable	3	66 °C
F5 (Tris)	6 nM	14	4	51 °C
F5 (Hepes)	15 nM	27	3	N/A
G3 (Tris)	208 nM	12	3	58 °C
G3 (Hepes)	364 nM	27	3	N/A
A2 (Tris)	>1 μ M	N/A	2	48 °C

To evaluate the affinities of ProBi variants to IL-10, we utilized the microscale thermophoresis technique that utilizes low material consumption [64]. We used a commercial kit to fluorescently label the IL-10 with C-terminal His-tag as a target molecule and titrated it by evolved ProBi variants with the N-terminal Strep-tag. The measured affinities are shown in Table 3. We did not detect binding of IL-10 to the parental wild-type ProBi scaffold in our binding buffer (50 mM Tris-HCl, pH 8.0, 300 mM NaCl, 0.1% Pluronic F-127). We cannot measure the affinities to BSA and milk in our MST setup because they do not possess His-tag for labeling.

(c) Characterization of ProBi variants with the highest affinity. The chromatograms from size exclusion chromatography and SDS-PAGE analysis of purified proteins are shown in Figure S5. We measured the melting temperature (T_m) of the variants (Table 3) finding that T_m was lower than for the WT protein, but still in a range acceptable for practical

purposes. We confirmed the folded structure of the selected ProBi variants with a high content of alpha helices according to their circular dichroism spectra (Figure S6).

(d) Inhibitory assay. We tested potential of the G3 and F5 variants to inhibit the IL-10 signaling pathway by a competitive binding assay on the RAW264.7 cell line, which expresses both IL10R1 and IL10R2 receptors on the cell surface. We used ProBi-WT protein as a negative control. Using these experimental conditions, we observed no inhibition of the IL-10 signaling pathway by either G3 or F5 (Figure S7). We hypothesize that these ProBi variants bind to the surface of IL-10 in such a way that they do not prevent IL-10 binding to the receptors IL10R1 and/or IL10R2 and do not block the signalization.

In order to identify truly inhibitory binders with a potential medical use, we need to include more ProBi variants, correlate their activity with the effect of neutralizing anti-IL-10 antibodies, test the inhibition on more cell types (e.g., THP-1 or U937), and possibly monitor signalization by outcomes other than STAT3 phosphorylation. The ProBi IL-10 binders developed as a proof of principle will have to be engineered further in order to inhibit the signaling pathway of IL-10 cytokine.

3.2.4. Further Development of Scaffold Selection and Improvement of Probi-Based Binders

We are aware that the procedure of scaffold selection can be optimized, and here we discuss possible future modifications of the present protocol.

(a) The first step of our procedure, the visual screening of the PDB, can be performed more systematically. A possible way would be to automate selection of monomeric small proteins and the following identification of mutable patches on their surfaces by in silico screening by employing the FoldX [36] or Rosetta [65] programs. We can also include proteins that were produced not only in *E. coli* expression systems because the expression level and solubility of the tested scaffolds can be tested in a high-throughput format.

(b) The proposed workflow will be further tested by development of our second candidate scaffold, protein alpha-X beta2 integrin I domain (UniProt ID P20702, structure of PDB ID 1N3Y [52]) in the near future.

(c) The selectivity of the best ProBi binders to other IL-10 family cytokines was tested only by the ELISA pre-screening against IL-29 (Section 3.2.2). Further development of the binders would undoubtedly require thorough checking of their cross-reactivity to more cytokines and other proteins.

(d) A substantial challenge for possible medical use of the binders is their immunogenicity [24]. We do not expect the ProBi-based binders to be immunogenic as the scaffold is derived from the human PIH1 domain-containing protein 1 (UniProt ID Q9NWS0, structure of PDB ID 4PSF [42]). However, potentially immunogenic scaffolds could be repurposed for molecular imaging [16].

(e) The directed evolution methodologies [66,67] offer avenues to development of proteins with new properties. Over the years, several display techniques [68,69] have evolved and they offer alternative and complementary ways to the selection of optimal protein molecules for the task. In this work, we make use only one of the display techniques, ribosome display. Because the yeast display offers certain advantages compared to ribosome display, we designed the final ProBi scaffold construct to be directly used by both methods. Therefore, we included the C-terminal c-Myc-tag that is widely used for high-throughput detection in Fluorescence-activated cell sorting (FACS).

(f) The protein scaffolds as well as antibodies typically bind just one interaction partner. Two independently mutable patches on one protein scaffold molecule could open a way to train binders to interact simultaneously with two partners. Therefore, we aimed at scaffolds with two mutable patches. Such a feature would mimic a function of natural proteins, such as cytokines and/or other proteins signaling through simultaneous binding to two receptors i.e., via formation of a ternary complex. The protein scaffolds can also work as “synthekines” to engineer non-natural receptor heterodimers that could activate new unexplored cellular responses [70].

4. Conclusions

Protein scaffolds represent a great engineering tool that could complement functions of more commonly used antibodies in high-affinity binding of biomolecular targets. We think that there is no “one-scaffold-fits-all” and that the development of new scaffolds tailored to specific functions is crucial for real-life applications, e.g., regulation of signaling pathways *in vivo*, biologics, and molecular imaging.

Visual inspection of several hundred structures from the PDB, *in silico* investigation of about 100 selected candidates, and finally experimental examination of 12 of them, led to selection of two potentially useful scaffold proteins. The first candidate was based on the human PIH1 domain-containing protein 1 (UniProt ID Q9NWS0, structure of PDB ID 4PSF [42]) and the second one on the alpha-X beta2 integrin I domain (UniProt ID P20702, structure of PDB ID 1N3Y [52]). The latter of the two candidates is going to be developed further in the near future.

We preferred the 4PSF protein structure because it contained two surface patches amenable for independent mutagenesis. Thus, we modified the 4PSF protein construct into the protein scaffold construct called ProBi that was ready to be used in both ribosome and yeast display technology. For the purpose of this work, we focused on one of the patches and utilized the ribosome display to evolve the ProBi scaffold into the binders of interleukin-10 with nanomolar affinity. In the future, we plan to include more scaffold candidates and concentrate on their other features, such as signaling inhibition, immunogenicity, and selectivity.

In this work, we present a proof of concept methodology to identify protein structures that could be converted into a new protein scaffold constructs. We experimentally proved that at least one of them could be adapted into binders of a medically important target with nanomolar affinity by methods of directed evolution.

Supplementary Materials: The following are available online at <https://www.mdpi.com/1999-4915/13/2/190/s1>, Table S1: List of primers, Table S2: Data processing statistics of PDB entry 7AVC. Figure S1: DNA sequences of internal arrangement within (A) the pRDVsm and (B) pETsm vectors. Figure S2: Testing of non-specific binding of scaffold candidates. Figure S3: Structural alignment. Figure S4: The phylogenetic tree of ten ProBi scaffold variants. Figure S5: SDS-PAGE (15%) analysis of purified ProBi variants. Figure S6: Circular dichroism spectra of (A) ProBi scaffold. Figure S7: Inhibition of the IL-10 signaling pathway estimated by a competitive binding assay.

Author Contributions: Conceptualization, B.S. and P.M.; methodology, B.S., P.M. and J.Z.; computational analysis, L.B., J.Č. and B.S.; molecular biology experiments, P.N.P., M.H., L.K. and P.M.; biophysical experiments P.N.P., M.H., T.C., G.F., P.K., Š.H. and J.P.; data analysis, M.H., P.N.P., Š.H., L.K., P.K., J.P. and J.Z.; writing—original draft preparation, B.S., P.M. and L.B.; writing—review and editing, B.S., P.M., P.N.P. and M.H.; visualization, P.M., M.H. and P.N.P.; supervision, B.S.; project administration, B.S. and P.M.; funding acquisition, B.S.; P.N.P. and M.H. contributed equally to the manuscript preparation. All authors have read and agreed to the published version of the manuscript.

Funding: This research was funded by the Czech Science Foundation, grant 16-20507S, Czech Academy of Sciences, grant RVO 86652036, Ministry of Education, Youth, and Sports of the Czech Republic, grant LM2015043, LM2018127.

Institutional Review Board Statement: Not applicable.

Informed Consent Statement: Not applicable.

Data Availability Statement: The structural data presented in this study are openly available in the Protein Data Bank, identification number 7AVC. All other data presented in this study are available on request from the corresponding authors.

Acknowledgments: We thank Marketa Janovska for her invaluable technical assistance.

Conflicts of Interest: The authors declare no conflict of interest.





References

- Bryson, J.W.; Desjarlais, J.R.; Handel, T.M.; DeGrado, W.F. From coiled coils to small globular proteins: Design of a native-like three-helix bundle. *Protein Sci.* **1998**, *7*, 1404–1414. [\[CrossRef\]](#) [\[PubMed\]](#)
- Khoury, G.A.; Smadbeck, J.; Kieslich, C.A.; Floudas, C.A. Protein folding and de novo protein design for biotechnological applications. *Trends Biotechnol.* **2014**, *32*, 99–109. [\[CrossRef\]](#) [\[PubMed\]](#)
- Burnside, D.; Schoenrock, A.; Moteshareie, H.; Hooshyar, M.; Basra, P.; Hajikarimlou, M.; Dick, K.; Barnes, B.; Kazmirchuk, T.; Jessulat, M.; et al. In Silico Engineering of Synthetic Binding Proteins from Random Amino Acid Sequences. *iScience* **2019**, *11*, 375–387. [\[CrossRef\]](#) [\[PubMed\]](#)
- Kortemme, T.; Baker, D. Computational design of protein-protein interactions. *Curr. Opin. Chem. Biol.* **2004**, *8*, 91–97. [\[CrossRef\]](#) [\[PubMed\]](#)
- Mikulecky, P.; Cerny, J.; Biedermannova, L.; Petrokova, H.; Kuchar, M.; Vondrasek, J.; Maly, P.; Sebo, P.; Schneider, B. Increasing affinity of interferon-gamma receptor 1 to interferon-gamma by computer-aided design. *BioMed Res. Int.* **2013**, *2013*, 752514. [\[CrossRef\]](#)
- Smith, G.P.; Petrenko, V.A. Phage Display. *Chem. Rev.* **1997**, *97*, 391–410. [\[CrossRef\]](#)
- Hosse, R.J.; Rothe, A.; Power, B.E. A new generation of protein display scaffolds for molecular recognition. *Protein Sci.* **2006**, *15*, 14–27. [\[CrossRef\]](#)
- Brender, J.R.; Shultis, D.; Khattak, N.A.; Zhang, Y. An Evolution-Based Approach to De Novo Protein Design. *Methods Mol. Biol.* **2017**, *1529*, 243–264.
- Goldenzweig, A.; Goldsmith, M.; Hill, S.E.; Gertman, O.; Laurino, P.; Ashani, Y.; Dym, O.; Unger, T.; Albeck, S.; Prilusky, J.; et al. Automated Structure- and Sequence-Based Design of Proteins for High Bacterial Expression and Stability. *Mol. Cell* **2016**, *63*, 337–346. [\[CrossRef\]](#)
- Musil, M.; Stourac, J.; Bendl, J.; Brezovsky, J.; Prokop, Z.; Zendulka, J.; Martinek, T.; Bednar, D.; Damborsky, J. FireProt: Web server for automated design of thermostable proteins. *Nucleic Acids Res.* **2017**, *45*, W393–W399. [\[CrossRef\]](#)
- Zahradnik, J.; Kolarova, L.; Peleg, Y.; Kolenko, P.; Svidenska, S.; Charnavets, T.; Unger, T.; Sussman, J.L.; Schneider, B. Flexible regions govern promiscuous binding of IL-24 to receptors IL-20R1 and IL-22R1. *FEBS J.* **2019**, *286*, 3858–3873. [\[CrossRef\]](#) [\[PubMed\]](#)
- Banta, S.; Dooley, K.; Shur, O. Replacing antibodies: Engineering new binding proteins. *Annu. Rev. Biomed. Eng.* **2013**, *15*, 93–113. [\[CrossRef\]](#)
- Yu, X.; Yang, Y.P.; Dikici, E.; Deo, S.K.; Daunert, S. Beyond Antibodies as Binding Partners: The Role of Antibody Mimetics in Bioanalysis. *Annu. Rev. Anal. Chem.* **2017**, *10*, 293–320. [\[CrossRef\]](#) [\[PubMed\]](#)
- Skerra, A. Engineered protein scaffolds for molecular recognition. *J. Mol. Recognit.* **2000**, *13*, 167–187. [\[CrossRef\]](#)
- Hey, T.; Fiedler, E.; Rudolph, R.; Fiedler, M. Artificial, non-antibody binding proteins for pharmaceutical and industrial applications. *Trends Biotechnol.* **2005**, *23*, 514–522. [\[CrossRef\]](#)
- Simeon, R.; Chen, Z. In vitro-engineered non-antibody protein therapeutics. *Protein Cell* **2018**, *9*, 3–14. [\[CrossRef\]](#)
- Nord, K.; Gunneriusson, E.; Ringdahl, J.; Stahl, S.; Uhlen, M.; Nygren, P.A. Binding proteins selected from combinatorial libraries of an alpha-helical bacterial receptor domain. *Nat. Biotechnol.* **1997**, *15*, 772–777. [\[CrossRef\]](#)
- Binz, H.K.; Amstutz, P.; Pluckthun, A. Engineering novel binding proteins from nonimmunoglobulin domains. *Nat. Biotechnol.* **2005**, *23*, 1257–1268. [\[CrossRef\]](#)
- Skerra, A. Alternative non-antibody scaffolds for molecular recognition. *Curr. Opin. Biotechnol.* **2007**, *18*, 295–304. [\[CrossRef\]](#)
- Barinka, C.; Ptacek, J.; Richter, A.; Novakova, Z.; Morath, V.; Skerra, A. Selection and characterization of Anticalins targeting human prostate-specific membrane antigen (PSMA). *Protein Eng. Des. Select.* **2016**, *29*, 105–115. [\[CrossRef\]](#)
- Bedford, R.; Tiede, C.; Hughes, R.; Curd, A.; McPherson, M.J.; Peckham, M.; Tomlinson, D.C. Alternative reagents to antibodies in imaging applications. *Biophys. Rev.* **2017**, *9*, 299–308. [\[CrossRef\]](#) [\[PubMed\]](#)
- Rothe, C.; Skerra, A. Anticalin(R) Proteins as Therapeutic Agents in Human Diseases. *BioDrugs* **2018**, *32*, 233–243. [\[CrossRef\]](#) [\[PubMed\]](#)
- Kosztyu, P.; Kuchar, M.; Cerny, J.; Barkocziava, L.; Maly, M.; Petrokova, H.; Czernekova, L.; Liskova, V.; Raskova Kafkova, L.; Knotigova, P.; et al. Proteins mimicking epitope of HIV-1 virus neutralizing antibody induce virus-neutralizing sera in mice. *EBioMedicine* **2019**, *47*, 247–256. [\[CrossRef\]](#) [\[PubMed\]](#)
- Vazquez-Lombardi, R.; Phan, T.G.; Zimmermann, C.; Lowe, D.; Jermutus, L.; Christ, D. Challenges and opportunities for non-antibody scaffold drugs. *Drug Discov. Today* **2015**, *20*, 1271–1283. [\[CrossRef\]](#) [\[PubMed\]](#)
- Azhar, A.; Ahmad, E.; Zia, Q.; Rauf, M.A.; Owais, M.; Ashraf, G.M. Recent advances in the development of novel protein scaffolds based therapeutics. *Int. J. Biol. Macromol.* **2017**, *102*, 630–641. [\[CrossRef\]](#)
- Ahmad, J.N.; Li, J.; Biedermannova, L.; Kuchar, M.; Sipova, H.; Semeradtova, A.; Cerny, J.; Petrokova, H.; Mikulecky, P.; Polinek, J.; et al. Novel high-affinity binders of human interferon gamma derived from albumin-binding domain of protein G. *Proteins* **2012**, *80*, 774–789. [\[CrossRef\]](#)
- Kuchar, M.; Vankova, L.; Petrokova, H.; Cerny, J.; Osicka, R.; Pelak, O.; Sipova, H.; Schneider, B.; Homola, J.; Sebo, P.; et al. Human interleukin-23 receptor antagonists derived from an albumin-binding domain scaffold inhibit IL-23-dependent ex vivo expansion of IL-17-producing T-cells. *Proteins* **2014**, *82*, 975–989. [\[CrossRef\]](#)

28. Kruziki, M.A.; Bhatnagar, S.; Woldring, D.R.; Duong, V.T.; Hackel, B.J. A 45-Amino-Acid Scaffold Mined from the PDB for High-Affinity Ligand Engineering. *Chem. Biol.* **2015**, *22*, 946–956. [[CrossRef](#)]
29. Alsultan, A.M.; Chin, D.Y.; Howard, C.B.; de Bakker, C.J.; Jones, M.L.; Mahler, S.M. Beyond Antibodies: Development of a Novel Protein Scaffold Based on Human Chaperonin 10. *Sci. Rep.* **2016**, *5*, 37348. [[CrossRef](#)]
30. Berman, H.M.; Battistuz, T.; Bhat, T.N.; Bluhm, W.F.; Bourne, P.E.; Burkhardt, K.; Feng, Z.; Gilliland, G.L.; Iype, L.; Jain, S.; et al. The Protein Data Bank. *Acta Crystallogr. D Biol. Crystallogr.* **2002**, *58 Pt 6*, 899–907. [[CrossRef](#)]
31. El Kasmi, K.C.; Smith, A.M.; Williams, L.; Neale, G.; Panopoulos, A.D.; Watowich, S.S.; Hacker, H.; Foxwell, B.M.; Murray, P.J. Cutting edge: A transcriptional repressor and corepressor induced by the STAT3-regulated anti-inflammatory signaling pathway. *J. Immunol.* **2007**, *179*, 7215–7219. [[CrossRef](#)] [[PubMed](#)]
32. Asadullah, K.; Sterry, W.; Volk, H.D. Interleukin-10 therapy—Review of a new approach. *Pharmacol. Rev.* **2003**, *55*, 241–269. [[CrossRef](#)] [[PubMed](#)]
33. Liu, Y.; de Waal Malefyt, R.; Briere, F.; Parham, C.; Bridon, J.M.; Banchereau, J.; Moore, K.W.; Xu, J. The EBV IL-10 homologue is a selective agonist with impaired binding to the IL-10 receptor. *J. Immunol.* **1997**, *158*, 604–613. [[PubMed](#)]
34. Larkin, M.A.; Blackshields, G.; Brown, N.P.; Chenna, R.; McGettigan, P.A.; McWilliam, H.; Valentin, F.; Wallace, I.M.; Wilm, A.; Lopez, R.; et al. Clustal W and Clustal X version 2.0. *Bioinformatics* **2007**, *23*, 2947–2948. [[CrossRef](#)] [[PubMed](#)]
35. Okonechnikov, K.; Golosova, O.; Fursov, M.; Ugene Team. Unipro UGENE: A unified bioinformatics toolkit. *Bioinformatics* **2012**, *28*, 1166–1167. [[CrossRef](#)] [[PubMed](#)]
36. Schymkowitz, J.; Borg, J.; Stricher, F.; Nys, R.; Rousseau, F.; Serrano, L. The FoldX web server: An online force field. *Nucleic Acids Res.* **2005**, *33*, W382–W388. [[CrossRef](#)]
37. Mikulecky, P.; Zahradnik, J.; Kolenko, P.; Cerny, J.; Charnavets, T.; Kolarova, L.; Necasova, I.; Pham, P.N.; Schneider, B. Crystal structure of human interferon-gamma receptor 2 reveals the structural basis for receptor specificity. *Acta Crystallogr. D Struct. Biol.* **2016**, *72 Pt 9*, 1017–1025. [[CrossRef](#)]
38. Kabsch, W. Xds. *Acta Crystallogr. D Biol. Crystallogr.* **2010**, *66 Pt 2*, 125–132. [[CrossRef](#)]
39. Evans, P.R.; Murshudov, G.N. How good are my data and what is the resolution? *Acta Crystallogr. D Biol. Crystallogr.* **2013**, *69 Pt 7*, 1204–1214. [[CrossRef](#)]
40. Winn, M.D.; Ballard, C.C.; Cowtan, K.D.; Dodson, E.J.; Emsley, P.; Evans, P.R.; Keegan, R.M.; Krissinel, E.B.; Leslie, A.G.; McCoy, A.; et al. Overview of the CCP4 suite and current developments. *Acta Crystallogr. D Biol. Crystallogr.* **2011**, *67 Pt 4*, 235–242. [[CrossRef](#)]
41. McCoy, A.J.; Grosse-Kunstleve, R.W.; Adams, P.D.; Winn, M.D.; Storoni, L.C.; Read, R.J. Phaser crystallographic software. *J. Appl. Crystallogr.* **2007**, *40 Pt 4*, 658–674. [[CrossRef](#)]
42. Horejsi, Z.; Stach, L.; Flower, T.G.; Joshi, D.; Flynn, H.; Skehel, J.M.; O'Reilly, N.J.; Ogorodowicz, R.W.; Smerdon, S.J.; Boulton, S.J. Phosphorylation-dependent PIH1D1 interactions define substrate specificity of the R2TP cochaperone complex. *Cell Rep.* **2014**, *7*, 19–26. [[CrossRef](#)] [[PubMed](#)]
43. Murshudov, G.N.; Skubak, P.; Lebedev, A.A.; Pannu, N.S.; Steiner, R.A.; Nicholls, R.A.; Winn, M.D.; Long, F.; Vagin, A.A. REFMAC5 for the refinement of macromolecular crystal structures. *Acta Crystallogr. D Biol. Crystallogr.* **2011**, *67 Pt 4*, 355–367. [[CrossRef](#)]
44. Emsley, P.; Lohkamp, B.; Scott, W.G.; Cowtan, K. Features and development of Coot. *Acta Crystallogr. D Biol. Crystallogr.* **2010**, *66 Pt 4*, 486–501. [[CrossRef](#)]
45. Williams, C.J.; Headd, J.J.; Moriarty, N.W.; Prisant, M.G.; Videau, L.L.; Deis, L.N.; Verma, V.; Keedy, D.A.; Hintze, B.J.; Chen, V.B.; et al. MolProbity: More and better reference data for improved all-atom structure validation. *Protein Sci.* **2018**, *27*, 293–315. [[CrossRef](#)] [[PubMed](#)]
46. Dreier, B.; Pluckthun, A. Ribosome display: A technology for selecting and evolving proteins from large libraries. *Methods Mol. Biol.* **2011**, *687*, 283–306. [[PubMed](#)]
47. Zahnd, C.; Amstutz, P.; Pluckthun, A. Ribosome display: Selecting and evolving proteins in vitro that specifically bind to a target. *Nat. Methods* **2007**, *4*, 269–279. [[CrossRef](#)]
48. Lam, S.Y.; Yeung, R.C.; Yu, T.H.; Sze, K.H.; Wong, K.B. A rigidifying salt-bridge favors the activity of thermophilic enzyme at high temperatures at the expense of low-temperature activity. *PLoS Biol.* **2011**, *9*, e1001027. [[CrossRef](#)]
49. Armstrong, E.H.; Goswami, D.; Griffin, P.R.; Noy, N.; Ortlund, E.A. Structural basis for ligand regulation of the fatty acid-binding protein 5, peroxisome proliferator-activated receptor beta/delta (FABP5-PPARbeta/delta) signaling pathway. *J. Biol. Chem.* **2014**, *289*, 14941–14954. [[CrossRef](#)]
50. Cheung, Y.Y.; Lam, S.Y.; Chu, W.K.; Allen, M.D.; Bycroft, M.; Wong, K.B. Crystal structure of a hyperthermophilic archaeal acylphosphatase from *Pyrococcus horikoshii*—Structural insights into enzymatic catalysis, thermostability, and dimerization. *Biochemistry* **2005**, *44*, 4601–4611. [[CrossRef](#)]
51. Kumagai, A.; Ando, R.; Miyatake, H.; Greimel, P.; Kobayashi, T.; Hirabayashi, Y.; Shimogori, T.; Miyawaki, A. A bilirubin-inducible fluorescent protein from eel muscle. *Cell* **2013**, *153*, 1602–1611. [[CrossRef](#)] [[PubMed](#)]
52. Vorup-Jensen, T.; Ostermeier, C.; Shimaoka, M.; Hommel, U.; Springer, T.A. Structure and allosteric regulation of the alpha X beta 2 integrin I domain. *Proc. Natl. Acad. Sci. USA* **2003**, *100*, 1873–1878. [[CrossRef](#)] [[PubMed](#)]

53. Buchko, G.W.; Ni, S.; Robinson, H.; Welsh, E.A.; Pakrasi, H.B.; Kennedy, M.A. Characterization of two potentially universal turn motifs that shape the repeated five-residues fold—Crystal structure of a luminal pentapeptide repeat protein from *Cyanospora* 51142. *Protein Sci.* **2006**, *15*, 2579–2595. [[CrossRef](#)] [[PubMed](#)]
54. McKay, D.B.; Xi, L.; Barthel, K.K.B.; Cech, T.R. Structure and function of steroid receptor RNA activator protein, the proposed partner of SRA noncoding RNA. *J. Mol. Biol.* **2014**, *426*, 1766–1785. [[CrossRef](#)] [[PubMed](#)]
55. Kanagawa, M.; Satoh, T.; Ikeda, A.; Nakano, Y.; Yagi, H.; Kato, K.; Kojima-Aikawa, K.; Yamaguchi, Y. Crystal structures of human secretory proteins ZG16p and ZG16b reveal a Jacalin-related beta-prism fold. *Biochem. Biophys. Res. Commun.* **2011**, *404*, 201–205. [[CrossRef](#)]
56. Becker, A.K.; Mikolajek, H.; Paulsson, M.; Wagener, R.; Werner, J.M. A structure of a collagen VI VWA domain displays N and C termini at opposite sides of the protein. *Structure* **2014**, *22*, 199–208. [[CrossRef](#)]
57. Groves, M.A.; Osbourn, J.K. Applications of ribosome display to antibody drug discovery. *Expert Opin. Biol. Ther.* **2005**, *5*, 125–135. [[CrossRef](#)]
58. Pluckthun, A. Ribosome display: A perspective. *Methods Mol. Biol.* **2012**, *805*, 3–28.
59. Bohm, G.; Muhr, R.; Jaenicke, R. Quantitative analysis of protein far UV circular dichroism spectra by neural networks. *Protein Eng.* **1992**, *5*, 191–195. [[CrossRef](#)] [[PubMed](#)]
60. Lefevre, F.; Remy, M.H.; Masson, J.M. Alanine-stretch scanning mutagenesis: A simple and efficient method to probe protein structure and function. *Nucleic Acids Res.* **1997**, *25*, 447–448. [[CrossRef](#)] [[PubMed](#)]
61. Weiss, G.A.; Watanabe, C.K.; Zhong, A.; Goddard, A.; Sidhu, S.S. Rapid mapping of protein functional epitopes by combinatorial alanine scanning. *Proc. Natl. Acad. Sci. USA* **2000**, *97*, 8950–8954. [[CrossRef](#)] [[PubMed](#)]
62. Morrison, K.L.; Weiss, G.A. Combinatorial alanine-scanning. *Curr. Opin. Chem. Biol.* **2001**, *5*, 302–307. [[CrossRef](#)]
63. Miknis, Z.J.; Magracheva, E.; Li, W.; Zdanov, A.; Kotenko, S.V.; Wlodawer, A. Crystal structure of human interferon-lambda1 in complex with its high-affinity receptor interferon-lambdaR1. *J. Mol. Biol.* **2010**, *404*, 650–664. [[CrossRef](#)] [[PubMed](#)]
64. Jerabek-Willemsen, M.; Wienken, C.J.; Braun, D.; Baaske, P.; Duhr, S. Molecular interaction studies using microscale thermophoresis. *Assay Drug Dev. Technol.* **2011**, *9*, 342–353. [[CrossRef](#)]
65. Moretti, R.; Lyskov, S.; Das, R.; Meiler, J.; Gray, J.J. Web-accessible molecular modeling with Rosetta: The Rosetta Online Server that Includes Everyone (ROSIE). *Protein Sci.* **2018**, *27*, 259–268. [[CrossRef](#)]
66. Hibbert, E.G.; Dalby, P.A. Directed evolution strategies for improved enzymatic performance. *Microb. Cell Factories* **2005**, *4*, 29. [[CrossRef](#)]
67. Bloom, J.D.; Arnold, F.H. In the light of directed evolution: Pathways of adaptive protein evolution. *Proc. Natl. Acad. Sci. USA* **2009**, *106* (Suppl. 1), 9995–10000. [[CrossRef](#)]
68. Packer, M.S.; Liu, D.R. Methods for the directed evolution of proteins. *Nat. Rev. Genet.* **2015**, *16*, 379–394. [[CrossRef](#)]
69. Xiao, H.; Bao, Z.; Zhao, H. High Throughput Screening and Selection Methods for Directed Enzyme Evolution. *Ind. Eng. Chem. Res.* **2015**, *54*, 4011–4020. [[CrossRef](#)]
70. Moraga, I.; Spangler, J.B.; Mendoza, J.L.; Gakovic, M.; Wehrman, T.S.; Krutzik, P.; Garcia, K.C. Synthekines are surrogate cytokine and growth factor agonists that compel signaling through non-natural receptor dimers. *eLife* **2017**, *6*, e22882. [[CrossRef](#)]

De novo developed protein binders mimicking Interferon lambda signaling

Lucie Kolářová¹, Jiří Zahradník² , Maroš Huličiak¹, Pavel Mikulecký¹ , Yoav Peleg², Maya Shemesh², Gideon Schreiber²  and Bohdan Schneider¹ 

¹ Institute of Biotechnology of the Czech Academy of Sciences, BIOCEV, Vestec, Czech Republic

² Department of Biomolecular Sciences, Weizmann Institute of Science, Rehovot, Israel

Keywords

cytokine signaling; cytokines; directed evolution; IFN- λ ; IL-29; interferon lambda; protein scaffolds; yeast display

Correspondence

B. Schneider, Institute of Biotechnology of the Czech Academy of Sciences, BIOCEV, CZ-252 50 Vestec, Czech Republic
 Tel: +420 728 303 566
 E-mail: bohdan.schneider@ibt.cas.cz

(Received 15 September 2021, revised 12 November 2021, accepted 25 November 2021)

doi:10.1111/febs.16300

We hereby describe the process of design and selection of nonantibody protein binders mimicking cytokine signaling. We chose to mimic signaling of IFN- λ 1, type 3 interferon (also known as IL-29) for its novelty and the importance of its biological functions. All four known interferons λ signal through binding to the extracellular domains of IL-28 receptor 1 (IL-28R1) and IL-10 receptor 2 (IL-10R2). Our binders were therefore trained to bind both receptors simultaneously. The bifunctional binder molecules were developed by yeast display, a method of directed evolution. The signaling capacity of the bivalent binders was tested by measuring phosphorylation of the JAK/STAT signaling pathway and production of mRNA of six selected genes naturally induced by IFN- λ 1 in human cell lines. The newly developed bivalent binders offer opportunities to study cytokine-related biological functions and modulation of the cell behavior by receptor activation on the cell surfaces alternative to the use of natural IFN- λ .

Introduction

Medical treatment by therapeutics based on protein molecules has expanded dramatically over the last 40 years since the approval of recombinant insulin [1]. Currently, over 200 different protein drugs and peptides have been approved by the US Food and Drug Administration [2]. The development of biologicals has accelerated with advancement of protein engineering methods that opened ways to modify the specificity, affinity, function and activity of protein molecules [3,4].

Monoclonal antibodies represent the most successful and rapidly growing class of human therapeutics, but they have some disadvantages related to their large molecular weight, high price and limited stability.

Therefore, researchers look for alternatives keeping the medical effectiveness of antibodies but eliminating their imperfections. A great potential is attributed to high-affinity protein binders based on so-called small protein scaffolds [5,6]. Examples of scaffold-based biologicals approved for the clinical use are Kunitz domain (Ecallantide), a plasma kallikrein inhibitor used for the treatment of hereditary angioedema [7,8].

One of target systems for medical treatment are cytokines, an important class of signaling proteins serving as modulators of native immunity barrier against bacteria and viruses. Interferons lambda, also known as type III interferons (IFN- λ s), has been

Abbreviations

BiBi, bivalent binder based on two monovalent binders linked by a short peptide; FACS, fluorescence-activated cell sorting; GP2, DNA libraries of the scaffolds variants; IFN- λ , interferon lambda; IL-10R2, interleukin 10 receptor 2; IL-28R1, interleukin 28 receptor 1; IL-29, interleukin 29; JAK/STAT, janus kinase/signal transducer and activator of transcription signaling pathway; Kan-Nfr, Scaffold aminoglycoside-3'-phosphotransferase of type VIII N-terminal domain fragment (aminoacid H(-5) – 90P); Knottin, cystine knot scaffold; ProBi, protein bivalent Binder based on the in-house developed protein scaffold; ProBi-PatchC, Protein Binder with mutable positions on C-terminus; ProBi-PatchN, Protein Binder with mutable positions on N-terminus; RT-qPCR, real-time quantitative polymerase chain reaction; Sso7d, DNA binding protein 7.

discovered by two independent research groups [9,10], IFN- λ s consist of four members: IFN- λ 1 (also called IL-29), IFN- λ 2 (IL-28A), IFN- λ 3 (IL-28B) and IFN- λ 4 [10,11]. All four belong to the IL-10 family of cytokines as they share genomic organization, and signal through the common IL-10 receptor subunit 2 (IL-10R2). They also share a similar fold with other IL-10 cytokines [12] and the subfamily of monomeric IL-20, -22, -24, and all four IFN- λ s also share the architecture of the ternary signaling complex [13–16]. Interferons λ signal through the heterodimeric receptor complex composed of shared IL-10R2 and specific IL-28 receptor (IL-28R1). Complex formation initiates phosphorylation of intracellular STAT1 and STAT2 proteins (signal transducer and activator of transcription proteins) and the subsequent chain of events leading to the expression of downstream genes. Activation of alternative STAT3, STAT4 and STAT5 was also reported [9,10,17,18].

Overall, the IFN- λ response is similar to the response of type I interferons (IFN- α and IFN- β) but in contrast to the type I interferons, the IFN- λ -specific receptor is expressed only in epithelial cells [19,20]. Inhibition or stimulation of the IFN- λ signaling, therefore, influences only specific tissues and potential adverse side effects are less likely than in the case of influencing the more general IFN- α and IFN- β signaling. IFN- λ s thus represent a promising alternative therapeutic target for the treatment of respiratory and gastrointestinal viral infections. Especially, its profound ability to control the inflammatory response at mucosal sites makes this cytokine subfamily a timely target in the light of the SARS-CoV-2 pandemic [21].

Considering the potential of IFN- λ s for medical use as antiviral agents, we focused on triggering the signalization of one of the IFN- λ s, IFN- λ 1 (IL-29), by *de novo* engineered nonantibody protein binders. To achieve the goal, we adopted one of the powerful techniques of directed evolution [22], yeast display [23], that allows screening for desired properties. We

combined the binder selection process with fluorescence-activated cell sorting (FACS) to achieve high-throughput quantitative screening of combinatorial libraries. To simplify the overall process, we applied protein engineered tailored reporter proteins [24]. The final *de novo*-developed protein binders initiate IFN- λ 1 signaling as shown by the analysis of STAT1 phosphorylation and induction of selected genes detected by RT-qPCR analysis.

Results and discussion

Overview

De novo development of a protein molecule mimicking the IFN- λ signaling requires engineering of a protein molecule that simultaneously binds to two receptors, IL-28R1 and IL-10R2 and the analysis of whether the binder can turn on the signalization pathway. The latter may depend on the stereo-specificity of the ternary complex [25]. We describe the process of selection in four parts. Part I reports on engineering of protein scaffolds that interact separately with either IL-28R1 or IL-10R2. In Part II, we recount how these monovalent protein binders were further modified to create bivalent binders capable of simultaneous binding to both IL-28R1 and IL-10R2. Part III describes IFN- λ signalization screening. The signalization of the binder variant population was measured as phosphorylation in the IFN- λ -responsive HeLa cells induced by the binders displayed directly on the yeast cells. In Part IV, we tested whether two promising *de novo* purified binders induce expression of genes in a similar way to IFN- λ .

Part I: Engineering of IL-28R1 and IL-10R2 high-affinity binders

Design of DNA libraries

We started with five protein scaffolds (Table 1, Fig. 1) to increase the odds for identification of high-affinity

Table 1. Yeast display DNA library based on pJYDNn plasmid.

Scaffold	PDB ID	Uniprot	Residues PDB	Size (kDa)	Random codons ^a	FACS selection
ProBi (PatchC) [26]	4psf [31]	O9NWS0	Q17-I144	15	6	IL-28R1
ProBi (PatchN) [26]	4psf [31]	O9NWS0	Q17-I144	15	6	IL-10R2
Sso7d [27]	1sso [32]	P61991	A1-K62	7	7	IL-28R1
Kan-Nfr [24]	4h05 [33]	O9F9M5	H(-5)-P90	10	10	IL-10R2
GP2 [28]	2wnm [34]	P03704	K35-P79	5	9	< 7%
Knottin [29]	1cbh [35]	P62694	T1-L36	5	8	< 7%

Following the selection results, further experiments continued against IL-28R1 with ProBi PatchC and Sso7d, and against IL-10R2 with ProBi PatchN and Kan-Nfr. Scaffolds GP2 and Knottin did not achieve any significant enrichment.

^aNumber of randomized codons. The NNK/NNS degeneration was used.

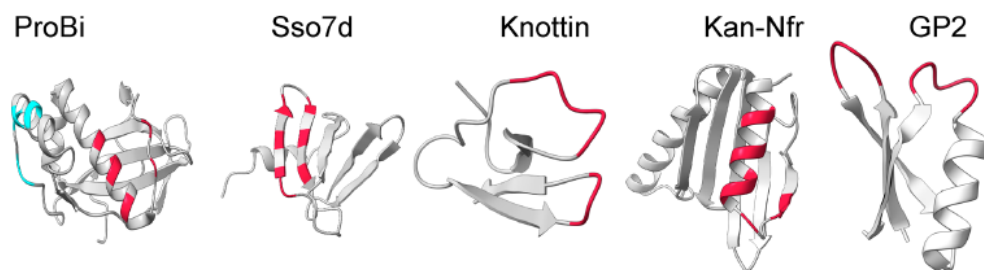


Fig. 1. Protein scaffolds used to create six different libraries. The mutable patches are color highlighted, the N-terminal ProBi patch in cyan, the C-terminal in red. Sequences of the scaffolds are listed in Table S1. Cartoons were drawn by the ChimeraX program [43].

binding proteins. The DNA and protein sequences of all protein scaffolds are listed in Table S1. The ProBi scaffold has two mutable surface patches (called PatchN and PatchC, Fig. 1). They were initially established for ribosome display, so each Patch contains 10 mutable amino acid positions [26]. For yeast display, we used six positions to reduce the complexity of library. We also created four libraries according to previously published protein scaffolds: Sso7d [27], GP2 [28], Knottin [29] and Kan-Nfr [24]. The quality of all libraries was verified by DNA sequencing of 20 randomly selected clones. Sequence alignment showed no redundant clones implying high diversity (Fig. S1).

Yeast display

We utilized an enhanced yeast display selection technique, in which the protein expression is detected by bilirubin inducible fluorescent protein [24]. The high-affinity variants were selected against target proteins, purified recombinant extracellular parts of IL-28R1 and IL-10R2. The yeast display method and production of all proteins used in the study (IFN- λ , receptors, all scaffolds and their variants) are described in the Methods section.

Selection of protein scaffolds binding to monovalent receptor

We performed four consecutive rounds of yeast display by Fluorescence-Activated Cell Sorting (FACS) [30]. We collected yeast cells based on two parameters, (a) expression level of protein scaffold on the yeast surface, and (b) amount of target protein bound to yeasts. We regularly sorted between 20 000 and 50 000 cells in the double-positive area. The sorting and gating strategy is shown in the Fig. S2. Naïve libraries were screened against the target protein with a starting concentration

of 4 μM . Subsequently, we gradually decreased the concentration from 2.5 μM to 1 μM and a final concentration 500 nM was used to increase selection stringency. The selection with the lowest concentration of IL-28R1 was repeated to reach higher enrichment of the double-positive population. Two libraries, Kan-Nfr and ProBi-PatchN, showed enrichment in the population of IL-10R2-binding cells from an initial 2% in the first round of selection to approximately 20% in the fourth run. Knottin, GP2, Sso7d and ProBi-PatchC showed no significant enrichment to IL-10R2 (< 7%). Only libraries ProBi-PatchC and Sso7d showed enrichment of binding population of IL-28R1 to approximately 25%. On the basis of these selection results we decided to continue with libraries showing enrichment of binding population to IL-28R1 and IL-10R2 above 20% after the fourth round of FACS selection – ProBi (PatchN and PatchC), Sso7d and Kan-Nfr libraries (summarized in Table 1). Knottin and GP2 libraries were not enriched for any receptor.

Part II: Selection of protein scaffold candidates showing simultaneous binding

Design of bivalent libraries

Simultaneous binding of protein scaffold variants to both receptors is a prerequisite to trigger signalization. The previous experiments resulted in four DNA libraries – ProBi-PatchC and Sso7d for IL-28R1, ProBi-PatchN and Kan-Nfr for IL-10R2 (Table 1). These monovalent DNA libraries were combined by the restriction-free cloning technique [36] and homologous recombination in *Saccharomyces cerevisiae* EBY100 [37] to create bivalent DNA libraries. All constructs were based on pJYDnN plasmid (Addgene ID: 162450) [24]. Since the binding sites on receptors were unknown, we applied two different strategies to create

scaffold constructs binding both receptors with fundamentally different binding modalities.

(a) We utilize the unique feature of the ProBi scaffold – two mutable patches (PatchN and PatchC) on one protein molecule (Fig. 2A, reported previously in [26]). This approach imitates the natural signaling

molecules such as interleukins and interferons. The fact that bivalent ProBi is one compact molecule simplifies the downstream process. We combined the DNA library of ProBi-PatchC preselected against IL-28R1 and ProBi-PatchN against IL-10R2 to produce a new DNA library of scaffold variant called ProBi-NC.

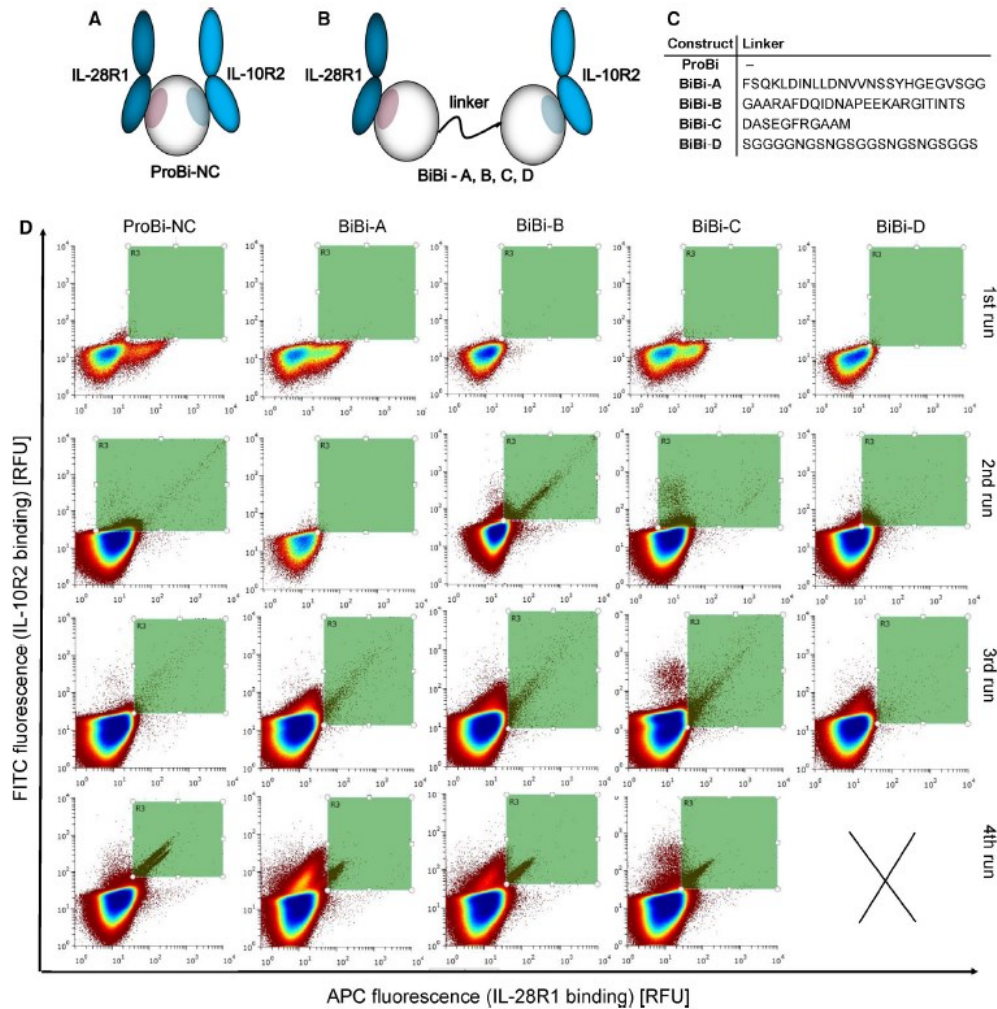


Fig. 2. Design of bivalent binders and simultaneous binding of IL-28R1 and IL-10R2 measured by FACS. Two different approaches to create a double binder were used: (A) combination of two mutable patches in one molecule (ProBi scaffold), and (B) fusion of two different scaffolds (Sso7d and Kan-Nfr) by a linker peptide. (C) Table of linkers used to create bivalent binders. (D) Simultaneous binding measured by FACS. The x-axis represents IL-28R1 binding (APC fluorescence), the y-axis represents IL-10R2 binding (FITC fluorescence). Each FACS-sorting dot plot represents 100 000 binding events. The green area highlights the region containing selected double binders (gating strategy).

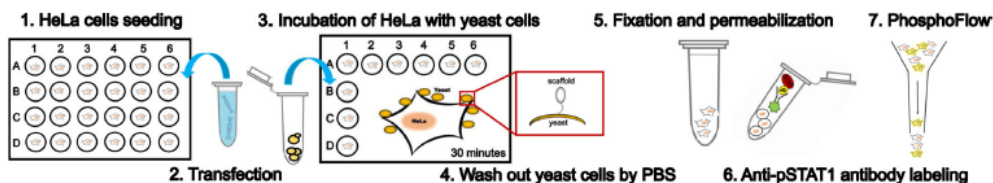


Fig. 3. Schematic procedure of the Cell-Cell Interaction PhosphoFlow method. The detailed procedure is described in the method section.

(b) The second approach is the fusion of independent protein scaffold molecules into a two-domains protein scaffold (Fig. 2B). We merged the DNA library of Sso7d and Kan-Nfr preselected against IL-28R1 and IL-10R2, respectively, using flexible polypeptide linkers. The resulted bivalent DNA libraries of scaffold variant are called BiBi-A, -B, -C and -D where -A, -B, -C and -D denote the used linker. The length and composition of a particular linker (Fig. 2C) can influence the interactions. Therefore, we tested multiple possibilities to achieve the optimal configuration to trigger an artificial signalization.

Selection of protein scaffolds simultaneously binding to two receptors

Initially, we preselected bivalent scaffold libraries against each receptor independently. Following this, we created five bivalent libraries coding for potential bivalent binders. These libraries, called ProBi-NC and BiBi-A, BiBi-B, BiBi-C and BiBi-D, were subjected to another four selection rounds against IL-28R1 and IL-10R2 receptors. The concentration of each receptor was 200 nM in each sorting run. The receptors were labeled by different amino-reactive fluorescent dyes. In the subsequent round, we incubated both receptors with yeast cells displaying the binder variants on their surfaces. We collected double-positive cells that appear near the diagonal of the FACS records (Fig. 2D).

Despite that, bivalent libraries were designed to bind both IL-28R1 and IL-10R2, not all FACS selections enriched double binders. Of the five screened libraries, only four, ProBi-NC, BiBi-A, BiBi-B, BiBi-C, were enriched during the four rounds of yeast display; BiBi-D showed no significant enrichment after the third round. The populations after the fourth sorting were plated and 10 single colonies were analyzed by DNA sequencing. The resulting sequences (Fig. S3) suggest certain level of sequence convergence. The sequences of the ProBi-PatchN and Sso7d N-terminal parts of the binders are variable, but they do show preferences. For instance, the Sso7d part of the BiBi-A, -B, -C, -D

libraries displays 5 serine and 5 aspartate residues at mutable position 20, 7 leucine residues at position 21 and 10 proline residues at the position 25 (Fig. S3). As will be shown later, overall, the best tested binder is BiBi-A1. Quite significantly, the mutable residues of BiBiA1 (in yellow in Fig. S3) are SLGP^HTHV-GHRGMVGRRL, the residues among two most frequently occurring residues when one aligns sequences of BiBi-A, -B, -C and -D libraries. In this sense, the evolution of the BiBi-A library is close to convergence. In contrast, we do not have any immediate explanation for a low complexity of the ProBi-Patch C library and its resemblance to the WT sequence and decided to report ProBi-P binders because one of the tested binders, ProBi-P5, signals as discussed in section IV.

Part III: Screening of signalization of yeast-displayed binders by Cell-Cell Interaction PhosphoFlow method

The IFN- λ s' signalization starts with formation of the cytokine-receptor complex on the cell surface, followed by signal transduction and resulting in phosphorylation of STAT molecules that could be detected by antibodies. Western blot detecting the p-STAT molecules is the most routinely used method, but it is laborious and has low throughput. Another approach to evaluate the intracellular phosphorylation at single cell level is p-STAT fluorescence flow cytometry (PhosphoFlow Cytometry). To avoid a time-consuming protein purification, we developed the process utilizing direct interaction between responsive human cell line and whole yeast cells expressing proteins on their surface. We called this new approach Cell-Cell Interaction PhosphoFlow method (CCIPF). Schematic representation of our process approach is shown in Fig. 3.

Cell-cell interaction phosphoflow method screening

Scaffold variants showing simultaneous binding to both receptors were subjected to signalization screening experiments on a single-cell resolution level. The

BDTMPhosphoFlow procedure for fixation and permeabilization of the HeLa cells (<https://www.bdbiosciences.com/en-us/resources/protocols>) was optimized and followed by purified IFN- λ 1 calibrations using western blot and PhosphoFlow. The immunoblot analysis suggested that doses between 100 and 200 ng·mL⁻¹ of IFN- λ 1 are optimal to activate STAT1 phosphorylation. Indeed, the same concentrations triggered a strong PhosphoFlow signal as identified by Phospho-STAT1 (Tyr701) antibody conjugated with Alexa Fluor® 647 (Fig. S4). Having identified the optimal signaling condition, we examined whether the signalization can be triggered by IFN- λ 1 displayed on EBY-100 *Saccharomyces cerevisiae* instead of a purified protein. In our proof-of-concept experiment, HeLa cells were transfected with IL-28R1 and IL-10R2 and incubated with either purified IFN- λ 1 protein or IFN- λ 1-expressing yeast cells. By comparing FACS plots ‘Yeast displayed IFN- λ 1’ and ‘Purified IFN- λ 1’ (Fig. 4A), we conclude that the yeast surface-exposed IFN- λ 1 protein triggers phosphorylation of STAT1 molecules in HeLa cells. Therefore, the new procedure is a viable approach to screen for signaling clones. We screened over 100 randomly picked clones from all libraries binding both receptors receiving more than 20 signaling variants. According to the CCIPF data, we identified six best signaling candidates. These positive hits were subjected to validation and characterization steps (Part IV).

Part IV: Gene expression of purified binders

The unique hits obtained from the screening experiments were cloned to an *E. coli* expression system, proteins were purified and characterized and further subjected to signaling analysis by PhosphoFlow cytometry and gene induction experiments.

Expression and purification of the signaling variants

The unique hits were cloned into two different *E. coli* expression system vectors: pET26b with N-terminal His-tag and pET28bdSumo with N-terminal his-bdSumo tag [38]. The recombinant protein candidates (BiBi-A1, -A7, -B2, -C1 and ProBi-P4, -P5) were produced in *E. coli* BL21(DE3) and *E. coli* BL21(GOLD). Among all tested expressions, only two produced in pET26 (BiBi-A1, ProBi-P5) met our requirements for protein quality represented by high solubility, stability and low aggregation properties; sequences of both variants are in Table S2. We measured binding affinities of these two variants to both receptors by flow cytometry binding analysis (Fig. 4B, C). The ProBi-P5

and BiBi-A1 had a binding affinity to IL-28R1 of about 500 nM and 450 nM respectively. The binding to IL-10R2 had an affinity of $K_D > 2 \mu\text{M}$ for both bivalent binders. We attempted to determine K_D values by microscale thermophoresis (MST), but no successful setup was found for IL-28R1, likely because of its stickiness.

Signaling assay and gene induction evaluation

To evaluate the ability of the most promising IFN- λ -mimicking candidates BiBi-A1 and ProBi-P5, we tested their ability to trigger STAT1 phosphorylation by applying our optimized BDTMPhosphoFlow. HeLa cells do not express naturally high level of the receptors. In order to reach a higher expression level of both IFN- λ receptors and test the activity of the binders in HeLa cells, we overexpressed HeLa cells by transfection with IL-28R1 and IL-10R2. The HeLa cells were treated with 2 μM of the purified double binder variants for 30 min and 200 ng·mL⁻¹ (~ 6 nM) IFN- λ 1 as a positive control. Results are shown in Fig. 4A. The signal of the BiBi-A1- and ProBi-P5-purified proteins is approximately three times lower than for the IFN- λ 1-positive control. This was expected considering affinities of these two candidates to both receptors. Unlike the IFN- λ 1 control, both candidate proteins were tested in a concentration below their affinity saturation level (> 90% binding).

To further test the ability of BiBi-A1 and ProBi-P5 to mimic the IFN- λ signaling, we measured induction of genes known to be upregulated in response to IFN- λ s stimulus [39], MX1, OAS1, OAS3, IFIT1, IFI6, BST2, OASL, CXCL10, IFIT3, IFIH1, by RT-PCR. HaCat and HeLa cells were induced with 200 ng·mL⁻¹ (~ 6 nM) of purified IFN- λ 1 or binders for 24 h; the experiments were performed in duplicates. We observed a more than two-fold increase in induction of nine genes in nontransfected HaCat cells but only three genes in nontransfected HeLa cells (data not shown). We overexpressed IL-28R1 and IL-10R2 in HeLa cells, but the level of gene expression remained low, especially compared to HaCat cells. We, therefore, decided to continue experiments only with HaCat cells and to measure the expression levels of just six genes (MX1, OAS1, OAS3, IFIT1, IFI6, BST2) that showed the highest response to IFN- λ 1 treatment.

Expression of the six genes induced by IFN- λ 1, BiBi-A1 and ProBi-P5 binders in HaCat cells is summarized in Fig. 5A. Cells were treated with 200 ng·mL⁻¹ (~ 6 nM) IFN- λ 1, 2 μM BiBi-A1 and ProBi-P5 for 24 h; the mRNA concentrations were

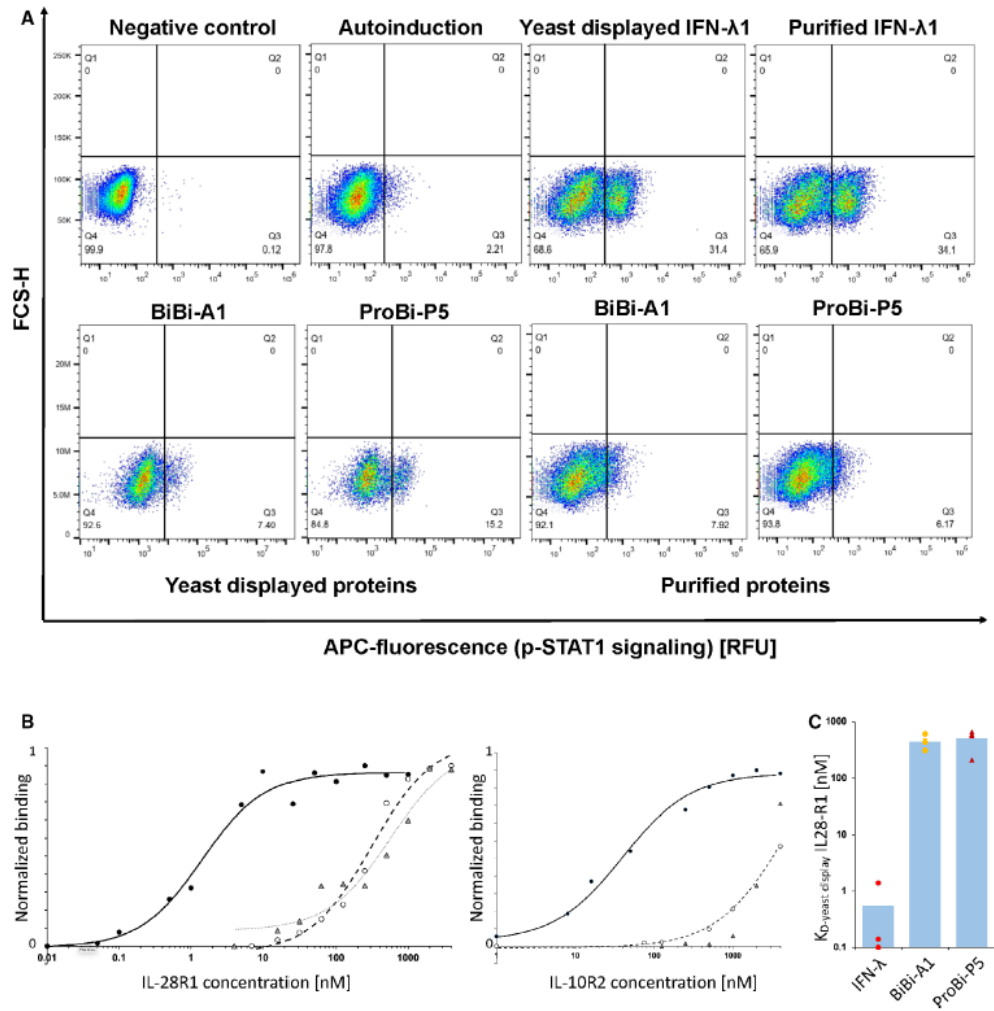


Fig. 4. Screening of signaling variants binding both IL-28R1 and IL-10R2. (A) PhosphoFlow screening performed on BD LSRFortessa™ SORP. The x-axis represents phosphorylation of STAT1 (APC-fluorescence channel-p-STAT1 (Tyr701) conjugated with Alexa Fluor® 647), the y-axis represents FCS-H side scatter. The plots show negative control (only HeLa cells), autoinduction (HeLa cells transfected with IL-28R1 and IL-10R2, not induced), positive control of the purified IFN- λ 1 protein from S2 cells (200 ng·mL⁻¹) and IFN- λ 1 displayed on EBY-100 surface (10⁷–10⁸ yeast cells). The plots below show examples of two yeast display signaling variants (BiBi-A1 and ProBi-P5) and the signaling of the same variants after two-step purification (described in Part IV). (B) Flow cytometry-based binding affinity analysis of ProBi-P5 (triangles), BiBi-A1 (empty dots) and IFN- λ 1 (black dots) binding to fluorescently labeled IL-28R1 (left graph) and IL-10R2 (the middle graph). The experiment was performed in triplicates. (C) Histogram of the affinity assessment by FACS. The left bar shows the average of the K_D values measured for IFN- λ 1, the middle one K_D for BiBi-A1, the right one for ProBi-P5. Colored points indicate values of the individual measurements.

analyzed by RT-qPCR. The bivalent binder BiBi-A1 showed higher than a two-fold increase in all six genes, whereas the induction caused by ProBi-P5 was

significant (about four-fold) only in one gene, OAS1. Therefore, we decided to demonstrate the dose effect on the gene expression only for BiBi-A1 (Fig. 5B).

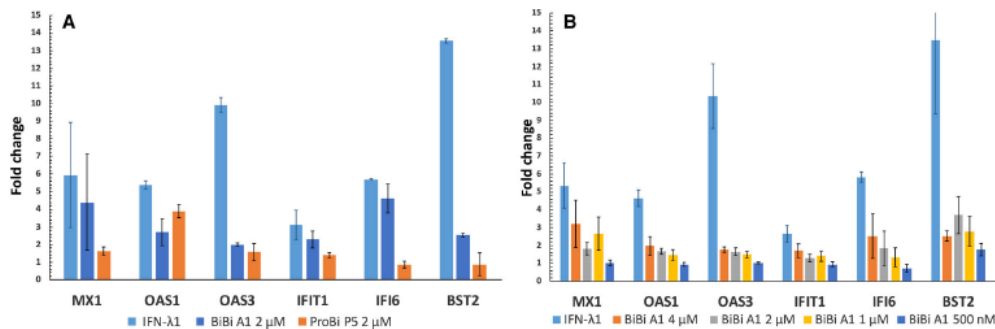


Fig. 5. Relative gene expression in HaCat cells responding to IFN- λ 1, BiBi-A1 and ProBi-P5 treatment. (A) HaCat cells were treated with 200 ng·mL⁻¹ IFN- λ 1, 2 μ M BiBi-A1 and 2 μ M ProBi-P5 for 24 h and analyzed by RT-qPCR. (B) HaCat cells were treated for 24 h with 4, 2, 1 μ M and 500 nM BiBi-A1, the IFN- λ 1 concentration was always 200 ng·mL⁻¹. The fold change is presented in the y axis as the relative expression levels compared to the negative control cells and normalized to the B2M gene. The data are means and their standard estimated errors calculated from two independent experiments (A) and from four independent experiments (B) are indicated.

Cells were treated with 4, 2, 1 μ M and 500 nM of purified BiBi-A1 and 200 ng·mL⁻¹ (~6 nM) IFN- λ 1 as a positive control and were compared to their non-treated (NT) controls and negative controls represented by HaCat cells treated with the Kan-Nfr scaffold protein.

The lower gene induction observed for ProBi-P5 may be a result of stereospecific hindrance of the two receptors, one relative to the other, when binding ProBi-P5. In contrast, BiBi-A1 has its two binding surfaces located on two domains fused by a linker. The resulting flexibility apparently solves the stereospecific hindrance. The observed difference in behavior of BiBi-A1 and ProBi-P5 also suggests that having a precise relative conformation of the two receptors one relative to the other is not crucial for signaling [25,40]. In summary, expression of six analyzed genes induced by exposure to IFN- λ 1 were all increased by the bivalent binder BiBi-A1, but response was weaker than in the control treatment with IFN- λ 1.

Conclusions

We applied protein engineering techniques to develop *de novo*-developed nonantibody protein binders able to trigger the biological response of one of the IFN- λ s, IFN- λ 1 (aka IL-29). To match or even beat the ability of evolution-tested antibodies to bind at high affinity and specificity is a challenging task but we were motivated by the proven plasticity of the used protein scaffolds, available protein engineering tools and successes of others.

The development of an agonist protein in this project contrasts with most others that typically aim at inhibiting the targeted biomolecule. In our work, we combined new approaches with the yeast display methodology using engineered reporter proteins [24] and high-throughput quantitative screening by FACS.

IFN- λ 1 triggers signaling by binding to two receptors, specific IL-28R1 and receptor IL-10R2 shared with other cytokines of the IL-10 group. The 'double binders', binding both IL-28R1 and IL-10R2, were selected from five different scaffolds; three of them turned more useful. In the first step, we separately sorted binders of IL-28R1 and IL-10R2. These preselected libraries were then linked to form new libraries with two preselected interfaces combined, one for IL-28R1 and the other for IL-10R2. Double binders were selected by using four rounds of FACS experiments by measuring simultaneous binding to both receptors fluorescently labeled by different dyes. These FACS experiments were followed by PhosphoFlow cytometry choosing only signaling variants; the signaling clones were identified easily. We improved a method of measuring protein signalization by PhosphoFlow cytometry, where the inducer of the signalization is displayed directly on the yeast surface and signalization is measured in HeLa cells.

To prove the usability of the binders, we expressed, purified and characterized six best signaling variants but only two of them, BiBi-A1 and ProBi-P5, were purified in high yield and passed our quality requirements. The ability to trigger biological response of BiBi-A1 and ProBi-P5 was tested on the HaCat cell line

by RT-qPCR. The lower gene induction observed for ProBi-P5 is likely linked to its lower binding affinities (Fig. 4B) or may be a result of stereospecific hindrance of the two receptors, one relative to the other [25].

Further development of the binders for therapeutic application would require several additional steps. Binders affinity and signaling capacity need to be increased, their production and stability optimized. Furthermore, studies of their biological properties need to be performed including the critical issue of immunogenicity, a complex phenomenon that is known to be influenced by factors outside of the molecular structure of the therapeutic agent [5].

To summarize, we present here a new approach for the generation of artificial protein binders mimicking signaling of a human cytokine, in our case IFN- λ 1. We experimentally proved that two *de novo*-developed proteins switch the IFN- λ 1 signaling as shown by PhosphoStat and increased expression of the six relevant genes as detected by RT-qPCR analysis of mRNA expression. We propose that our approach represents a viable way to develop new biologics that activate cytokine signaling pathways.

Materials and methods

Cell lines

HeLa and HaCat cell lines were kindly provided by Dr. Cyril Bařinka and Dr. Petr Malý (Institute of Biotechnology) respectively. The cell lines were maintained in Dulbecco's Modified Eagle Medium (DMEM) high glucose medium (catalog number 41965039, Thermo Fisher Scientific, Waltham, MA, USA) and regularly subcultured according to the ATCC culturing method (cat. CCL-2). The *Drosophila melanogaster* Schneider S2 cells were cultivated in the HyClone SFX Insect medium (Cat.N-HYCLSH30278.02, Cytiva, Freiburg im Breisgau, Germany) supplemented with 10% FBS for subculturing or in serum-free medium for protein expression experiments.

Cloning, expression and purification of the lambda proteins by Drosophila S2 expression system

Cloning, expression and purification were processed similarly to [41] and [38].

Construction of DNA libraries for yeast display with a single randomized patch

The library of ProBi scaffold (PatchC) was synthesized by the GENEWIZ company using NNK codons technology

[26]. The DNA library of ProBi scaffold (PatchN) was constructed by the restriction-free cloning technique described by Peleg *et al.* [42]. DNA library was amplified by PCR using NNS randomized primers (six codons) and KAPA HiFi Hot Start Ready Mix (Cat. N. KK2602, Roche, Switzerland, Basel). The PCR fragment (amplified DNA library) was purified with NucleoSpin Gel and PCR Cleanup kit (Macherey-Nagel) according to manufacturer's protocol. Purified DNA (10–12 μ g per library) was mixed with pJYDnN (pJYDnN, Addgene ID 162450) plasmid (4 μ g) cleaved by *Nde*I and *Bam*HI restriction enzymes, and electroporated to *Saccharomyces cerevisiae* EBY100 strain and grown overnight as described in [37]. The library size was estimated to be $\sim 10^8$ by plating serial dilutions on selection plates lacking tryptophan. The library was further examined for the correct gene insertion and for targeted mutations introduced into the gene by sequencing of 20 single clones. The remaining four DNA protein libraries of protein scaffolds – Sso7d, Kan-Nfr, GP2 and Knottin – using pJYDnN plasmid optimized for labeling-free yeast display were provided by Prof. Gideon Schreiber (Laboratory of Protein-Protein interaction, Weizmann Institute of Science).

Construction of DNA libraries for yeast display for bivalent scaffold constructs

DNA from preselected libraries with the single randomized patch was isolated by Zymoprep kit (Zymo Research) according to the manufacturer's protocol and amplified by PCR. We combined the pre-selected library of ProBi (PatchN) scaffold and the pre-selected library of ProBi (PatchC) scaffold by recombination procedure in yeast [37] to obtain a new bivalent ProBi library in pJYDnN plasmid. Similarly, the DNA of preselected Sso7d and Kan-Nfr libraries were cloned in yeast plasmid pJYDn by homologous recombination in yeast in the position between *Nhe*I and *Bam*HI restriction sites. Sso7d and Kan-Nfr were fused together by polypeptide linkers to create multiple constructs with different flexible linkers, resulting in four new libraries-BiBi-A, -B, -C and -D.

Yeast plasmid isolation and sequencing

Aliquots of transformed yeast cells were collected by centrifugation (3000 g, 3 min) and DNA was isolated using a Zymoprep kit (Zymo Research) according to the manufacturer's protocol. Two microliters of DNA were electroporated in *E. coli* Cloni 10G strain, cells were plated on selective LB plates with 100 mg-L⁻¹ kanamycin and colonies were grown overnight at 37 °C. Single-colony plasmid DNA was isolated using a Qiagen miniprep kit according to the manufacturer's instructions from 3 mL of LB media.

Yeast display preselection runs of DNA libraries

Yeast libraries grown in SD-CAA media (composition: 20 g glucose, 6.7 g yeast nitrogen base, 5 g Bacto casamino acids, 5.4 g Na₂HPO₄, 8.56 g NaH₂PO₄ per 1 L) overnight at 30 °C were used as inoculum. The overnight culture was diluted in SG-CAA medium (prepared as for SD-CAA, but used 20 g galactose instead of glucose, supplemented with 1 nM bilirubin dissolved in DMSO, to final OD₆₀₀ = 0.5–1 and grown at 20 °C for 24–48 h). One milliliter of induced yeast cells was collected (3000 g, 3 min), washed twice in cold PBS supplemented with 0.1% (w/v) BSA at pH 7.4 (PBSB buffer), the pellet was resuspended in 50 μ L of PBSB and mixed with biotinylated receptors (IL-10R2 and IL-28R1) to the final concentration and incubated on ice for 1 h. Then, yeast cells were collected, washed with PBSB buffer and labeled with secondary reagent streptavidin-allophycocyanin (APC) in the final volume of 50 μ L (1 : 100 dilution) and incubated for 1 h on ice. Yeast cells were washed three times and resuspended in 1 mL of PBSB buffer and sorted on BD FACSAria™ Fusion. Expression signal of displayed libraries was analyzed by fusion with reporter protein – bilirubin-inducible fluorescence protein eUnaG2 (pJYDNn vector, excitation 498 nm, emission 527) [24]. Targeted proteins were covalently modified with biotin, amine reactive biotinylation reagent (EZ-Link Sulfo-NHS-LC-Biotin) and subsequently labeled with streptavidin conjugated with fluorochrome (Streptavidin-APC). No compensation was applied. Negative cells, EBY100 cells, without plasmid or nonlabeled cells were used to determine the negative population and set quadrant gating. Selected yeast cells (double-positive) were sorted into SD-CAA medium and grown for 24–48 h. Overnight grown culture was used as inoculum for a consecutive round of selection. Aliquots of the sorted yeast cells were routinely plated in parallel as single colonies on SD-CAA agar plates, picked and grown on 1 mL of SD-CAA for further sequencing and affinity determination.

Yeast display for simultaneous binding

The new bivalent libraries were sorted four times against IL-28R1 and IL-10R2 following the same procedure as described above (Yeast surface display). The receptors were labeled by different amino-reactive fluorescent dyes, IL-28R1 by far-red CF@640R succinimidyl ester dye (APC fluorescence analog) and IL-10R2 by CF@488A succinimidyl ester dye (FITC fluorescence analog) which allowed its detection by standard FACS laser/filter setup. The labeling with 1 : 4 (Protein : dye) ratio was performed in 0.1 M bicarbonate buffer (pH 8.2). Excess of unreacted/hydrolyzed dye was removed by dialysis (GebaFlex tubes, Geba, 8000 MWCO) to PBS supplemented with 1 mM Tris-HCl, pH 8.0 overnight at 4 °C.

Screening of the bivalent candidates by PhosphoFlow cytometry and biological characterization

PhosphoFlow cytometry: Cell–cell interaction PhosphoFlow

The human HeLa cell line was grown in high-glucose DMEM (Cat. N. D5796, Sigma Aldrich, Schnellendorf, Germany) supplemented with 10% fetal bovine serum (FBS) and 1 \times penicillin–streptomycin. HeLa cells were cultivated in a 24-well plate, incubated overnight at 37 °C and transfected with full length of IL-28R1 and IL-10R2 cloned into pcDNA3.1 expression vector. Transfection was performed according to the jetPRIME® transfection reagent procedure (Polyplus). HeLa cells were treated with IFN- λ 1 as positive control and yeast cells displayed bivalent binders (or purified proteins) for 30 min. Following, the cells were washed with PBS and treated with 0.5% trypsin and incubated for 5 min in 37 °C, centrifugated (800 g, 5 min, 4 °C) and washed in PBSB buffer. Stimulated/unstimulated cells were fixed with 1 mL of 2% paraformaldehyde (10 min, RT) and then permeabilized with 1 mL of MeOH (30 min, ice). Permeabilized samples were spun (1600 r.p.m., 5 min, 4 °C), washed in PBSB buffer and stained with Phospho-Stat1 (Tyr701), Alexa Fluor® 647 Conjugate and incubated for 1 h on ice. The spin cells were washed and resuspended in 200 μ L of PBSB buffer and analyzed by BD LSRFortessa™ SORP flow cytometer.

Screening and affinity determination by flow cytometry

Aliquots of expressed cells (10⁶) were collected (3000 g, 3 min) and washed in PBSB buffer. Subsequently, the cell pellets were suspended in analysis solutions across a range of concentrations (μ M–nM range) of biotinylated receptors (IL-10R2 and IL-28R1). The expression and binding signals were determined by flow cytometry using BD LSRFortessa™ SORP. Green fluorescence channel (FL-1, FITC) was used to record the expression of positive cells, and a far-red fluorescent channel (FL-4, APC) for binding signals. No compensation was applied. The mean FL4-A fluorescence signal values of FL1-A-positive cells, reduced by mean FL4-A- of FL1-A-negative cells, were subjected for $K_{D,YD}$ (K_D measured by Yeast display) computations of the standard noncooperative Hill equation fitted by nonlinear least-squares regression using Python 3.7 [24].

Western blot assay

Examination of p-STAT1 was measured by western blot assay using the following antibodies: polyclonal anti-pSTAT1 (Tyr701) (Santa Cruz Biotechnology Inc., Dallas, TX, USA), polyclonal anti-STAT1 (Santa Cruz Biotechnology Inc.) and monoclonal anti- α -tubulin (Cat.N. T9026-

100UL, Sigma Aldrich). HeLa cells were treated as described above. Levels of phosphorylation were followed after 30 min treatment with IFN- λ 1 as the positive control (10–200 ng·mL⁻¹). Total protein concentration was determined by bicinchoninic acid (BCA) protein assay (Thermo Scientific), and equal amounts were separated by SDS/PAGE electrophoresis. Quantitative analysis of band intensities on western blots was performed with Image Studio Lite software.

Reverse transcriptase and quantitative Polymerase Chain Reaction analysis

The extent of expression of IFN- λ 1-stimulated genes was measured using RT-PCR and qPCR performed in Gene Core facility in Biocev, Czech Republic. The sequences of the primers used are detailed in Table S3. HeLa and HaCat cells (treated and nontreated group) were collected in 1.5-mL tubes containing 1 mL of TRI Reagent® - RNA isolation reagent (Sigma-Aldrich, T9424) and stored in a -80 °C freezer. Samples were homogenized using vortex. Total RNA was isolated following the manufacturer's manual. The final total RNA was diluted in 100 μ L of 1xTE buffer (Invitrogen, 12 090-015). The concentration of RNA was measured using Nanodrop 8000 (Thermo Scientific), and the quality of RNA was analyzed using Fragment Analyzer (AATI, Standard Sensitivity RNA analysis kit, DNF-471). RT-qPCR analysis was performed using 800 ng of total RNA obtained from isolation. Reverse transcription was performed using Grand Script Super Mix (Tataa Biocenter) according to the manufacturer's protocol in 20 μ L volume. Synthesized cDNA was diluted four times in 1xTE buffer and 2 μ L of final cDNA was added to the qPCR reaction (2x SYBRGreen mix, TATAA Biocenter, 400 nm primers mix and Nuclease-free water to final volume 10 μ L). Protocol for qPCR was: 30 s at 95 °C; 50 cycles of 95 °C for 5 s, 60 °C for 30 s and 72 °C for 10 s; followed by melting curve analysis. Relative expression levels were calculated by the CT (cycle threshold) relative quantitation (RQ) method, using the untreated control and negative control cells as the calibrator sample and (B2M) as the endogenous control detector (reference gene levels measured on the same sample). All the experiments were performed using biological triplicates. For qPCR data, the average of at least three independent biological replicates is shown, with their affiliated standard errors.

Cloning, expression and purification of the signaling variants

The DNA from selected signaling bivalent binder candidates were isolated from yeast by ZymoPrep kit (Zymo Research) and recloned into the pET28(+) vector using RF

cloning. Verified plasmids were transformed to expression *E. coli* BL21(DE3). Cells were incubated at 30 °C (220 r.p.m.) to OD₆₀₀ = 0.6 and then they were transferred to 20 °C and expression was initialized by the addition of IPTG (0.5 mM) and expression continued for 16 h. Cultures were harvested by centrifugation (5000 g, 15 min, 4 °C), washed once with PBS buffer. Cells were disintegrated by sonication (15 min of cycles 20 s pulse and 40 s cooling, 30% intensity) in Tris-HCl buffer, pH 8 and a soluble fraction was isolated by centrifugation (40 000 \times g). Classified lysates were purified by gravity flow columns loaded with Pure Cube Ni-NTA agarose resin (1 mL, Cube Biotech, Germany) and pre-equilibrated with 50 mM Tris-HCl pH 8, 300 mM NaCl. The unbound fraction was washed with 50 mM Tris-HCl, 300 mM NaCl, 10 mM imidazole, pH 8 (10 CV) and the proteins were eluted 50 mM Tris-HCl, 100 mM NaCl, 250 mM imidazole, pH 8. All proteins were further purified to homogeneity by size exclusion chromatography at 16 °C using Superdex75 10/300 Increase or Superdex 75 16/600 column (GE Healthcare). The column was equilibrated in PBS pH 7. Samples were analyzed by 15% SDS/PAGE.

Acknowledgements

We thank Dr. Lucie Langerová from the Institute of Biotechnology for performing the RT-qPCR measurements and to Dr. Tamar Unger from Israeli Structural Proteomics Center, Weizmann Institute of Science for protein production in baculovirus systems. This study was supported by the Czech Science Foundation grant 19-17398S and the institutional grant to the Institute of Biotechnology of the Czech Academy of Sciences RVO 86652036. We acknowledge CMS-Biocev (Biophysical techniques and Structural mass spectrometry) supported by MEYS CR (LM2018127).

Conflict of interest

The authors declare no conflict of interest.

Author contributions

BS and JZ conceived the project, LK, JZ, PM, GS and BS planned experiments, LK, JZ, PM and BS wrote the paper, LK, JZ, MH, PM, YP, MS and GS performed experiments and analyzed data.

Peer Review

The peer review history for this article is available at <https://publons.com/publon/10.1111/febs.16300>.

Data Accessibility

The supporting data are contained in the manuscript as Supplementary Information.

References

- Goeddel DV, Kleid DG, Bolivar F, Heyneker HL, Yansura DG, Crea R, Hirose T, Kraszewski A, Itakura K & Riggs AD (1979) Expression in *Escherichia coli* of chemically synthesized genes for human insulin. *Proc Natl Acad Sci USA* **76**, 106–110.
- Usmani SS, Bedi G, Samuel JS, Singh S, Kalra S, Kumar P, Ahuja AA, Sharma M, Gautam A & Raghava GPS (2017) THPdb: Database of FDA-approved peptide and protein therapeutics. *PLoS One* **12**, e0181748.
- Fosgerau K & Hoffmann T (2015) Peptide therapeutics: current status and future directions. *Drug Discov Today* **20**, 122–128.
- Leader B, Baca QJ & Golan DE (2008) Protein therapeutics: a summary and pharmacological classification. *Nat Rev Drug Discov* **7**, 21–39.
- Vazquez-Lombardi R, Phan TG, Zimmermann C, Lowe D, Jermutus L & Christ D (2015) Challenges and opportunities for non-antibody scaffold drugs. *Drug Discov Today* **20**, 1271–1283.
- Simeon R & Chen Z (2018) *In vitro*-engineered non-antibody protein therapeutics. *Protein Cell* **9**, 3–14.
- Levy JH & O'Donnell PS (2006) The therapeutic potential of a kallikrein inhibitor for treating hereditary angioedema. *Expert Opin Invest Drugs* **15**, 1077–1090.
- Gompels MM, Lock RJ, Abinun M, Bethune CA, Davies G, Grattan C, Fay AC, Longhurst HJ, Morrison L, Price A et al. (2005) C1 inhibitor deficiency: consensus document. *Clin Exper Immunol* **139**, 379–394.
- Kotenko SV, Gallagher G, Baurin VV, Lewis-Antes A, Shen M, Shah NK, Langer JA, Sheikh F, Dickensheets H & Donnelly RP (2003) IFN-lambdas mediate antiviral protection through a distinct class II cytokine receptor complex. *Nat Immunol* **4**, 69–77.
- Sheppard P, Kindsvogel W, Xu W, Henderson K, Schlutsmeyer S, Whitmore TE, Kuestner R, Garrigues U, Birks C, Roraback J et al. (2003) IL-28, IL-29 and their class II cytokine receptor IL-28R. *Nat Immunol* **4**, 63–68.
- Prokunina-Olsson L, Muchmore B, Tang W, Pfeiffer RM, Park H, Dickensheets H, Hergott D, Porter-Gill P, Mumy A, Kohaar I et al. (2013) A variant upstream of IFNL3 (IL28B) creating a new interferon gene IFNL4 is associated with impaired clearance of hepatitis C virus. *Nat Genetics* **45**, 164–171.
- Gad HH, Dellgren C, Hamming OJ, Vends S, Paludan SR & Hartmann R (2009) Interferon-lambda is functionally an interferon but structurally related to the interleukin-10 family. *J Biol Chem* **284**, 20869–20875.
- Miknis ZJ, Magracheva E, Li W, Zdanov A, Kotenko SV & Wlodawer A (2010) Crystal structure of human interferon-lambda1 in complex with its high-affinity receptor interferon-lambdaR1. *J Mol Biol* **404**, 650–664.
- Logsdon NJ, Deshpande A, Harris BD, Rajashankar KR & Walter MR (2012) Structural basis for receptor sharing and activation by interleukin-20 receptor-2 (IL-20R2) binding cytokines. *Proc Natl Acad Sci USA* **109**, 12704–12709.
- Mendoza JL, Schneider WM, Hoffmann HH, Vercauteren K, Jude KM, Xiong A, Moraga I, Horton TM, Glenn JS, de Jong YP et al. (2017) The IFN-lambda-IFN-lambdaR1-IL-10Rbeta complex reveals structural features underlying type III IFN functional plasticity. *Immunity* **46**, 379–392.
- Lubkowski J, Sonmez C, Smirnov SV, Anishkin A, Kotenko SV & Wlodawer A (2018) Crystal structure of the labile complex of IL-24 with the extracellular domains of IL-22R1 and IL-20R2. *J Immunol* **201**, 2082–2093.
- Zhang D, Wlodawer A & Lubkowski J (2016) Crystal structure of a complex of the intracellular domain of interferon lambda receptor 1 (IFNLR1) and the FERM/SH2 domains of human JAK1. *J Mol Biol* **428**, 4651–4668.
- Kotenko SV & Durbin JE (2017) Contribution of type III interferons to antiviral immunity: location, location, location. *J Biol Chem* **292**, 7295–7303.
- Muir AJ, Arora S, Everson G, Flisiak R, George J, Ghalib R, Gordon SC, Gray T, Greenbloom S, Hassanein T et al. (2014) A randomized phase 2b study of peginterferon lambda-1a for the treatment of chronic HCV infection. *J Hepatol* **61**, 1238–1246.
- Lazear HM, Schoggins JW & Diamond MS (2019) Shared and distinct functions of type I and type III interferons. *Immunity* **50**, 907–923.
- Feld JJ, Kandel C, Biondi MJ, Kozak RA, Zahoor MA, Lemieux C, Borgia SM, Boggild AK, Powis J, McCready J et al. (2021) Peginterferon lambda for the treatment of outpatients with COVID-19: a phase 2, placebo-controlled randomised trial. *Lancet Respir Med* **9**, 498–510.
- Packer MS & Liu DR (2015) Methods for the directed evolution of proteins. *Nat Rev Genetics* **16**, 379–394.
- Schreuder MP, Brekelmans S, van den Ende H & Klis FM (1993) Targeting of a heterologous protein to the cell wall of *Saccharomyces cerevisiae*. *Yeast* **9**, 399–409.
- Zahradník J, Dey D, Marciano S & Schreiber G. (2020) An enhanced yeast display platform demonstrates the binding plasticity under various selection pressures. *bioRxiv* [PREPRINT].

- 25 Li H, Sharma N, General IJ, Schreiber G & Bahar I (2017) Dynamic modulation of binding affinity as a mechanism for regulating interferon signaling. *J Mol Biol* **429**, 2571–2589.
- 26 Pham PN, Hulciak M, Biedermannova L, Cerny J, Charnavets T, Fuertes G, Herynek S, Kolarova L, Kolenko P, Pavlicek J *et al.* (2021) Protein binder (ProBi) as a new class of structurally robust non-antibody protein scaffold for directed evolution. *Viruses* **13**, 190.
- 27 Gera N, Hussain M, Wright RC & Rao BM (2011) Highly stable binding proteins derived from the hyperthermophilic Sso7d scaffold. *J Mol Biol* **409**, 601–616.
- 28 Kruziki MA, Bhatnagar S, Woldring DR, Duong VT & Hackel BJ (2015) A 45-amino-acid scaffold mined from the PDB for high-affinity ligand engineering. *Chem Biol* **22**, 946–956.
- 29 Hosse RJ, Rothe A & Power BE (2006) A new generation of protein display scaffolds for molecular recognition. *Prot Sci* **15**, 14–27.
- 30 Chao G, Lau WL, Hackel BJ, Sazinsky SL, Lippow SM & Wittrup KD (2006) Isolating and engineering human antibodies using yeast surface display. *Nat Protoc* **1**, 755–768.
- 31 Horejsi Z, Stach L, Flower TG, Joshi D, Flynn H, Skehel JM, O'Reilly NJ, Ogrodowicz RW, Smerdon SJ & Boulton SJ (2014) Phosphorylation-dependent PIH1D1 interactions define substrate specificity of the R2TP cochaperone complex. *Cell Rep* **7**, 19–26.
- 32 Baumann H, Knapp S, Lundbäck T, Ladenstein R & Härd T (1994) Solution structure and DNA-binding properties of a thermostable protein from the archaeon *Sulfolobus solfataricus*. *Nat Struct Biol* **1**, 808–819.
- 33 Boyko KM, Gorbacheva MA, Korzhenevskiy DA, Alekseeva MG, Mavletova DA, Zakharevich NV, Elizarov SM, Rudakova NN, Danilenko VN & Popov VO (2016) Structural characterization of the novel aminoglycoside phosphotransferase AphVIII from *Streptomyces rimosus* with enzymatic activity modulated by phosphorylation. *Biochem Biophys Res Commun* **477**, 595–601.
- 34 Cámara B, Liu M, Reynolds J, Shadrin A, Liu B, Kwok K, Simpson P, Weinzierl R, Severinov K, Cota E *et al.* (2010) T7 phage protein Gp2 inhibits the *Escherichia coli* RNA polymerase by antagonizing stable DNA strand separation near the transcription start site. *Proc Natl Acad Sci USA* **107**, 2247–2252.
- 35 Kraulis PJ, Clore GM, Nilges M, Jones TA, Pettersson G, Knowles J & Gronenborn AM (1989) Determination of the three-dimensional solution structure of the C-terminal domain of cellobiohydrolase I from *Trichoderma reesei*. A study using nuclear magnetic resonance and hybrid distance geometry-dynamical simulated annealing. *Biochemistry* **28**, 7241–7257.
- 36 Peleg Y & Unger T (2014) Application of the Restriction-Free (RF) cloning for multicomponents assembly. *Methods Mol Biol* **1116**, 73–87.
- 37 Benatuil L, Perez JM, Belk J & Hsieh CM (2010) An improved yeast transformation method for the generation of very large human antibody libraries. *Protein Eng Des Sel* **23**, 155–159.
- 38 Zahradnik J, Kolarova L, Peleg Y, Kolenko P, Svidenska S, Charnavets T, Unger T, Sussman JL & Schneider B (2019) Flexible regions govern promiscuous binding of IL-24 to receptors IL-20R1 and IL-22R1. *FEBS J* **286**, 3858–3873.
- 39 Diegelmann J, Beigel F, Zitzmann K, Kaul A, Göke B, Auernhammer CJ, Bartenschlager R, Diepolder HM & Brand S (2010) Comparative analysis of the lambda-interferons IL-28A and IL-29 regarding their transcriptome and their antiviral properties against hepatitis C virus. *PLoS One* **5**, e15200.
- 40 Sharma N, Longjam G & Schreiber G (2016) Type I interferon signaling is decoupled from specific receptor orientation through lenient requirements of the transmembrane domain. *J Biol Chem* **291**, 3371–3384.
- 41 Mikulecky P, Zahradnik J, Kolenko P, Cerny J, Charnavets T, Kolarova L, Necasova I, Pham PN & Schneider B (2016) Crystal structure of human interferon-gamma receptor 2 reveals the structural basis for receptor specificity. *Acta Cryst* **72**, 1017–1025.
- 42 Peleg Y & Unger T (2008) Application of high-throughput methodologies to the expression of recombinant proteins in *E. coli*. *Methods Mol Biol* **426**, 197–208.
- 43 Pettersen EF, Goddard TD, Huang CC, Meng EC, Couch GS, Croll TI, Morris JH & Ferrin TE (2021) UCSF ChimeraX: Structure visualization for researchers, educators, and developers. *Prot Sci* **30**, 70–82.

Supporting information

Additional supporting information may be found online in the Supporting Information section at the end of the article.

Table S1. List of DNA and amino acid sequences of scaffold libraries.

Table S2. List of amino acid sequences of signaling variants ProBi P5 and BiBi A1.

Table S3. Overview of primers of 10 genes used to verify signalization of bivalent binder in HeLa and HaCat cells.

Fig. S1. Sequencing of scaffold libraries.

Fig. S2. Gating strategy.

Fig. S3. Sequencing after simultaneous selection to IL-28R1 and IL-10R2.

Fig. S4. PhosphoFlow and western Blot of concentration range of IFN- λ 1.

Combined in vitro and cell-based selection display method producing specific binders against IL-9 receptor in high yields

Maroš Huličiak, Lada Biedermanová, Daniel Berdár, Štěpán Herynek, Lucie Kolářová, Jakub Tomala, Pavel Mikulecký, and Bohdan Schneider

*Institute of Biotechnology of the Czech Academy of Sciences,
Průmyslová 595, 252 50 Vestec, Czech Republic*

Correspondence

Bohdan Schneider, Institute of Biotechnology of the Czech Academy of Sciences,
BIOCEV, CZ-252 50 Vestec, Czech Republic,
Tel: +420 728 303 566, e-mail: bohdan.schneider@ibt.cas.cz

Running title

Protein binders targeting IL-9R α

Abbreviations

IL-9R α : interleukin 9 receptor alpha; HSA: human serum albumin; IL-9: interleukin 9; VEGF-A: Vascular Endothelial Growth Factor A; IL-10: interleukin 10; IL-2: interleukin 2; SubP: subtractive panning; RiD: ribosome display; YstD: yeast display; WT: wild type; BSA: bovine serum albumin; PVP: polyvinylpyrrolidone; PBS: Phosphate-buffered saline; scFvs: single chain variable antibody fragments; HM-1: *Hansenula mrakii*-1; *E. coli*: *Escherichia coli*; ELISA: Enzyme-linked immuno sorbent assay; gammaC: gamma chain; APC: allophycocyanin; FITC: fluorescein isothiocyanate; PE: phycoerythrin; PCR: polymerase chain reaction; BiP: binding protein; ILRG2: interleukin 2 receptor gamma; S2 cells: Schneider 2 insect cells; IPEI: polyethyleneimine; SDS: sodium dodecyl sulfate polyacrylamide gel electrophoresis; LB: lysogeny broth; *S. cerevisiae*: *Saccharomyces cerevisiae*; EDTA: ethylenediaminetetraacetic acid; EB: elution buffer; YPD: yeast extract-peptone-dextrose; DTT: dithiothreitol; FACS: Fluorescent Activated Cell Sorting; HRP: horseradish peroxidase; TMB: 3,3',5,5'-tetramethylbenzidine; MST: Microscale thermophoresis

Keywords

57aBi scaffold, 57bBi scaffold, interleukin 9, interleukin 9 receptor alpha, directed evolution, ribosome display, yeast display

Conflict of interest

The authors declare no conflict of interest.

Abstract

We combined cell-free ribosome display and cell-based yeast display selection to build specific protein binders to the extracellular domain of the human interleukin 9 receptor alpha (IL-9R α). The target, IL-9R α , is the receptor involved in the signaling pathway of IL-9, a pro-inflammatory cytokine medically important for its involvement in respiratory diseases. The successive use of modified protocols of ribosome and yeast displays allowed us to combine their strengths - the virtually infinite selection power of ribosome display and the production of (mostly) properly folded and soluble proteins in yeast display. The described experimental protocol is optimized to produce binders highly specific to the target, including selectivity to common proteins such as BSA, and proteins potentially competing for the binder such as receptors of other cytokines. The binders were trained from DNA libraries of two protein scaffolds called 57aBi and 57bBi developed in our laboratory. We show that the described unconventional combination of ribosome and yeast displays is effective in developing selective small protein binders to the medically relevant molecular target.

Introduction

Small engineered non-antibody molecules derived from protein scaffolds are promising alternatives to antibodies as research tools or for medical applications [1]. The properties of small, stable protein molecules - protein scaffolds - can be modified to selectively bind specific targets by randomizing amino acids in carefully selected positions.

Protein scaffolds are used as alternatives and/or supplements to monoclonal antibodies for research [2], diagnostics [3], and treatment purposes [4] because they possess several advantages over the more frequently used monoclonal antibodies: they are smaller, non-glycosylated, and easier to produce in prokaryotes. Of increasing importance seems to be that there is no need for animal immunization to produce them and that their production can be cheaper than production of antibodies.

Some scaffolds have been successfully exploited to develop binders that are currently in advanced stages of clinical trials [5] [6]. Treatment by protein binders derived from the Anticalin scaffold is promising in the areas of immuno-oncology, metabolic and respiratory diseases [7]. For instance, the Anticalin scaffold variant PRS050 was engineered into a variant effectively recognizing and preventing activation of VEGF-A, a marker of solid tumors [8]. Despite that tens of scaffolds are in use, they are mostly used in basic research projects and only a few have undergone biopharmaceutical development up to the clinical stage [9]. We believe this is an indication that there is a need for enrichment of the portfolio of scaffolds to suit a wider range of applications and to improve their applicability.

The standard strategy to develop high affinity binders based on a scaffold protein is to perform selection from combinatorial DNA libraries using one of the selection display methods. Widely used techniques for this purpose are the non-cell-based ribosome display and the cell-based yeast display; each has its strengths and limitations. Ribosome display is an *in vitro* method, providing the highest complexity. Its theoretical number of 10^{14} produced variants is practically limited only by the number of the ribosomes used in the reaction [10]. However, this technique can lead to the selection of incompletely translated and poorly expressed variants. This is a lesser issue in yeast display, where the final binding variants need to be properly folded to be displayed on the surface of a single yeast cell [11]. On the other hand, the complexity of yeast display cannot compete with the complexity of ribosome display, its automatization is also complicated.

For our display selection experiments, we used two scaffold molecules developed in our laboratory [12]. The first scaffold called 57aBi has already been successfully trained to bind human IL-10 [12] and to function as interferon-lambda 1 surrogate [13]. The second scaffold called 57bBi is used here for the first time. 57aBi and 57bBi are trained to recognize the extracellular domain of the human IL-9 receptor α -chain (IL-9R α). We decided to target the IL-9 signaling pathway because IL-9 is an important pro-inflammatory cytokine that signals *via* binding to its specific receptor IL-9R α and common gamma chain cytokine receptor subunit which IL-9 shares with the other members of the IL-2 interleukin family [14]. Besides its normal function in defense against viruses, IL-9 is involved in triggering several respiratory diseases such as asthma [15]. Specific inhibition of IL-9R α might therefore prove beneficial in treatment of these illnesses.

Successful development of a protein binder is typically evaluated by the affinity to its target molecule. However, a high specificity of the binding is of the same if not of higher importance. While the problem of a lower affinity can be solved by increasing the concentration of the binder in the system, binder's non-specificity can cause severe side effects rendering the binder useless for any therapeutic purposes. This was the call for development of our methodical platform where highly specific protein binders would be selected and trained. The platform we present here offers an unconventional combination of modified *in vitro* subtractive ribosome display and cell-based competitive yeast display selection techniques in one workflow to boost their advantages and

minimize flaws. The pipeline is employed here for development of protein binders produced in a soluble form and in high yields and specifically binding the medically relevant target, IL-9R α .

Results and Discussion

Preparation of DNA libraries of the protein scaffolds

Our target for development of protein binders is the extracellular domain of the human IL-9 receptor α -chain (IL-9R α , Uniprot code Q01113, residues 41-270). To generate the binders, we used variants of two protein scaffolds called 57aBi and 57bBi, which were previously developed in our group [12]. In each scaffold protein, we identified ten mutable residues (Figure 1), for which we created degenerated DNA libraries. The usability of the 57aBi scaffold was shown previously by successful selection of variants binding the human IL-10 at ~10 nM affinity [12]. 57aBi is based on PIH1D1 N-terminal domain Alpha-X beta2 integrin I domain, PDB ID 4PSF [16]. Performance of the other scaffold, 57bBi, is tested in this work; it is based on the crystal structure of alpha-X beta2 integrin domain, PDB ID 1N3Y [17].

The combinatorial DNA libraries for the ribosome display were synthesized using NNK codons technology. This partial randomization approach has been very successful in both academia and industry, as it introduces only one STOP codon, compared to the fully randomized NNN methodology that can introduce up to all three STOP codons to libraries. The NNK approach still has a better price-performance ratio compared to a potentially more powerful TRIM or Trimer technology that cannot generate STOP codons and lowers the risk of synonymous mutations [18].

Overview of the workflow of binder selection

We used the combinatorial libraries of the 57aBi and 57bBi scaffolds to select binders against extracellular domain of IL-9R α using directed evolution. For the initial steps of our workflow, we used the ribosome display technique, since it allowed us to screen the largest applicable library size amongst the display methods [10]. However, we modified the typical ribosome display workflow in three ways; (a) we utilized protein-free blocking reagents, (b) we introduced one to three subtractive pre-selection rounds (subtractive panning), and (c) after the fifth round of ribosome display, we performed one round of competitive yeast display to increase the specificity of binders and ensure good expression levels. The pipeline can be schematized as follows:

SubP - RiD1 - SubP - RiD2 - SubP - RiD3 - SubP - RiD4 - SubP - RiD5 - YstD - SubP - RiD6

where SubP stands for subtractive panning, RiD for ribosome display, and YstD for yeast display. The steps of the selection process are discussed below.

Ribosome display using protein-free blocking reagents

To increase binding specificity, we utilized protein-free blocking reagents in the ribosome display process. In the standard protocols, the target protein is immobilized on the surface of microplates and their surface is blocked by protein-based blockers, BSA protein [19] [20], non-fat skimmed milk [21] or gelatin [22] [23]. These proteins can and apparently do serve as unwanted selection targets, lowering the specificity of the selected variants.

To increase the selective power of ribosome display we utilized protein-free blocking reagents. One of the first protein-free solution used as blocking agent in immunochemical studies was polyvinylpyrrolidone (PVP) [24]. Nowadays, there are several protein-free reagents available on the market that are suitable for use in both membrane- and plate-based binding assays; we used Pierce Protein-Free (PBS) Blocking Buffer (Thermo Scientific, USA).

(A)		Position																									
57aBi variants		109	110	111	112	113	114	115	116	117	118	119	120	121	122	123	124	125	126	127	128	129	130	131	132	133	134
57aBi-WT	R	E	L	V	I	Y	I	A	R	E	G	L	E	D	K	Y	N	L	Q	L	N	P	E	W	R	M	
57aBi-A_01	R	W	L	V	I	R	I	A	S	K	G	L	E	W	K	Y	G	L	H	L	Y	P	W	W	L	M	
57aBi-A_02	R	L	L	V	I	S	I	A	L	T	G	L	E	V	K	Y	R	L	F	L	H	P	G	W	I	M	
57aBi-A_03	R	R	L	V	I	T	I	A	L	R	G	L	E	L	K	Y	P	L	C	L	R	P	A	W	H	M	
57aBi-A_06	R	C	L	V	I	P	I	A	R	Q	G	L	E	Q	K	Y	C	L	P	L	R	P	F	W	T	M	
57aBi-A_10	R	Q	L	V	I	L	I	A	W	S	G	L	E	M	K	Y	W	L	K	L	D	P	W	W	P	M	
57aBi-A_11	R	C	L	V	I	S	I	A	Y	L	G	L	E	M	K	Y	F	L	R	L	T	P	G	W	C	M	
57aBi-A_12	R	R	L	V	I	S	I	A	F	R	G	L	E	F	K	Y	S	L	L	S	P	S	W	S	M		
57aBi-A_13	R	A	L	V	I	Y	I	A	R	A	G	L	E	G	K	Y	L	L	T	L	P	P	I	W	P	M	
57aBi-A_14	R	S	L	V	I	D	I	A	F	S	G	L	E	W	K	Y	F	L	K	L	R	P	G	W	T	M	
57aBi-A_15	R	F	L	V	I	G	I	A	S	L	G	L	E	Y	K	Y	P	L	A	L	R	P	L	W	D	M	
57aBi-D_11	R	G	L	V	I	Y	I	A	A	P	G	L	E	S	K	Y	S	L	L	S	P	P	W	Y	M		
57aBi-D_14	R	L	L	V	I	D	I	A	C	P	G	L	E	C	K	Y	S	L	L	V	P	L	W	N	M		

(B)		Position																																		
57bBi variants		18	19	20	21	22	23	24	25	26	27	28	29	30	31	32	33	34	-	44	45	46	47	-	65	66	67	68	69	70	71	72	73	74	75	76
57bBi-WT	S	R	N	F	A	T	M	M	N	F	V	R	A	V	I	S	Q	-	-	L	M	Q	S	-	S	N	P	L	S	L	L	A	S	V	H	Q
57bBi-A_01	M	M	N	F	E	T	M	M	S	F	V	R	C	V	I	S	D	-	-	L	M	Q	S	-	S	C	P	L	D	L	L	-	S	V	M	Q
57bBi-A_05	S	G	N	F	L	T	M	M	Q	F	V	R	G	V	I	S	-	-	L	M	Q	S	-	S	E	P	L	T	L	L	P	S	V	I	Q	
57bBi-A_06	K	V	N	F	T	T	M	M	H	F	V	R	C	V	I	S	T	-	-	L	M	Q	S	-	S	R	P	L	Y	L	L	C	S	V	S	Q
57bBi-A_07	G	G	N	F	P	T	M	M	R	F	V	R	G	V	I	S	L	-	-	L	M	Q	S	-	S	I	P	L	G	L	L	P	S	V	A	Q
57bBi-A_08	-	H	N	F	T	T	M	M	A	F	V	R	G	V	I	S	R	-	-	L	M	Q	S	-	S	H	P	L	A	L	L	R	S	V	N	Q
57bBi-A_10	T	L	N	F	F	T	M	M	H	F	V	R	-	V	I	S	P	-	-	L	M	Q	S	-	S	G	P	L	Q	L	L	L	S	V	I	Q
57bBi-A_11	W	A	N	F	Q	T	M	M	D	F	V	R	W	V	I	S	L	-	-	L	M	Q	S	-	S	P	L	L	L	L	L	V	S	V	P	Q
57bBi-A_13	G	L	N	F	S	T	M	M	Y	F	V	R	S	V	I	S	H	-	-	L	M	Q	S	-	S	C	P	L	S	L	L	P	S	V	S	Q
57bBi-A_15	S	V	N	F	V	T	M	M	E	F	V	R	L	V	I	S	W	-	-	L	M	Q	S	-	S	P	L	L	L	L	L	S	S	V	D	Q
57bBi-A_16	-	Q	N	F	L	T	M	M	L	F	V	R	V	I	S	-	-	-	-	L	M	Q	S	-	S	V	P	L	V	L	L	M	S	V	T	Q
57bBi-D_06	A	G	N	F	R	T	M	M	N	F	V	R	V	I	S	D	-	-	-	L	M	Q	S	-	S	S	P	L	A	L	L	N	S	V	S	Q
57bBi-D_14	A	Y	N	F	G	T	M	M	V	F	V	R	L	V	I	S	T	-	-	L	M	Q	S	-	S	I	P	L	A	L	L	P	S	V	A	Q

Figure 1. Protein sequences of the combinatorial libraries of the (A) 57aBi and (B) 57bBi scaffolds. On top, the initial, “wild type” sequences are displayed with their ten mutable sites highlighted in yellow. The following ten sequences demonstrate sequence variability after the fifth round of the ribosome display (mutated residues in cyan, inadvertently mutated in black); the last two lines show sequences of the best binders after the 6th round of ribosome display and yeast display (the mutations in pink). The sequences are shown for the region with the 10 mutable residues corresponding to residues 138-164 of UniProt Q9NWS0 for 57aBi and residues 164-221 of UniProt P20702 for 57bBi. Position numbers refer to positions on the scaffold proteins 57aBi and 57bBi.

Preselection by subtractive panning

To avoid the selection of non-specific binders, we decided to include subtractive panning into our workflow. The method of subtractive panning has been introduced to ribosome display selection to increase the binding specificity of single chain variable antibody fragments (scFvs) [25]. It was shown to be effective to avoid binding to the carrier protein [26], to develop specific antibodies recognizing HM-1 killer toxin [27], or to identify MKN-45, a poorly differentiated diffuse gastric adenocarcinoma cell line [28].

Every ribosome display selection round of the 57aBi and 57bBi combinatorial libraries towards IL-9R α was preceded by one-step subtractive panning against BSA. After the fifth round of selection, 16 variants of each scaffold were cloned into a vector for protein expression in *E. coli* BL21-Gold (DE3) strain. The DNA of these clones was isolated and sent for sequence analysis. Even after five rounds of ribosome display, the sequences still showed high variability in the ten mutated positions (Figure 1). The 57aBi scaffold had mutations only in the randomized positions, while the 57bBi scaffold had two clones (A_05, A_11) with mutations outside of the randomized positions and five clones (A_01, A_05, A_8, A_10, A_16) with codon deletion without open reading frame shift.

The elegance of the subtractive ribosome display method is that only the non-binding variants in the supernatant from the non-specific target well are displaced into the neighboring well on one microplate that contains the specific target. This setup makes this method suitable for further automatization, which is a big advantage of ribosome display compared with *in vivo* selection.

Targets for pre-selection steps can be chosen independently in each round and they do not need to be labeled with fluorescent antibodies, which decreases the costs.

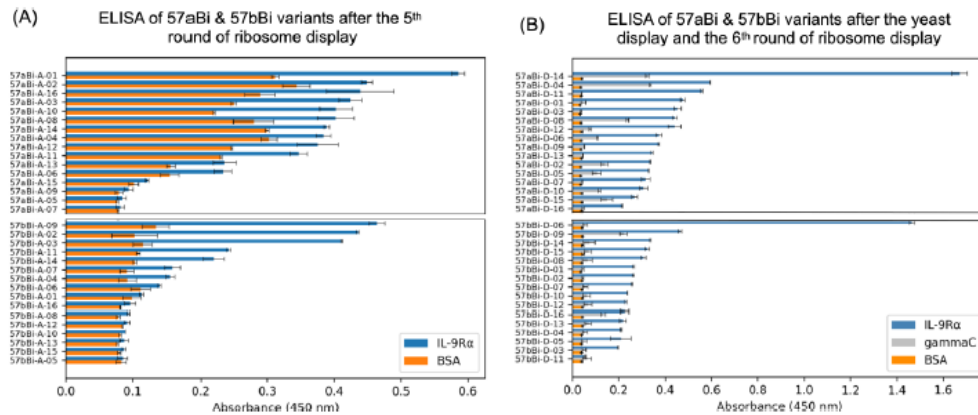


Figure 2. ELISA binding assays of the 57aBi and 57bBi scaffold variants towards IL-9R α , BSA and towards common gamma chain cytokine receptor subunit, labeled gammaC in the figure. Variants are ordered according to the strongest binding towards IL-9R α . (A) Clones selected after 5th round of the ribosome display. (B) Clones selected after the additional yeast display and the 6th round of ribosome display with three step subtractive preselection.

Pre-selection strategies in the 6th round of ribosome display

We evaluated the binding of the variants after the 5th round using ELISA assays (Figure 2A). Binding of some variants is relatively strong but binding to BSA remains also high. We therefore decided to test the power of the pre-selection process by running the 6th round of ribosome display in two different setups: (1) one round and (2) three rounds of subtractive panning. However, even these preselection steps did not resolve the issue of no or low expression and relatively high affinity to BSA. In addition, we detected only a small number of variants recognizing IL-9R α . Some defective variants can be proteins shortened by the STOP codons present at the mutable sites of 57aBi or 57bBi, some can simply be insoluble. To eliminate clones with low expression and/or low solubility, we incorporated yeast display into the pipeline, as described in the next section.

Competitive yeast display improved expression and solubility

To alleviate low production and solubility of binders after the 5th round of ribosome display, we decided to implement a yeast display step into the selection workflow. Firstly, only properly folded, and soluble protein scaffold variants could be secreted and exposed on the yeast surface. Secondly, only fully translated scaffold variants retained the C-terminal c-myc tag, which was detected by a fluorescent-labeled antibody. Expressed and soluble binders presented on the yeast surface then competed for IL-9R α (used at 100 nM concentration). Bound IL-9R α was detected by another antibody with conjugated fluorophore (Figure 3A).

Following the competitive yeast display, the resulting DNA library underwent another 3-step subtractive preselection against BSA and the 6th round of ribosome display selection against IL-9R α . The harvested variants were tested for binding towards IL-9R α , BSA, and the shared receptor for IL-9, the common gamma chain cytokine receptor subunit (UniProt P31785 ILRG2_HUMAN, residues 23-255). The results of the ELISA assay showed that the additional selection by yeast display improved dramatically the selectivity of binding to IL-9R α compared

to BSA and common gamma chain cytokine receptor subunit (Figure 2B). While the affinity to BSA is still detectable after 5th round of ribosome display (Figure 2A), it is at the background level after the yeast display and 6th round of ribosome display. In addition, binding to the common gamma chain cytokine receptor subunit is also undetectable for most variants.

Switching between two display techniques significantly improved binding specificity of selected binders to the target and decreasing it to unwanted molecules, in our case BSA and common gamma chain. It can be explained by the different environment in each technique, the non-specific variants occurring in one of them lose their binding partners in the other selection technique and are discarded during the selection process. A few rounds of ribosome display should be used in the initial steps of the selection to take advantage of the ability of ribosome display to deal with high complexity of libraries. After the complexity is reduced, yeast display eliminates selection of incompletely and/or poorly expressed variants. The final round of ribosome display ensures that binders can be produced by a prokaryotic expression system (albeit in the cell-free system).

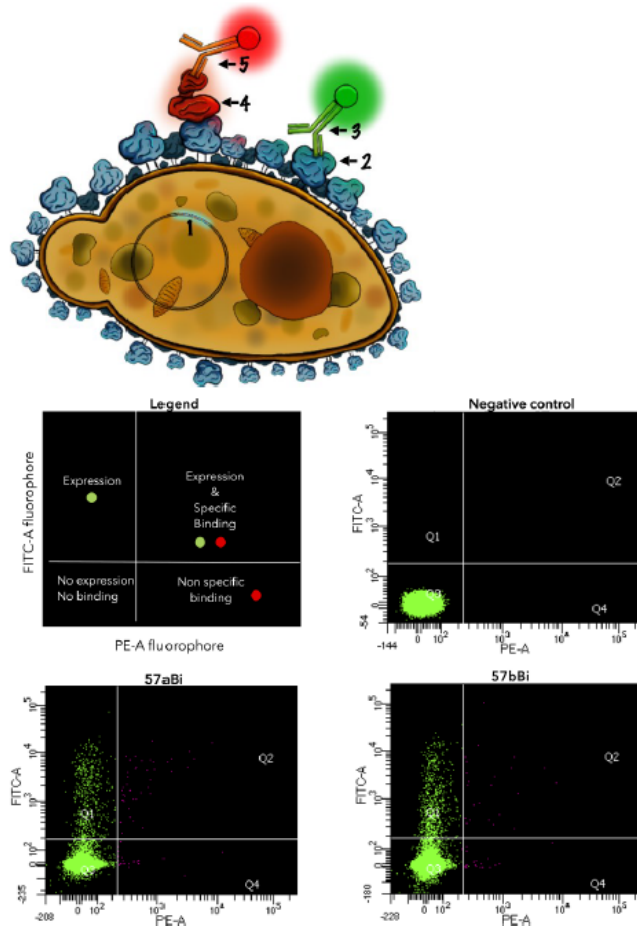


Figure 3. Yeast display of 57aBi and 57bBi scaffolds trained to bind IL-9R α protein. (A) Scheme of competitive yeast display selection: (1) vector with cloned combinatorial library, (2) protein binder variant displayed on the yeast surface, (3) anti c-myc APC conjugated antibody used to detect fully translated scaffold variant, (4) IL-9R α , (5) anti-IL-9R α PE conjugated antibody used to detect bound target IL-9R α . (B) Flow cytometry assisted yeast display selection of the combinatorial libraries of the 57aBi and 57bBi scaffolds performed after the 5th round of ribosome

display. The panel Legend shows strategy of the detection of expression of the variants on the yeast cell surface and binding to IL-9R α subunit with fluorescent antibodies. Variants of the 57aBi and 57bBi combinatorial libraries presented on the yeast cell surface were incubated with 100 nM IL-9R α and were competing for binding for 1 hour. Cells with fluorescence positivity on FITC22-A and PE-A (double positives) in quadrant Q2, which exhibit both good expression level and binding affinity to IL-9R α , were sorted and their plasmid DNA was isolated.

Affinity measurement of two best binder candidates

Affinities of the IL9-R α binders were measured for two best binders, one derived from the 57aBi scaffold and one from the 57bBi scaffold by Microscale thermophoresis (MST) as dissociation constants K_d (Figure 4, Table 1) in triplicates. The affinity measured for the best 57aBi variant 57aBi-D14 was 5 μ M, the best 57bBi variant 57bBi-D06 had a higher affinity, 510 nM. Untrained 57aBi-WT used as a negative control had unmeasurably low affinity to IL9-R α . The affinity of natural ligand of IL9-R α , IL-9, was 43 nM. The IL-9 affinity to IL-9R α has been previously reported in literature as sub nanomolar [29]. This high affinity has been estimated for the mouse IL-9/ IL9-R α system by MST-unrelated method directly in the cell culture of murine T-cell population.

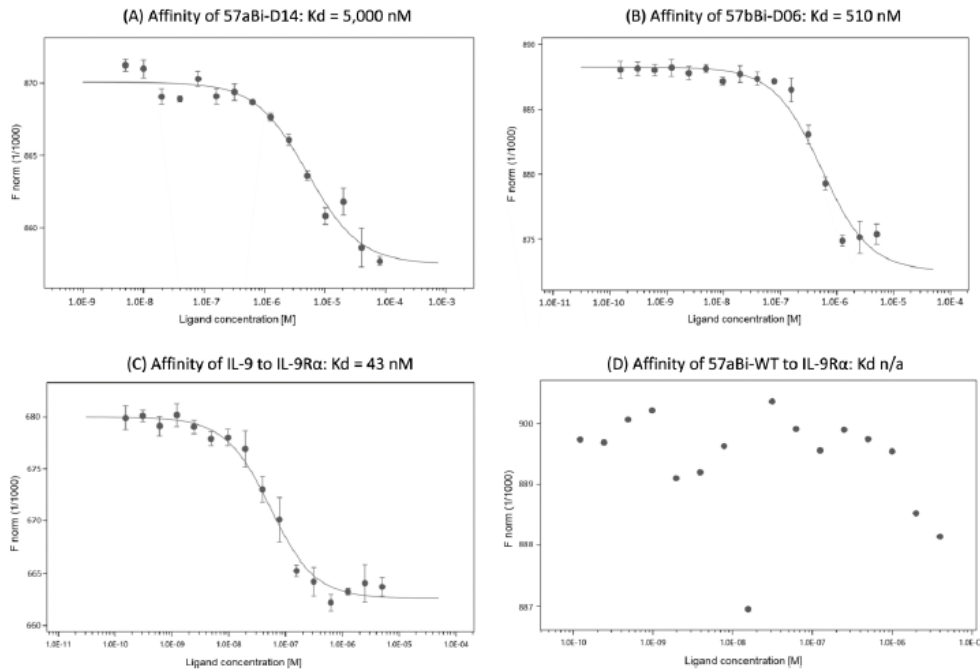


Figure 4. Affinity measurement between human interleukin 9 receptor alpha (IL-9R α) and its ligands measured by microscale thermophoresis (MST). The curves show level of binding between IL-9R α and (A) 57aBi-D14 variant, (B) 57bBi-D06 variant, (C) IL-9 (natural ligand, positive control), (D) 57aBi-WT (negative control).

Table 1. Results of the affinity measurement between human interleukin 9 receptor alpha (IL-9R α) and its ligands measured by microscale thermophoresis (MST).

	Affinity [nM]	Amplitude	No. of replicates
57aBi-WT	not measurable	-	3
IL-9	43	17	3
57aBi-D14	5,000	13	3
57bBi-D06	510	16	3

Comparing the MST affinities of the binders and IL-9 indicates a need for further affinity maturation of binders. The difference between the measured affinities of the binders and IL-9 suggests that further use of secondary mutagenesis tools such as error-prone PCR, and rational computer-driven design has a good chance to further increase of binder affinities. Increasing binder's affinity would be the first step towards their use for diagnostic or therapeutic purposes that would need to be followed by proving their power to disrupt the IL-9 signaling pathway. However, these steps are beyond the scope of this methodological work.

Conclusions

In this work, we present a proof-of-concept study combining two display selection methods into one workflow. We demonstrated that the combination of *in vitro* ribosome and cell-based yeast display methods presents a powerful tool for the selection of highly expressed and specific protein binders. We used this platform to select binders against the specific IL-9 receptor, IL-9R α , an important member of the IL-9 signaling pathway that is involved in regulating inflammation and response to viruses.

We used ribosome display technique in the initial selection steps, as it enabled us to cover the high-complexity libraries. After several rounds of ribosome display, as the complexity of the combinatorial library was reduced, we introduced yeast display. This enabled us to select only well-folded and fully translated protein variants with a high expression level in the soluble form. Importantly, the implementation of yeast display into the workflow increased the specificity of the selected variants to IL-9R α and eliminated non-specific binding to BSA and to the common gamma chain cytokine receptor subunit.

During the selection process in the ribosome display we applied subtractive panning against a non-specific BSA target. This, together with the usage of non-protein blocking reagents instead of protein-based solutions helped to increase the specificity of binders to the target protein, IL-9R α .

For the creation of combinatorial libraries of protein variants, we used two protein scaffolds, 57aBi and 57bBi, previously designed in our laboratory. The experiments presented here show that the newly developed pipeline combining *in vitro*, and cell-based selection display methods is effective in producing soluble specific binders.

Materials and methods

Construction of DNA library of scaffolds

The 57aBi and 57bBi scaffolds were designed and ten amino acid positions for randomization in each of them were selected in previous studies (Figure 5) [12]. The combinatorial libraries of both 57aBi and 57bBi scaffolds were synthesized by the GENEWIZ company using NNK codons technology. The DNA construct contained an open reading frame coding the protein scaffold sequence, elements for *in vitro* transcription and translation (T7 promoter, 5' stem loop and

ribosome binding site), and restriction sites on both termini. In addition, the libraries consisted of N-terminal Strep-tag II peptide for further purification and C-terminal c-myc detection tag followed by TolA-spacer. For further selection by ribosome display technique, there was an absence of STOP codon for creation of a stable complex of mRNA/ribosome/protein. The ordered DNA libraries were amplified by PCR using T7b and TolAk primers (Table 2).

Cloning of recombinant proteins

Gene for human IL-9R α extracellular domain (Uniprot Q01113 residues 41-270) was ordered in the form of DNA string (Thermo Fisher, Waltham, MA, USA) with optimized codons for their expression in the eukaryotic system. The DNA was cloned into a pMTH vector [12] to obtain a final construct of human IL-9R α extracellular subunit with N-terminal BiP signal peptide and C-terminal His-tag purification tag (UniProt code Q01113 residues 41-270) containing C-terminal 6xHis purification tag, and cloning sites in bold.

RSSVTGEGQG PRSRTFTCLT NNILRIDCHW SAPELGQGSS PWLLFTSNQA PGGTHKCILR
 GSECTVVLPP EAVLVPSDNF TITFHHCMMSG REQVSLVDPE YLPRRHVKLD PPSDLQSNIS
 SGHCILTWSI SPALEPMTTL LSYELAFKKQ EEAWEQAQHR DHIVGVTWLI LEAFELDPGF
 IHEARLRVQM ATLEDDVVEE ERYTGQWSEW SQPVCFQAPQ RQGPLIPPWG **WPLEHHHHHH**

The DNA coding human common gamma chain cytokine receptor subunit (UniProt code P31785 residues 23-255) was kindly provided by prof. Jamie Spangler (Johns Hopkins University, Baltimore, MD). The gene was cloned into gWiz vector (Genlantis, San Diego, CA, USA).

Table 2. List of used DNA primers. Specific set of 57aBi_for/rev and 57bBi_for/rev were used for amplification of scaffolds open reading frame sequence. Primers T7b and TolAk served for amplification of ordered DNA libraries including ribosome display elements.

Primer name	Sequence
57aBi_for	AAGTCCATGGCACAGGGA
57aBi_rev	GTTCCGATCCGATGGAGCCCATGAATG
57bBi_for	AAGTCCATGGCAAGACAGGAG
57bBi_rev	GTTCCGATCCACCCTCAATG
T7b	ATACGAAATTAATACGACTCACTATAGGGAGACCACAACGG
TolAk	CCGCACACCAGTAAGGTGTGCGGTTTCAGTTGCCGCTTTCTTTCT

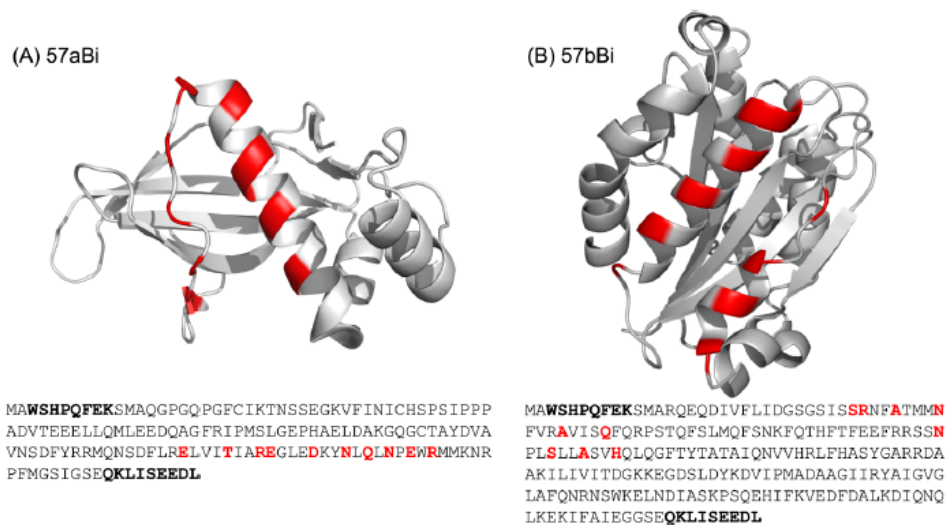


Figure 5. Structures of (A) 57aBi scaffold and (B) 57bBi scaffold and their amino acid sequences. Ten red labeled positions of each scaffold were chosen for further randomization. Scaffolds contain Strep-tag II purification tag on N-terminus and c-myc detection tag on their C-terminus (in bold).

Expression and purification of proteins

The recombinant human IL-9R α extracellular domain was produced similarly as described elsewhere [30]. Briefly, the Schneider 2 insect (S2) cells were transfected and further cultivated in an Insect-XPRESS Protein-free Insect Cell Medium (Lonza, Bazel, Switzerland). Protein expression was induced by addition of CuSO₄ and secreted IL-9R α protein was purified via Ni-NTA affinity chromatography followed with size exclusion chromatography using Superdex 200 Increase 10/300 GL column (Figure 6, Figure 7A). The column was equilibrated into the buffer containing 50 mM Tris pH 8.0 and 300 mM NaCl. Human IL-9 (UniProt P15248 residues 19-144) used as a positive control in the microscale thermophoresis affinity assay was produced as a recombinant protein in the S2 insect cells and purified in the same way as IL-9R α .

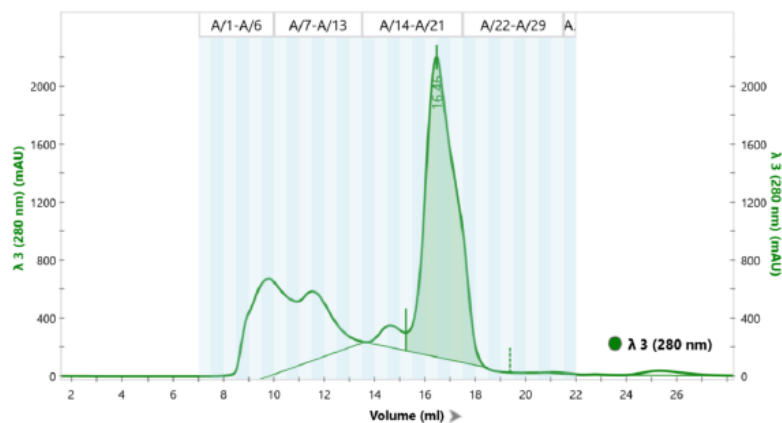


Figure 6. Size exclusion chromatography of IL-9R α extracellular domain followed after Ni-NTA affinity chromatography. Elution fractions 19-21 were collected for further assays and were analyzed via SDS PAGE.

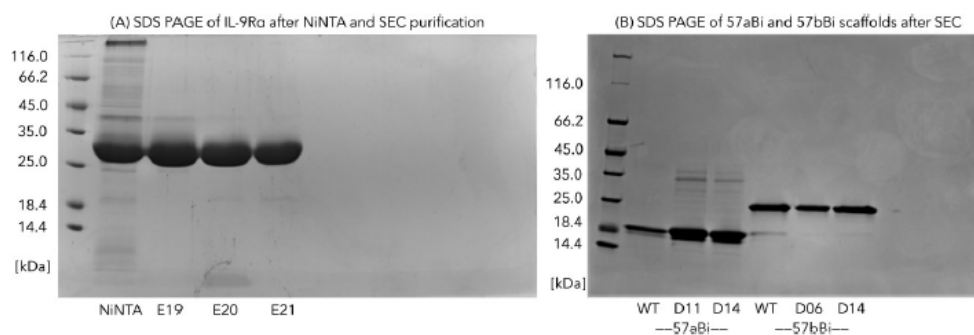


Figure 7. (A) SDS PAGE of IL-9R α extracellular domain purified by Ni-NTA affinity chromatography and size exclusion chromatography. (B) SDS PAGE of 57aBi and 57bBi WTs and two best binders of both scaffolds: 57aBi-D11, 57aBi-D14; 57bBi-D06, 57bBi-D14 after two-step purification (Streptactin XT purification and size exclusion chromatography).

The expression of human common gamma chain protein (CD132) was done in suspension adapted HEK293T cells kindly provided by Dr. Radu A. Aricescu [31]. The adaptation for suspension cultivation is described elsewhere [32]. The cells were transfected in high density. Briefly, 800×10^6 HEK293T cells were centrifuged (90 g, 5 min) and resuspended in 34 mL of ExCELL293 medium. The cell suspension was then transferred to 1 L square-bottom flask. To that, 800 μ g of plasmid DNA dissolved in 6 mL of PBS for cell cultures was sterile-filtered and mixed. Linear 25 kDa polyethyleneimine (IPEI) in a ratio of 1:3 DNA:IPEI (w/w) was added directly to the culture. The cell suspension was incubated on a shaker for 90 minutes at 37 °C, 135 rpm. The culture was topped with fresh medium to 400 mL and valproic acid [33] was added to a final 2 mM concentration. The culture was harvested 5 days post-transfection. The supernatant was filtered (0.22 μ m filter), diluted with PBS (1:1 volume ratio) and loaded to a 5 mL INDIGO Ni-Agarose column. Impurities were washed off with PBS and pre-eluted with 25 mM Imidazole in PBS. Protein was eluted with 250 mM Imidazole in PBS, concentrated to 250 μ L and loaded to Superdex 200 10/300 GL column equilibrated with 10 mM HEPES buffer pH 7.5 and the appropriate fractions were collected.

WTs of 57aBi and 57bBi scaffolds and two best binding variants derived of each scaffold were purified in-two steps, firstly by affinity chromatography using Streptactin XT resin (Iba, Göttingen, Germany) followed by size exclusion chromatography using Superdex 200 Increase 10/300 GL column (Figure 7B). The column was equilibrated into the buffer containing 50 mM Tris pH 8.0 and 300 mM NaCl. Purified proteins were then analyzed by SDS PAGE to demonstrate their solubility and expression level in *E. coli*.

Preparation of cell lysates for ELISA testing

Libraries after the fifth and sixth ribosome display selection were cloned into pETsm vector (a modified pET-26b(+)) vector containing N-terminal Strep-tag II peptide and C-terminal c-myc tag with Stop codon [12]. Chemically competent *E. coli* BL21-Gold (DE3) strain was transformed with this vector according to standard protocol for transformation of chemo-competent cells.

Protein expression was evaluated on 16 random clones of both 57aBi and 57bBi variants. Cells were cultivated in LB medium with kanamycin antibiotic in the deep 24-well plate. After the cultivation, cells were harvested by centrifugation (1100 g, 60 min). Cell pellets were resuspended and lysed in B-PER Bacterial Protein Extraction Reagent (ThermoFisher, Waltham, MA USA) by shaking at 300 rpm for 45 min. Lysates were clarified by centrifugation (1100 g, 60

min). Resulted supernatants containing binding variants were analyzed for binding to IL-9 receptor subunits and BSA by ELISA assay.

Construction of mRNA-ribosome-scaffold complex

Constructs coding combinatorial libraries of 57aBi and 57bBi scaffolds designed for ribosome display were transcribed and translated in one step at 30 °C for 6 hours using RTS 100 *E. coli* HY commercial kit (Biotechrabbit, Berlin, Germany). Because of the absence of STOP codon, a stable mRNA-ribosome-scaffold complex was formed. Complexes were held on ice until processed in the subtractive pre-selection in the ribosome display.

Subtractive pre-selection in ribosome display

Subtractive pre-selection was done before every round of ribosome display selection. Stable complexes of mRNA-ribosome-scaffold were supplemented by 0.5% BSA and 200 mg/mL of heparin in PBS buffer and incubated for either 1 x 60 min or 3 x 30 min at 4 °C with 3% BSA immobilized on the plastic surface of Nunc Polysorp plate (Invitrogen, Waltham, MA, USA).

Ribosome display selection

Supernatants from the pre-selection wells contained the pre-selected mRNA-ribosome-scaffold complexes then were transferred into the selection wells coated with IL-9R α diluted in Bicarbonate coating buffer pH 9.6. Concentrations of coated target protein, concentrations of used Pluronic F-127 detergent, and number of washing steps during the selection process varied in the individual rounds of display method (Table 3). Complexes of mRNA-ribosome-scaffold were incubated with IL-9R α for 60 min at 4 °C. The well was washed with TBS pH 7.4 buffer containing Pluronic F-127 detergent. The library complexes were incubated with an Elution buffer (EB) composed of 50 mM Tris acetate, 150 mM NaCl, 50 mM EDTA, final pH 7.5. EB contained 1 mg/mL of *S.cerevisiae* RNA and 200 mg/mL of heparin. EDTA causes disruption of the mRNA-ribosome-scaffold complex, and mRNA is then isolated using High Pure RNA isolation Kit (Roche, Switzerland) according to the manufacturer's instructions. The purified mRNA was reverse transcribed using GoScript Reverse Transcription System (Promega, Madison, WI, USA) using reverse primers 57aBi_rev and 57bBi_rev (Table 2) according to the manufacturer's protocol. The reverse transcribed cDNA was amplified by PCR using commercial Q5 polymerase (New England Biolabs, Ipswich, MA, USA) with 57aBi_for and 57aBi_rev primers for 57aBi library, and 57bBi_for and 57bBi_rev primers for 57bBi library. The amplified DNA was cloned into the pRDVsm vector [12] with NcoI and BamHI restriction enzymes and ligated with T4 ligase (New England Biolabs, Ipswich, MA, USA). Libraries cloned in pRDVsm vector were used for further selection and pre-selection processes. In final rounds of ribosome display selections, DNA libraries were cloned into the pETsm vector and transformed into *E. coli* BL21-Gold (DE3) chemocompetent cells (Agilent, Santa Clara, CA, USA) for analysis of sequences of the selected protein binders, and for evaluation of their binding properties by ELISA assays.

Table 3. Concentrations of coated target molecules (IL-9R α), concentrations of Pluronic F-127 detergent in washing buffer and number of washing steps of specific round during ribosome display selection.

Selection round	Target concentration [μ g/mL]	Pluronic F-127 concentration [%]	Number of washing steps
1	25	0.10	5
2	25	0.15	10
3	15	0.20	10
4	15	0.20	10
5	10	0.20	15
6	10	0.20	15

Construction of DNA libraries for yeast display selection and yeast cell transformation

DNA libraries after the fifth round of ribosome display selection were cleaved with NdeI and BamHI restriction enzymes and cloned into the pETcon(-) plasmid (Plasmid #41522, Addgene, Watertown, MA, USA) using T4 ligase (New England Biolabs, Ipswich, MA, USA).

S. cerevisiae EBY 100 competent cells (Invitrogen, Waltham, MA, USA) were cultivated in YPD medium (10 g/L Yeast nitrogen base, 20 g/L Peptone, 20 g/L Glucose) at 30 °C and until OD600 reached 1.6. Cells were collected by centrifugation (3000 rpm, 3 min). Pellets were washed twice with 50 mL of ice-cold water and once with 50 mL of ice-cold Electroporation buffer containing 1 M Sorbitol and 1 mM CaCl₂.

Pellets were resuspended in 20 mL of 0.1 M LiAc with 10 mM DTT and shaken in a culture flask for 30 min. Cells were again collected by centrifugation (3000 rpm, 3 min), washed once by 50 mL of ice-cold Electroporation buffer, and resuspended in 200 μ L of the same buffer. The cells were kept on ice until electroporation.

Cells were gently mixed with plasmid containing combinatorial libraries and transferred to a pre-chilled BioRad GenePulser cuvettes (BioRad, Hercules, CA, USA). Cuvettes were kept on ice for 5 min. Then, cells were transformed with prepared plasmid by electroporation at 2.5 kV and 25 μ F.

Electroporated cells were transferred into 8 mL of 1 M Sorbitol/YPD media in a ratio 1:1. Cells were cultivated at 30 °C for 1 hour, then collected by centrifugation (3000 rpm, 3 min), and resuspended in 50 mL of SDCAA media (6.7 g/L Yeast nitrogen base, 5 g/L Bacto casamino acids, 5.4 g/L Na₂HPO₄, 8.56 g/L NaH₂PO₄, 20 g/L Glucose) and grew overnight.

Yeast display selection

The electroporated yeast cells (1 mL) were added to a mixture of 1 mL of SDCAA media and 9 mL SG-CAA media (6.7 g/L Yeast nitrogen base, 5 g/L Bacto casamino acids, 5.4 g/L Na₂HPO₄, 8.56 g/L NaH₂PO₄, 20 g/L Galactose). Cells were cultivated overnight at 20 °C. When the yeast cells consumed all the glucose in the media mixture, they started to metabolize galactose. The protein scaffold variants were under the galactose promoter, therefore they were expressed and further displayed on the yeast cell surface.

Yeast cells presenting our protein binders on their surface were harvested by centrifugation (3000 rpm, 5 min) and resuspended in 1 mL of PBS buffer supplemented with 0.1 % BSA (PBS-B). IL-9R α in final concentration 100 nM was added and the reaction was incubated at 4 °C for 2 hours.

Cells were harvested by centrifugation (3000 rpm, 5 min), washed with PBS, and resuspended in 50 μ L of PBS-B buffer together with 1 μ L of chicken anti-c-myc tag antibody (BioLegend, San

Diego, CA, USA). Reaction was held on ice for 1 hour. After the incubation, cells were washed again, resuspended in 50 μ L of PBS-B buffer together with 1 μ L of anti-IL-9R α antibody conjugated with PE and 1 μ L of anti-chicken secondary antibody conjugated with APC (both BioLegend, San Diego, CA, USA). The reaction was incubated on ice for 1 hour. The cells were washed twice and resuspended in 1 mL of PBS-B buffer. Samples were analyzed using BD FACSAria flow cytometer. Variants with detected double fluorescence signals (Figure 3B) were sorted into a fresh SDCAA medium.

Yeast plasmid isolation

Sorted yeast cells with presented protein scaffold variants binding IL-9R α subunit were cultivated and recovered in SDCAA medium overnight at 30 °C. Cells were collected by centrifugation (3000 rpm, 5 min) and plasmid DNA was isolated using the ZymoPrep kit (Zymo Research, Irvine, CA, USA) according to the attached manufacturer's protocol. Isolated DNA was used for transformation of chemocompetent *E. coli* TOP10 strain. Cells were plated on LB agar plates with 100 μ g/L kanamycin antibiotic and colonies were grown overnight at 37 °C. Plasmids from single colonies were isolated using QIAprep Spin Miniprep Kit (Qiagen, Hilden, Germany) according to the attached manufacturer's protocol. DNA was then cleaved by NcoI and BamHI restriction enzymes and cloned into the pRDVsm vector for the sixth round of selection by ribosome display.

ELISA assay

Nunc Polysorp 96-well microplate from Invitrogen was covered with 10 μ g/mL of IL-9R α or common gamma chain cytokine receptor subunit diluted in Bicarbonate coating buffer pH 9.6. The plate was then blocked with 3% BSA diluted in PBS-P buffer (PBS buffer + 0.1% Pluronic F127). One control plate was also covered with 3% BSA for detection of negative background level of binding. Plates were washed three times with PBS-P buffer.

Each plate well was filled with a cell lysate prepared from a different single colony expressing protein scaffold variant. Binding reaction was running for 1 hour and plates were washed three times. The C-terminal c-myc detection tag of the binders was detected via anti-c-myc antibody conjugated with horseradish peroxidase (HRP) (Abcam, Cambridge, UK). Reaction was incubated for 1 hour and plates were washed three times to remove the unbounded antibody. Then a specific TMB-2 one step substrate (Thermo Scientific, Waltham, MA, USA) for the peroxidase was added and reaction was stopped with 2 M H₂SO₄. Absorbance at 450 nm was measured.

Microscale thermophoresis

According to ELISA results, affinity of 57-aBi-D14 and 57-bBi-D6 variants were estimated by Microscale thermophoresis (MST) using the Monolith NT.115 instrument; as a negative control was used 57aBi-WT, as the positive control S2-cell expressed IL-9. IL-9R α was labeled via c-terminal His tag with RED-tris-NTA labeling kit according to attached kit protocol. Protein binders were diluted in buffer 50 mM TRIS; pH=8, 300 mM NaCl and 0.1% Pluronic F-127. IL-9R α was then titrated by protein binders and mix was loaded into NT.115 Standard treated capillaries and MST was measured using Medium MST power and 60% of LED power. MST measurements were done in MO.Control program and data were analyzed in MO.Affinity Analysis v2.2.4 software (both NanoTemper Technologies, Munich, Germany).

Acknowledgements

We thank Jakub Svoboda from the Institute of Biotechnology for helping with design of graphical abstract. This study was supported by the Czech Science Foundation grant 20-13029S and the institutional grant to the Institute of Biotechnology of the Czech Academy of Sciences RVO

86652036, and by National Institute for Cancer Research (Program EXCELES LX22NPO5102) funded by the European Union Next Generation EU. We acknowledge CF Biophysic and CF Mass Spec of CIISB, Instruct-CZ Centre, supported by MEYS CR (LM2018127) and European Regional Development Fund-Project „UP CIISB“ (No. CZ.02.1.01/0.0/0.0/18_046/0015974).

Author contributions

PM, MH, and BS conceived the project, MH, PM, LB, and JT planned experiments, MH, DB, ŠH, LK and JT performed experiments and analyzed data, MH, JT, LB, PM and BS wrote the paper.

References

1. Nuttall SD & Walsh RB (2008) Display scaffolds: protein engineering for novel therapeutics, *Curr Opin Pharmacol.* **8**, 609-15.
2. Stiel AC, Feldmeier K & Hocker B (2014) Identification of protein scaffolds for enzyme design using scaffold selection, *Methods Mol Biol.* **1216**, 183-96.
3. Miao Z, Levi J & Cheng Z (2011) Protein scaffold-based molecular probes for cancer molecular imaging, *Amino Acids.* **41**, 1037-47.
4. Weidle UH, Auer J, Brinkmann U, Georges G & Tiefenthaler G (2013) The emerging role of new protein scaffold-based agents for treatment of cancer, *Cancer Genomics Proteomics.* **10**, 155-68.
5. Rothe C & Skerra A (2018) Anticalin((R)) Proteins as Therapeutic Agents in Human Diseases, *BioDrugs.* **32**, 233-243.
6. Samanta A, Aziz AA, Jhingan M, Singh SR, Khanani AM & Chhablani J (2020) Emerging Therapies in Neovascular Age-Related Macular Degeneration in 2020, *Asia Pac J Ophthalmol (Phila).* **9**, 250-259.
7. Deuschle FC, Ilyukhina E & Skerra A (2021) Anticalin(R) proteins: from bench to bedside, *Expert Opin Biol Ther.* **21**, 509-518.
8. Gille H, Hulsmeyer M, Trentmann S, Matschiner G, Christian HJ, Meyer T, Amirkhosravi A, Audoly LP, Hohlbaum AM & Skerra A (2016) Functional characterization of a VEGF-A-targeting Anticalin, prototype of a novel therapeutic human protein class, *Angiogenesis.* **19**, 79-94.
9. Gebauer M & Skerra A (2020) Engineered Protein Scaffolds as Next-Generation Therapeutics, *Annu Rev Pharmacol Toxicol.* **60**, 391-415.
10. Pluckthun A (2012) Ribosome display: a perspective, *Methods Mol Biol.* **805**, 3-28.
11. Boder ET & Wittrup, KD (1997) Yeast surface display for screening combinatorial polypeptide libraries, *Nat Biotechnol.* **15**, 553-7.
12. Pham PN, Huliciak M, Biedermannova L, Cerny J, Charnavets T, Fuertes G, Herynek S, Kolarova L, Kolenko P, Pavlicek J, Zahradnik J, Mikulecky P & Schneider B (2021) Protein Binder (ProBi) as a New Class of Structurally Robust Non-Antibody Protein Scaffold for Directed Evolution, *Viruses.* **13**.
13. Kolarova L, Zahradnik J, Huliciak M, Mikulecky P, Peleg Y, Shemesh M, Schreiber G & Schneider B (2022) De novo developed protein binders mimicking Interferon lambda signaling, *FEBS J.* **289**, 2672-2684.
14. Benczik M & Gaffen S L (2004) The interleukin (IL)-2 family cytokines: survival and proliferation signaling pathways in T lymphocytes, *Immunol Invest.* **33**, 109-42.
15. Shimbara A, Christodoulouopoulos P, Soussi-Gounni A, Olivenstein R, Nakamura Y, Levitt RC, Nicolaides NC, Holroyd KJ, Tsiopoulos A, Lafitte JJ, Wallaert B & Hamid QA (2000) IL-9 and its receptor in allergic and nonallergic lung disease: increased expression in asthma, *J Allergy Clin Immunol.* **105**, 108-15.

16. Horejsi Z, Stach L, Flower TG, Joshi D, Flynn H, Skehel JM, O'Reilly NJ, Ogradowicz RW, Smerdon SJ & Boulton SJ (2014) Phosphorylation-dependent PIH1D1 interactions define substrate specificity of the R2TP cochaperone complex, *Cell Rep.* **7**, 19-26.
17. Vorup-Jensen T, Ostermeier C, Shimaoka M, Hommel U & Springer TA (2003) Structure and allosteric regulation of the alpha X beta 2 integrin I domain, *Proc Natl Acad Sci USA.* **100**, 1873-8.
18. Lebl M (1999) Solid-phase synthesis of combinatorial libraries, *Curr Opin Drug Discov Devel.* **2**, 385-95.
19. Zahnd C, Amstutz P & Pluckthun A (2007) Ribosome display: selecting and evolving proteins in vitro that specifically bind to a target, *Nat Methods.* **4**, 269-79.
20. Mouratou B, Behar G, Paillard-Laurance L, Colinet S & Pecorari F (2012) Ribosome display for the selection of Sac7d scaffolds, *Methods Mol Biol.* **805**, 315-31.
21. Okda F, Liu X, Singrey A, Clement T, Nelson J, Christopher-Hennings J, Nelson EA & Lawson S (2015) Development of an indirect ELISA, blocking ELISA, fluorescent microsphere immunoassay and fluorescent focus neutralization assay for serologic evaluation of exposure to North American strains of Porcine Epidemic Diarrhea Virus, *BMC Vet Res.* **11**, 180.
22. Nolo R, Herbrich S, Rao A, Zweidler-McKay P, Kannan S & Gopalakrishnan V (2017) Targeting P-selectin blocks neuroblastoma growth, *Oncotarget.* **8**, 86657-86670.
23. Baldauf KJ, Salazar-Gonzalez RA, Doll MA, Pierce WM, Jr States JC & Hein DW (2020) Role of Human N-Acetyltransferase 2 Genetic Polymorphism on Aromatic Amine Carcinogen-Induced DNA Damage and Mutagenicity in a Chinese Hamster Ovary Cell Mutation Assay, *Environ Mol Mutagen.* **61**, 235-245.
24. Haycock JW (1993) Polyvinylpyrrolidone as a blocking agent in immunochemical studies, *Anal Biochem.* **208**, 397-9.
25. Rothe A, Nathanielsz A, Hosse RJ, Oberhauser F, Strandmann EP, Engert A, Hudson PJ & Power B E. (2007) Selection of human anti-CD28 scFvs from a T-NHL related scFv library using ribosome display, *J Biotechnol.* **130**, 448-54.
26. Sun Y, Ning B, Liu M, Gao X, Fan X, Liu J & Gao Z (2012) Selection of diethylstilbestrol-specific single-chain antibodies from a non-immunized mouse ribosome display library, *PLoS One.* **7**, e33186.
27. Kabir ME, Krishnaswamy S, Miyamoto M, Furuichi Y & Komiyama T (2009) An improved phage-display panning method to produce an HM-1 killer toxin anti-idiotypic antibody, *BMC Biotechnol.* **9**, 99.
28. Mehdipour T, Tohidkia MR, Ata Saei A, Kazemi A, Khajeh S, Rahim Rahimi AA, Nikfarjam S, Farhadi M, Halimi M, Soleimani R, Zubarev RA & Nouri M (2020) Tailoring subtractive cell biopanning to identify diffuse gastric adenocarcinoma-associated antigens via human scFv antibodies, *Immunology.* **159**, 96-108.
29. Uyttenhove C, Druetz C, Renauld JC, Hérin M, Noël H & Van Snick J (1991) Autonomous growth and tumorigenicity induced by P40/interleukin 9 cDNA transfection of a mouse P40-dependent T cell line, *J Exp Med.* **173**, 519-22.
30. Mikulecky P, Zahradnik J, Kolenko P, Cerny J, Charnavets T, Kolarova L, Necasova I, Pham PN & Schneider B (2016) Crystal structure of human interferon-gamma receptor 2 reveals the structural basis for receptor specificity, *Acta Crystallogr D Struct Biol.* **72**, 1017-25.
31. Aricescu AR, Lu W & Jones EY (2006) A time- and cost-efficient system for high-level protein production in mammalian cells, *Acta Crystallogr D Struct Biol.* **62**, 1243-50.
32. Blaha J, Pachel P, Novak P & Vanek O (2015) Expression and purification of soluble and stable ectodomain of natural killer cell receptor LLT1 through high-density transfection of suspension adapted HEK293S GnTI(-) cells, *Protein Expr Purif.* **109**, 7-13.
33. Backliwal G, Hildinger M, Kuettel I, Delegrange F, Hacker DL & Wurm FM (2008) Valproic acid: a viable alternative to sodium butyrate for enhancing protein expression in mammalian cell cultures, *Biotechnol Bioeng.* **101**, 182-9.